Dissecting Response and Resistance to CDK4/6 inhibition in ER+ Breast Cancer

A dissertation presented

by

Flora Luo

to

The Division of Medical Sciences

in partial fulfillment of the requirements

for the degree of

Doctor of Philosophy

in the subject of

Biological Chemistry and Molecular Pharmacology

Harvard University

Cambridge, Massachusetts

April 2017

Dissertation Advisor: Dr. Levi A. Garraway Flora Luo

Dissecting Response and Resistance to CDK4/6 Inhibition in ER+ Breast Cancer

Abstract

Highly specific cyclin-dependent kinase 4 and 6 (CDK4 and CDK6) inhibitors comprise a novel and exciting class of targeted therapeutics in oncology. CDK4/6 inhibitors, such as palbociclib, abemaciclib and ribociclib prevent cell cycle progression from the first growth phase (G1) to the DNA synthesis (S) phase of the cell cycle. CDK4/6 inhibition in combination with endocrine therapy is the new standard of care for metastatic breast cancers that express the estrogen receptor (ER+). Many preclinical biomarkers of sensitivity to CDK4/6 inhibition, however, are not clinically relevant. Furthermore, some ER+ breast cancer patients present with intrinsic resistance to CDK4/6 inhibitors and others are progressing on therapy. Consequently, effective treatment of metastatic breast cancer patients necessitates an understanding of response and resistance to CDK4/6 inhibition. To this end, we conducted two projects to 1) determine whether breast cancer cells that are dependent on ER signaling require CDK4/6 and 2) identify the landscape of resistance to CDK4/6 inhibition.

Recent sequencing studies have revealed that 20% of metastatic breast cancers harbor activating mutations in the gene encoding the ER (*ESR1*). Furthermore, ER+ breast cancer cells that are resistant to estrogen deprivation therapy exhibit a dependency on CDK4. We found that estrogen-independent growth of *ESR1*-mutant breast cancer cells require CDK4/6 and that sensitivity to CDK4/6 inhibition is dependent on an intact retinoblastoma protein (RB, the main downstream target of CDK4/6). Thus, *ESR1*-mutant breast cancer patients may benefit from CDK4/6 inhibition.

To systematically identify genes whose upregulation confer resistance to CDK4/6 inhibition, we conducted five near genome-wide open reading frame (ORF) screens. While most *in vitro* characterizations of resistance have utilized estrogen-rich media, CDK4/6 inhibitors are only approved in combination with endocrine therapy. Thus, to recapitulate the clinical setting more closely, our expression screens utilized two different CDK4/6 inhibitors alone and in combination with estrogen deprivation. Several novel resistance drivers were nominated. In particular, RB phosphorylation emerged as a convergent node of resistance to CDK4/6 inhibition. Together with cultured to resistance cell models and clinical sequencing of patient tumors, our studies identify several strategies to combat resistance and help pinpoint patient populations for CDK4/6 inhibitor treatment.

TABLE OF CONTENTS

List of Figures

List of Tables

Acknowledgements

There are numerous individuals whom I would like to thank for their unwavering support during my time in graduate school. From my first project on ARID2 to our resistance screens, my advisor Dr. Levi Garraway never lost faith in the significance of our research and always challenged me to see the bigger picture. I think what I will remember the most about Dr. Garraway is that it is not enough to be a great scientist; you must be a great person too.

I would also like to thank the many faculty members who have taken time out of their hectic schedules to be on my dissertation advisory committee. Dr. James Bradner, Dr. David Fisher and Dr. Charles Roberts were instrumental members of my original committee. They provided invaluable insights into chromatin remodeling in melanoma and continued to provide their expertise even when I transitioned into a breast cancer project. As chair of my dissertation committee, Dr. Myles Brown was pivotal in the success of our CDK4/6 inhibitor resistance story; he encouraged us to look beyond palbociclib and consider other CDK4/6 inhibitors, such as abemaciclib in our screens. Dr. Nikhil Wagle's clinical insights have also been invaluable. Thank you to Drs. Myles Brown, Andrew Aplin, William Hahn and Adam Bass for being on my dissertation defense committee.

Our collaborators at the Dana Farber Cancer Institute and the Broad Institute have greatly contributed to the success of our projects. Dr. Glenn Cowley was critical in helping with the optimization and sequencing of CDK4/6 inhibitor resistance screens. Other members of the Genetics Perturbation Platform, such as Dr. Federica Piccioni and Sasha Pantel conducted a follow-up CDK4/6 inhibitor resistance screen. Dr. Cory Johannssen helped secure funding from the Slim Initiative in Genomic Medicine for our large-scale screens. Dr. Seth Wander and Dr. Nikhil Wagle have been incredibly helpful in discussing our work and critical in obtaining patient samples to determine the clinical relevance of our screening results. Dr. Joseph Geradts and

the pathology team at Brigham and Women's have been incredibly helpful in helping us perform immunohistochemistry on our patient samples.

Whenever the science got difficult, I knew that I could always turn to the talented members of Dana 15 for advice. I'm fortunate to have been surrounded by so many strong women in the lab. Bokang Rabasha and Dr. Tiki Hayes were always there with the perfect song or meme to deal with a confusing experiment. Dr. Alison Taylor was always ready to listen and provide counsel. Dr. Eva Goetz, Dr. Chengyin Min, Dr. Shruti Malu, Dr. Ginerva Dr. Xiuning Le are also amazing scientists that have beautifully balanced research and family. Furthermore, Dr. Eva Goetz always volunteered her time to discuss my projects and help improve my writing. I am also grateful to have sat next to Dr. Chelsea Place Johnson and Daniel Treacy for much of my graduate studies. Their advice, technical support and positive outlooks were incredibly encouraging. Dr. Peter Choi was instrumental in the troubleshooting of my CRISPR experiments.

I also want to thank my family and friends. In life, my father didn't always get the opportunities he deserved but he taught me that true success is being able to make best out of any situation. I admire my mother for always navigating through life with a smile and for prioritizing family above all. From a very young age, my maternal grandmother taught me the importance of hard work and resilience—lessons that were quite relevant during long FACS days. I also would like to thank my fiancé Efraín Arias and our dog Koji for sitting through countless practice presentations and for reminding me to walk outside occasionally. The moral support from the Arias family throughout my PhD has been tremendous. My friends in the BBS program have also inspired me by their unbreakable spirit and dedication. Amelia Chang always reminds me that when science calls, you answer even if it's 10pm at night. Diana Cai has also been quite supportive. My family and friends have always been my biggest cheerleaders and their wisdom have guided me throughout graduate school and beyond.

Finally, I would like to thank our funding sources. The Slim Initiative for Genomic Medicine provided the funding for our open reading frame screens. The Ruth L. Kirschstein Research Service Award (F31 CA195751-03) has supported my graduate studies since 2015. The Howard Hughes Medical Institute Investigator Award is currently supporting our *in vivo* mouse work.

CHAPTER 1

INTRODUCTION

Overview

Breast cancer is one of the leading causes of cancer-related deaths among women. Globally, approximately 2.4 million women have breast cancer; in 2015 alone, there were 523,000 breast cancer deaths (1). Advances in understanding the etiology of this heterogeneous disease has helped decrease the breast cancer mortality rate over the past three decades (2,3).

The majority of breast cancers express the estrogen receptor (ER) and are denoted as ER+. Since the cell cycle is commonly deregulated in advanced ER+ breast cancers, the recent development of highly specific cell cycle inhibitors represents an exciting potential breakthrough in treatment (4-8). The molecular determinants governing response and resistance to these novel targeted agents, however, are not well-characterized. Effective treatment of breast cancer patients warrants an understanding of these factors. This dissertation is composed of two projects centered on inhibitors of the G1/S cell cycle checkpoint in ER+ breast cancer. The first project uncovers a potential marker of sensitivity, while the second project systematically identifies genes that confer resistance to cell cycle inhibition.

Cell cycle regulation in breast cancer

Cyclin-dependent kinases (CDKs) and the cell cycle

CDKs are serine/threonine kinases that control cell cycle progression and are activated by cognate cyclins. The mammalian cell cycle consists of four phases: G1 (growth phase 1), S (DNA synthesis phase), G2 (growth phase 2) and M (mitosis) **(Fig. 1.1A)**. At the start of G1, the tumor suppressor retinoblastoma protein (RB, hereafter RB) is hypophosphorylated and sequesters E2F transcription factors (9) **(Fig. 1.1B)**. This interaction blocks the transactivation

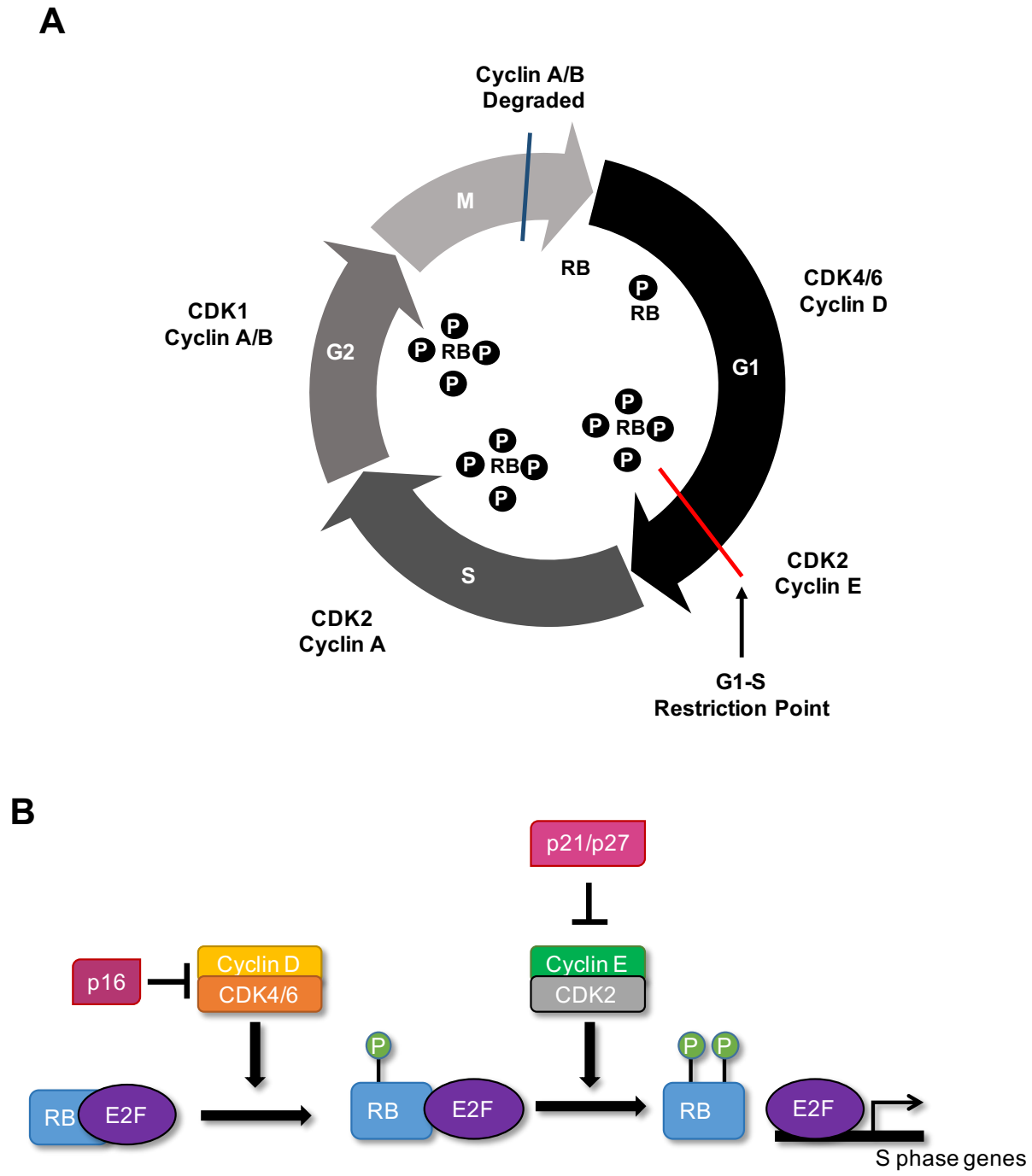

Figure 1.1. CDKs phosphorylate RB to drive cell cycle progression. **(A)** Schematic overview of the cell cycle. For each phase of the cell cycle, active cyclin-CDK complexes and RB phosphorylation status are indicated. Based on figure in Sherr *et al.*'s review (10). **(B)** Detailed depiction of the canonical G1/S cell cycle checkpoint.

domain of E2F family members, such as E2F1, and prevents expression of S phase genes (11). The three D-type cyclins (D1, D2, D3) often have overlapping functions but can confer differences in CDK substrate specificity (12) and are differentially expressed in cancer (13-15). In response to mitogenic signals, cyclin D levels rise (16). Cyclin D binds to and activates CDK4/6 (17-19). Activated cyclin D-CDK4/6 complexes then phosphorylate RB at serine 780, 807/811 and many other phosphorylation sites (17-19), weakening its interaction with E2F transcription factors (20). CDK4/6-cyclin D complexes can also phosphorylate and inactivate other pocket proteins in addition to RB such as p130 and p107 (21-23). As G1 progresses, cyclin E levels begin to rise, activating CDK2; CDK2-cyclin E complexes further phosphorylate and inactivate the retinoblastoma protein (24,25). Once freed from RB, E2F promotes expression of S phase genes, such as cyclin E and cyclin A (26-28). Full RB phosphorylation is required to progress through the G1/S restriction point **(Fig. 1.1A)** (10). In S phase, cyclin A-CDK2 complexes maintain RB phosphorylation, while cyclin A/B-CDK1 complexes maintain RB phosphorylation in G2. Cyclin A and B are degraded in mitosis (29), returning RB to the hypophosphorylated state and cells enter G1 (30).

Non-canonical interactions have also been detected between CDK2 and cyclin D1 in breast cancer cells (31). Chytl *et al.* generated a cyclin D1-CDK2 fusion protein to study the ability of cyclin D1-CDK2 complexes to phosphorylate RB. The fusion construct expressed a cyclin D1 mutant (T286A) together with CDK2. The T286A mutation stabilizes cyclin D1 by preventing its nuclear export and subsequent degradation (32,33). Characterization of this fusion construct revealed that CDK2 and cyclin D1 complexes phosphorylate RB at serine 780 and 807/811. Furthermore, functional cyclin D1 is necessary for CDK2 activation in cyclin D1-CDK2 complexes and for RB phosphorylation (34). Additional experiments by Chytl *et al.* comparing wild-type cyclin D1 and the T286A mutant suggested that stabilization of cyclin D1 increases CDK2's phosphorylation of RB at 249/252 (34). Thus, non-canonical cyclin D1 and CDK2 complexes are functional and can inactivate RB.

In cells, naturally occurring CDK inhibitors include members of the INK4 and CIP/KIP families. INK4 proteins such as p16, p15, p18 and p19 contain ankyrin repeats and exclusively bind to and inactivate CDK4/6 (35-39). In contrast, CIP/KIP proteins, such as p21, p27 and p57 (40-50) interact with cyclin D-, cyclin E- and cyclin A-CDKs. The activity of CIP/KIP proteins is dependent upon interaction with specific CDKs. For example, p21 and p27 inhibit the cell cycle by binding to cyclin E-CDK2 complexes (16). As proliferating cells progress through G1, cyclin D-CDK4/6 complexes sequester p27 and p21 (47,48,51), allowing for CDK2 activation. As described below, cancers often abrogate the G1/S cell cycle checkpoint.

Cell cycle gene alterations in breast cancer

Gene expression profiling has enabled prognostic and molecular stratification of breast cancers into five intrinsic subtypes: luminal A, luminal B, normal-like, HER2-positive, and basal-like (52-54). Luminal breast cancers comprise the largest subtype (~70%) (55). Since a defining characteristic of luminal breast cancers is expression of the hormone receptors progesterone receptor and estrogen receptor α, these cancers are estrogen-responsive and are amenable to hormonal therapy (56). There are two different isoforms of the estrogen receptor (ERα and ERβ) but estrogen predominantly signals through ERα in the luminal subtype (57,58); breast cancers that express ERα will henceforth be denoted as ER+. Luminal A tumors do not express HER2 and have the best prognosis (59). In contrast, HER2 expression is detected in a subset of luminal B tumors and this subtype is generally more aggressive than luminal A (59,60). While normal-like breast cancers may express the ER and resemble normal breast epithelial, patients with this subtype have an intermediate outcome (54). The PR-, ER- and HER2-enriched subtype accounts for another 10% of breast cancers (52,61,62). Breast cancers that are PR-, ER-, and HER2-negative and express basal epithelial markers have the worse prognosis (52).

Alteration of G1/S cell cycle genes is a key determinant of subtype specificity in breast cancer (55,63). Loss of p16 expression is correlated with ER positivity (64). Luminal A tumors have high RB expression and 29% amplify the cyclin D1 gene (*CCND1*) (55). In contrast, *CCND1* amplification is more prevalent in the luminal B subtype (58% harbor amplification of *CCND1*) (55,63). Luminal B breast cancers also have a higher proliferative index (as determined by Ki67 staining) compared to luminal A cancers; high Ki67 staining is further correlated with worse prognosis (59). *CCND1* amplification is detected in 38% of HER2-enriched breast cancers (55,63). While luminal and HER2-enriched breast cancers generally express wild-type RB, 20% of triple negative breast cancers have mutations or deletions in the *RB* gene (55). Cyclin E1 overexpression has also been detected in the basal subtype. Therefore, cyclin D1 overexpression is present in many subtypes, while RB loss mainly occurs in basal breast cancers.

Cyclin D1-CDK4/6 in breast cancer tumorigenesis

Numerous mouse studies have implicated the CDK4/6-cyclin D1 axis in breast cancer development. Cyclin D1 is a bona fide breast cancer oncogene as its expression from a transgenic mouse mammary tumor virus promoter (MMTV) is sufficient to induce tumor formation (65). Tumorigenesis of HER2- and RAS-driven mammary models of breast cancer is also cyclin D1-dependent (66,67). Yu *et al.* found that cyclin D1-mediated tumorigenesis requires CDK4 activity; HER2 can no longer induce tumors in mice expressing the cyclin $D1^{K112E}$ mutant (68). While the K112E mutant interacts with CDK4/6, it is unable to activate CDK4/6. As the authors note, CDK2 is still active in this mouse model, as cyclin $D1^{K112E}$-CDK4/6 complexes still sequester p21 and p27. Thus, CDK4/6 activation is specifically required for breast cancer tumorigenesis.

The ER and transcriptional regulation of cyclin D1

Approximately 70% of breast cancers are ER+. The gene encoding ERα, *ESR1*, was cloned over thirty years ago (69). In response to the steroid hormone estrogen, the ER stimulates expression of genes involved in development and cell growth (70). Similar to other members of the nuclear receptor superfamily, the ER contains a highly conserved DNA binding domain, a ligand binding domain (LBD), and two transactivation domains (71,72). Activation function 2 (AF-2) sits in the LBD and enables estrogen-dependent activation of the estrogen receptor; estrogen-independent activation of the ER occurs through the N-terminal activation function 1 (AF-1) domain. As discussed in the next chapter, growth factor receptor signaling often induces AF-1 phosphorylation and subsequent ligand-independent activation of the ER (73). According to the classical model of nuclear receptor action, estrogen binding induces ER dimerization, interaction with estrogen-responsive elements (EREs) and cofactors (coactivators or corepressors) to control gene expression (74,75). The ER can also regulate transcription in an ERE-independent manner. In particular, transcription factors such as AP-1 and SP-1 can bind their cognate promoter sequences and recruit the ER as a coactivator (76,77).

In breast cancer, the ER relies on its interaction with coactivators to drive cyclin D1 expression and cell cycle progression. These coactivators are particularly relevant as many breast cancers that overexpress cyclin D1 do not harbor *CCND1* amplification (78). Furthermore, unlike many ER target genes, the cyclin D1 promoter does not contain an ERE (79). Instead, in ER+ MCF7 cells, ATF-2/c-jun (transcription factors) heterodimers bind to the cAMP response element in the *CCND1* promoter and recruit the ER (80). In ER+ ZR-75-1 breast cancer cells, estrogen regulates cyclin D1 through PKA-dependent cAMP response elements and GC-rich rich SP-1 binding sites in the cyclin D1 promoter (81). Stable transfection studies have also implicated c-Jun/c-Fos heterodimers (AP-1) in ER recruitment to the cyclin D1 promoter (82). Thus, given the lack of an ERE in the *CCND1* promoter, the ER must be recruited by coactivators to regulate cyclin D1 expression.

Ectopic ER expression cannot induce cyclin D1 expression in breast cancers lacking endogenous ER (81), suggesting that the ER regulates cyclin D1 in a cell-type-specific manner. Using chromatin immunoprecipitation and DNA tile microarrays, Eeckhoute *et al.* identified an enhancer region downstream of the cyclin D1 gene that is required for ER-mediated transcription (83). This downstream enhancer was only activated in ER+ MCF7 cells and not triple negative MDA-MB-231 cells. The authors further found that the ER pioneer factor FOXA1 and was required for ER recruitment to this downstream cyclin D1 enhancer. Thus, the ER interacts with numerous coactivators to drive cyclin D1 expression. As discussed in the next section, cyclin D1 also plays a key role in endocrine resistance by activating the ER in a hormone- and CDK-independent manner (84,85).

Resistance to endocrine therapy

Since the ER is a lineage-survival oncogene (86), ER-directed therapies have been a successful mainstay of treatment for luminal breast cancers for forty years. Selective ER modulators (SERMs) like tamoxifen compete with estrogen for ER binding and inhibit ER activity in breast cancer cells (87). Although tamoxifen received FDA approval in 1977, it acts as an ER agonist in endometrial tissue and induces endometrial hyperplasia and even cancer (88-90). In contrast, aromatase inhibitors (AIs), such as anastrozole, letrozole and exemestane, prevent estrogen production. Anastrozole was first FDA-approved in 1995 for ER+ breast cancer patients who have progressed on prior tamoxifen treatment and subsequently shown to be superior to tamoxifen even in the first-line setting (91-93). While anastrozole and letrozole are nonsteroidal reversible inhibitors, exemestane is a steroidal compound that binds irreversibly (94). Letrozole suppresses aromatase activity upwards of 98.9%—the highest among the three AIs (95-97). Similar to anastrozole, exemestane and letrozole are also FDA approved for ER+ breast cancer patients in the adjuvant setting to combat tamoxifen resistance. The final class of

hormonal therapy includes selective ER degraders (SERDs) like fulvestrant. Fulvestrant is a pure ER antagonist (98,99) and decreases ER expression (100-102).

Despite the development of SERDs and AIs, resistance limits the long-term efficacy of these drugs (103,104). For example, while letrozole significantly increased median progression-free survival (PFS) by 3.4 months compared to tamoxifen in the first-line treatment of ER+ advanced breast cancer patients, there was no difference in overall survival after 2 years of therapy (105,106). Furthermore, for patients who have relapsed on prior AI treatment, fulvestrant only has a clinical benefit rate (partial response (PR) + complete response (CR) + stable disease (SD) >24 weeks) of 35% (107). Cultured to resistance cell models coupled with genetic screens and sequencing of metastatic tumors have revealed several convergent mechanisms of resistance to endocrine therapy. Three such mechanisms are highlighted below: alterations in the gene encoding ERα (*ESR1*), receptor tyrosine kinase (RTK) signaling through the PI3K/AKT pathway and activation of cell cycle genes.

ESR1 *alterations in advanced metastatic breast cancer*

In 1997, Zhang *et al.* combined single-strand conformation polymorphism analysis with DNA sequencing to search for *ESR1* mutations in metastatic breast cancer samples (108). Only one out of the thirty tumors studied harbored an activating Y537N missense mutation in the ER LBD. Unlike the wild-type ER, the Y537N mutant stimulated transcription from ERE-containing promoters even in the absence of estrogen. Subsequent whole genome and whole exome sequencing, however, revealed that *ESR1* mutations are quite rare in primary breast cancer; only 1-3% of treatment-naïve ER+ breast cancers harbor activating ER mutations (55,109).

In contrast, approximately 20% of metastatic ER+ breast cancers are *ESR1*-mutant (110-117). Numerous ERα point mutants and one *ESR1-YAP1* gene fusion have been identified (**Fig. 1.2A**). *ESR1* mutations are localized to the C-terminal LBD of the ER and

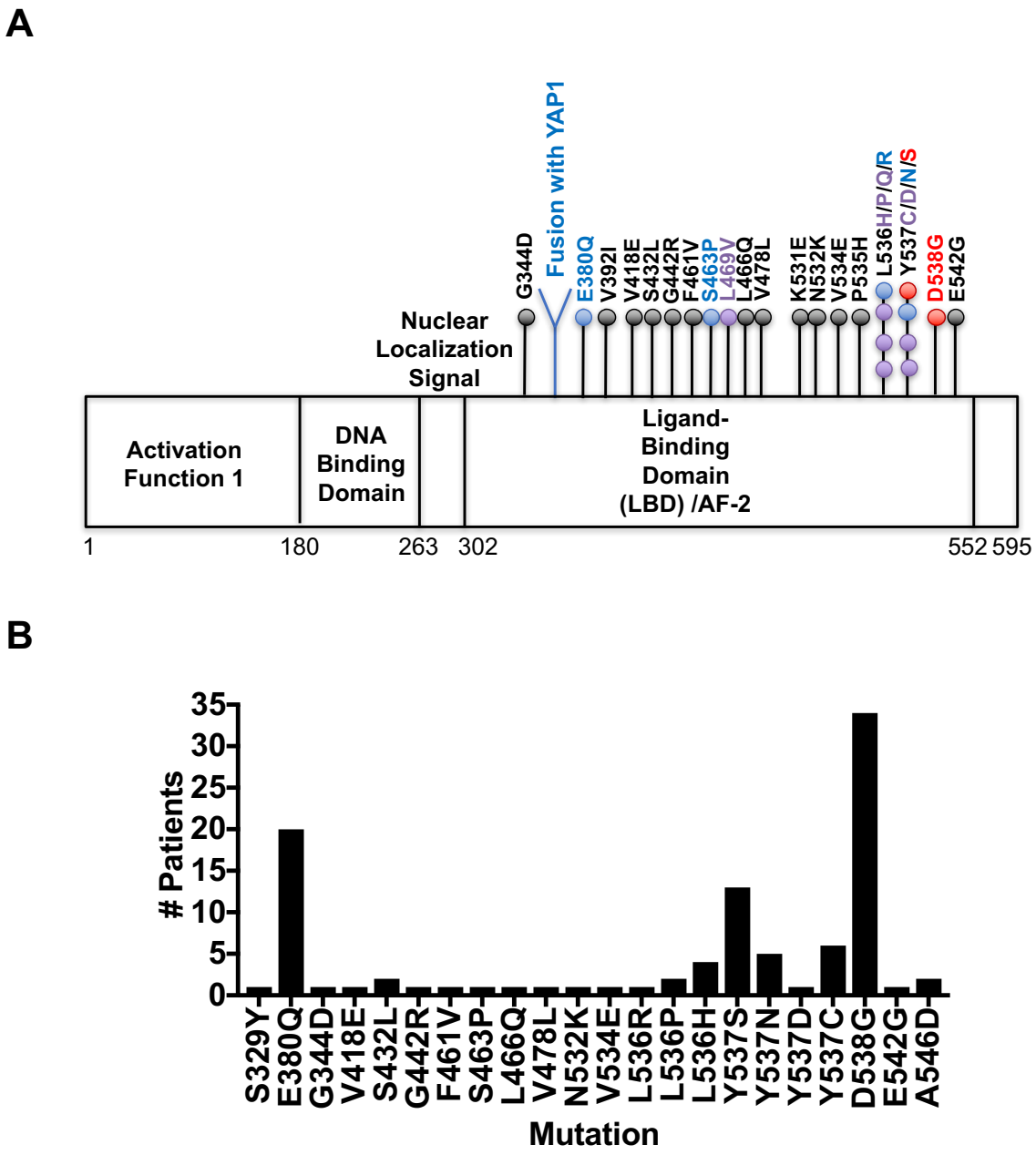

Figure 1.2. Functional annotation of *ESR1* alterations identified in advanced breast cancers (110-117). (A) Alterations that have been shown to stimulate ERE-reporter activity (purple), promote estrogen-independent growth *in vitro* (blue) and *in vivo* (red) are indicated. ER-YAP1 fusion includes the first 365 amino acids of ER and has only been shown to confer resistance to estrogen-deprivation *in vitro*. **(B)** Frequency distribution of LBD mutations in a cohort of 929 tumor biopsies (117). Total number of samples with detected mutation is indicated. Similar to figures by Segal *et al.* (114) and Ma *et al.* (103), but includes data from Toy *et al.* (117).

predominantly affect residues 380, 537 and 538 (**Fig. 1.2A-B**) (110-117). More recent analysis of 929 metastatic breast cancers confirmed that the three most common ER mutations are E380Q, Y537S and D538G (**Fig. 1.2B**) (117). Molecular dynamic simulations in the absence of ligand indicate that the Y537S and D538G variants alter the conformation of the ER and mimic the active agonist conformation (110).

Functionally, many of these mutants constitutively activate the ER (**Fig. 1.2A**); unlike wild-type ER, many LBD mutants stimulate expression of reporter genes attached to estrogen-responsive elements (EREs) even in the absence of ligand (110,112). Most importantly, variants such as Y537N, Y537S, S463P and D538G promote estrogen-independent growth of breast cancer cells *in vitro* (110-113,117) (**Fig. 1.2A**). Y537S and D538G mutations also enabled estrogen-independent growth of mouse xenografts (110). There are some differences in activity, however, among the LBD mutants. Although frequently detected, the E380Q mutation only modestly activates the ER (117,118). While the Y537S variant is a strong mediator of hormone-independent proliferation, cells expressing the Y537S mutant were reported to have poor basal growth compared to other ER mutants (113). Potent constitutive activation of the ER may cause some lethality in estrogen-replete normal growth media but is selected for under estrogen-deprived conditions (113).

Consistent with the ligand-independent activity of *ESR1* mutants observed in preclinical models, *ESR1* mutations are specifically associated with prior exposure to AI therapy in the metastatic setting (119). Analysis of circulating tumor DNA found no *ESR1* mutations in patients who only received tamoxifen therapy and there was no correlation between adjuvant AI treatment and the emergence of *ESR1* mutations (119). Furthermore, *ESR1* mutations predict resistance to aromatase inhibitor therapy (119). In contrast, *ESR1*-mutant breast cancer patients respond similarly to fulvestrant as patients with wild-type *ESR1* (118). Given the dependence of *ESR1*-mutant breast cancer cells on ligand-independent activity of the ER, ER degraders like fulvestrant inhibit the growth of mutant cells *in vitro*; the concentration of

fulvestrant needed for half-maximal inhibition of *ESR1*-mutant cells, however, is often 2-4 times higher than for cells with wild-type ER (112). Moreover, responses to fulvestrant may differ between *ESR1* mutants *in vivo* (117). While fulvestrant completely prevented the growth of mouse xenograft tumors that expressed either the E380Q or S463P mutant, fulvestrant only slowed the growth of Y537S-expressing tumors (117). As resistance to fulvestrant invariably develops, non-hormonal therapies are also needed to treat *ESR1*-mutant patients.

RTK signaling and AKT activation

Cross-talk between RTKs and the ER is another major driver of resistance to endocrine therapy (103,104). Expression and activation of numerous RTKs, such as members of the ERBB family (HER2 and EGFR), insulin-like growth factor 1 receptor (IGF1R) and fibroblast growth factor receptor 1 (FGFR1) render cells insensitive to anti-estrogens (120-127). Growth factor binding to cell surface RTKs induces dimerization, receptor autophosphorylation and activation (128). Although not well-understood, the ER can also interact with activated RTKs at the plasma membrane and promote proliferation in a nongenomic manner (129). Once phosphorylated, RTKs recruit adaptor proteins that activate downstream mitogen-activated protein kinase (MAPK) and phosphoinositide-3 kinase (PI3K) pathways to promote cell proliferation and survival (**Fig. 1.3**) (103,128).

Mechanistically, there are several ways in which MAPK and PI3K/AKT pathway activity drive endocrine resistance. Signaling through the RAF-MEK-ERK (MAPK) pathway promotes posttranslational modification and activation of the ER and its coregulators. For example, ERK induces estrogen-independent activation of the ER by phosphorylating serine 118 in the AF-1 domain (130). MAPK signaling can further induce transcription of ER-regulated genes by directly phosphorylating the ER coactivator AIB1 to recruit secondary coactivators such as p300 and CREB-binding protein (131). Several studies have also associated MAPK activity with

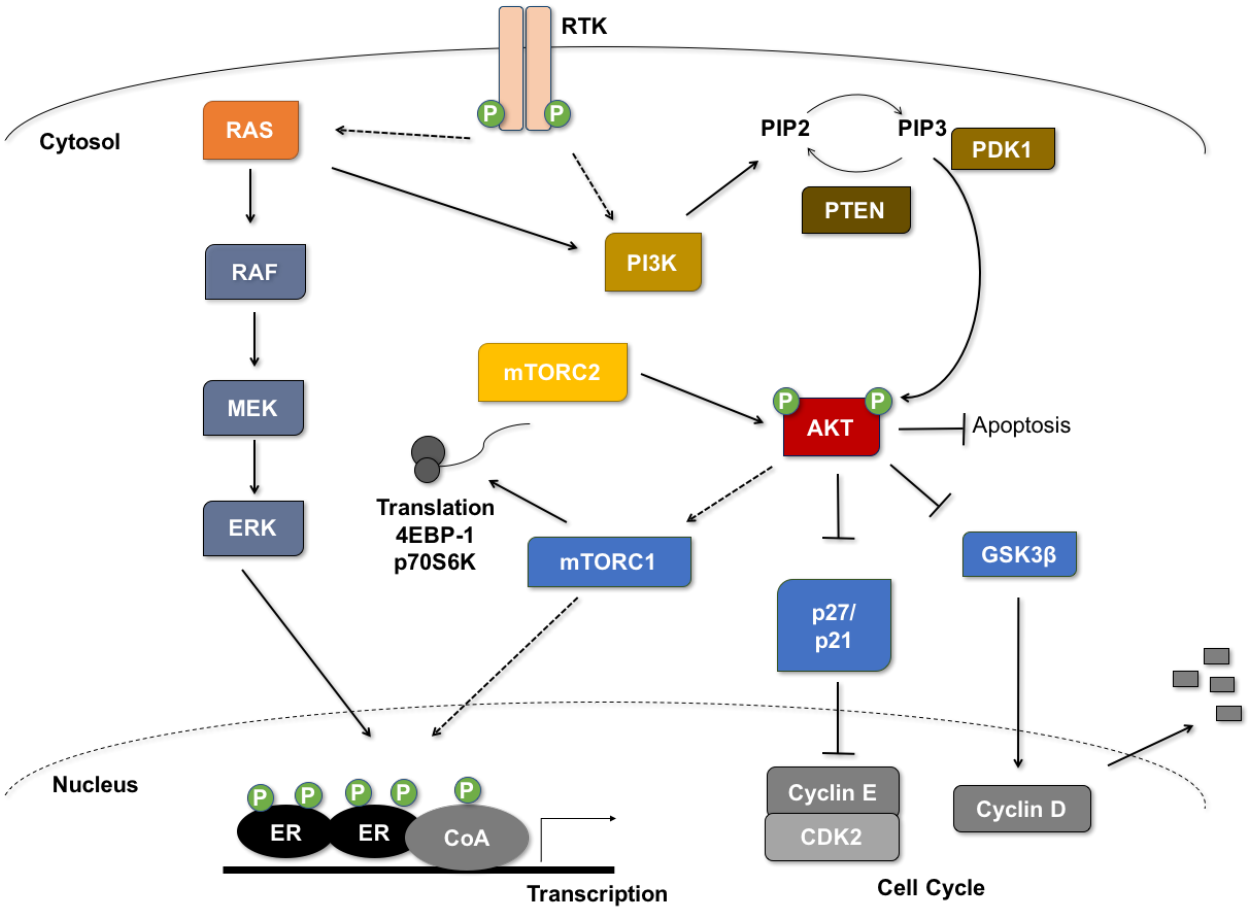

Figure 1.3. RTK and downstream MAPK and PI3K/AKT pathway signaling in endocrine resistance. Indirect signaling events are designated with dotted arrows. Based on figure from Ma et al.'s review (103). For clarity, only pathways discussed in this dissertation are highlighted. RTK signaling activates RAS GTPases and PI3Ks. RAS-initiated flux through the RAF-MEK-ERK pathway stimulates ERK's phosphorylation of ER and its coactivators (CoA), promoting expression of ER-target genes. Although not depicted, ER interacts with corepressors as well. PI3Ks are lipid kinases that convert phosphatidylinositide 4,5-bisphosphate (PIP2) to phosphatidylinositide (3,4,5)P3 (PIP3) (132). Phosphatase and tensin homolog (PTEN) counteracts PI3K activity by converting PIP3 into PIP2. PIP3 recruits PDK1 and AKT to the plasma membrane, where PDK1 can phosphorylate AKT on threonine 308. Full AKT activation requires mTOR complex 2 (mTORC2) phosphorylation on serine 473. AKT phosphorylates and inactivates the cell cycle inhibitors p21 and p27 and regulates cyclin D1 levels through GSK3β. Phosphorylation by AKT inhibits p21 and p27, activating CDK2 (133). GSK3β inactivation promotes cyclin D1 stability (134). AKT also activates mTORC1 by inhibiting TSC1/2 (135). mTORC1 stimulates protein synthesis and elongation by phosphorylating eukaryotic translation initiation factor 4E-binding protein 1 (4-EBP1) and p70 S6 kinase (p70S6K) (136). 4-EBP1 is a negative regulator of cap-dependent translation that is inactivated by mTORC1, while p70S6K promotes translation elongation. AKT signaling also promotes phosphorylation of the ER and its coregulators.

downregulation of ER expression and subsequent insensitivity to ER-directed therapy (137-139). Thus, flux through the MAPK signaling pathway modulates ER activity.

The PI3K pathway also operates downstream of RTKs and its oncogenic activity in breast cancer is well-documented (140,141). Mutations in the *PIK3CA* gene, which encodes the p110α subunit of class I PI3Ks, have been detected in over 30% of breast cancers and are associated with ER expression (142). *PIK3CA* hotspot mutations are located in the helical domain (e.g. E452K, E545K) and the catalytic domain (e.g. H1047R) (55,143). All three classes of PI3Ks (I, II and III) mediate signal transduction by phosphorylating lipids in the plasma membrane (144). Class I PI3Ks are heterodimers consisting of a p85 regulatory subunit and a p110 catalytic subunit and convert phosphatidylinositide 4,5-bisphosphate (PIP2) to phosphatidylinositide (3,4,5)P3 (PIP3). Phosphatase and tensin homolog (PTEN) counteracts PI3K activity by removing the phosphate from PIP3 to make PIP2. PIP3 recruits protein kinase B (AKT) to the plasma membrane, where PDK1 can phosphorylate AKT at threonine 308 in the kinase activation loop (145); mTORC2 phosphorylation at serine 473 fully activates AKT (146).

There are three isoforms of AKT (AKT1, AKT2 and AKT3). In breast cancer, high AKT1 protein expression is detected in 24% of tumors and AKT2 overexpression is present in about 4% (147). Approximately 3% of ER+ breast cancers harbor an activating mutation (E17K) mutation in the pleckstrin homology domain of AKT1 (148). Elevated AKT3 expression is more prevalent in ER negative tumors (147). Once phosphorylated, AKT acts on several substrates to stimulate cell cycle progression, translation initiation and prevent apoptosis (**Fig. 1.3**).

To drive S phase progression, AKT regulates G1/S cell cycle proteins, such as cyclin D1, p21 and p27. AKT stabilizes cyclin D1 by preventing GSK3β-mediated turnover of cyclin D1. AKT signaling prevents GSK3β from phosphorylating cyclin D1 at threonine 286, thereby inhibiting cyclin D1 degradation (134,149). Mutation of threonine 286 to alanine in cyclin D1 sufficiently prevents GSK3β phosphorylation (134). AKT also activates CDK2 by

phosphorylating and inactivating the cell cycle inhibitors p21 and p27 (133,150). Thus, AKT signaling can drive S phase progression by stabilizing cyclin D1 and activating CDK2.

The mammalian target of rapamycin (mTOR) is another key downstream effector of AKT (135). mTOR is a serine/threonine kinase that forms the catalytic subunit of two different multi-protein complexes: mTORC1 and mTORC2 (151). AKT specifically activates mTORC1 by inhibiting TSC1/2 (135). mTORC1 stimulates protein synthesis and elongation by phosphorylating eukaryotic translation initiation factor 4E-binding protein 1 (4-EBP1) and p70 S6 kinase (p70S6K) (136). 4-EBP1 is a negative regulator of cap-dependent translation that is inactivated by mTORC1, while p70S6K promotes translation. mTORC1 activity also regulates S phase progression. Inhibition of mTORC1 activity with the small molecule rapamycin induces a G1 cell cycle arrest (152). Mechanistically, rapamycin treatment decreases cyclin D1 protein levels in NIH3T3 cells and ER+ breast cancer cells (153,154). In HER2-driven mouse mammary tumors, mTOR inhibition with everolimus disrupts the formation of cyclin D1 and CDK2 complexes (155). Therefore, AKT signaling can also promote S phase progression through mTOR.

Long-term estrogen-deprived (LTED) cell culture models have been invaluable in interrogating the role of AKT in the development of hormone-independent breast cancer. Miller *et al.* chronically cultured ER+ breast cancer cell lines in estrogen-deprived (charcoal-stripped serum, CSS) media until resistant populations emerged (156). Reverse phase protein array analysis indicated that ER+ LTED cells hyperactivate the PI3K/AKT pathway compared to parental sensitive cells. Phosphorylation of AKT (threonine 308 and serine 473) and of the mTORC1 target p70S6K was significantly higher in LTED cells. Furthermore, estrogen-independent growth of LTED cells required PI3K/AKT signaling. BEZ235, a small molecule inhibitor of both PI3K and mTOR (157), prevented hormone-independent growth of LTED cells. Combined fulvestrant and BKM120 (pan-PI3K inhibitor) treatment also induced apoptosis in ER+ LTED MCF7 cells (158). Consistent with these data, PTEN loss also upregulates

PI3K/AKT activity and drives resistance to endocrine therapy (159). Similarly, myristolated-AKT, which is rendered constitutively active, also drives resistance to tamoxifen, fulvestrant and letrozole in an mTOR-dependent manner; rapamycin, a mTOR inhibitor, reduces AKT-mediated resistance (160). These data suggest that LTED cells are dependent on PI3K/AKT/mTOR signaling for estrogen-independent growth.

Clinical targeting of endocrine resistance

Clinically, many patients who have progressed on prior endocrine therapy derive clinical benefit from HER2 or mTOR inhibition (161-165). Durable responses to trastuzumab (antibody against HER2) and letrozole have been observed in patients with ER+ and HER2+ breast cancer (162). In a phase II study, the clinical benefit rate of combined trastuzumab and letrozole was 52% with a median duration of response of more than 20.6 months. Importantly, more than 80% of patients in this study received prior tamoxifen treatment, suggesting that anti-HER2 and estrogen deprivation therapy may be beneficial in the second-line setting. Trastuzumab and lapatinib (a small molecule HER2 inhibitor) are both approved for HER2+ breast cancers. In the BOLERO-2 study, the combination of everolimus (rapamycin derivative) and exemestane (a steroidal AI) more than doubled the PFS compared to exemestane alone (6.9 months vs. 2.8 months respectively) for patients who have progressed on a nonsteroidal AI (166). Similarly, nonsteroidal AI-resistant patients also benefit from co-treatment with everolimus and tamoxifen (167). RTK feedback activation of AKT, however, is a key of bypass mechanism to mTOR inhibition (168,169); combination therapy and inhibitors that hit multiple nodes of the PI3K/AKT pathway may mitigate resistance.

Despite the development of additional RTK and PI3K/AKT pathway inhibitors, tumor heterogeneity coupled with a lack of reliable biomarkers has limited the utility of these targeted agents for endocrine therapy-resistant patients (103,170). For example, gefitinib (an EGFR/HER2 inhibitor) reverses tamoxifen resistance in preclinical models (171) but the addition

of gefitinib did not improve PFS for breast cancer patients who have progressed on prior endocrine therapy. The clinical outcome was actually worse for patients given gefitinib and tamoxifen compared to tamoxifen alone (172). Similarly, the IGF-IR inhibitor (AMG 479) failed to improve PFS in patients who have progressed on prior endocrine therapy (173).

Clinical translation of PI3K pathway inhibitors has also been plagued by limited tumor regression and resistance. While PI3K inhibition preferentially suppress growth of *PIK3CA*-mutant cells (174,175), early clinical data indicated that only a few patients benefit from single agent treatment and responses are not durable (176). A recent phase Ib clinical trial evaluated the PI3K alpha isoform-specific inhibitor, BYL719, in combination with letrozole in patients who have progressed on prior endocrine therapy (177). Partial responses were observed in 19% of patients with a clinical benefit rate of 35%; amplification of *FGFR1/2* and mutations in *KRAS and TP53* were found in resistant patients. Preclinical characterization of the PI3K alpha isoform-specific inhibitor, BYL719, have also revealed several mechanisms of resistance to BYL719 in ER+ breast cancer including: PIM1 overexpression (178), CDK4/6 activation (179), cross-talk with the ER (180), signaling through PI3K p110β (181), PTEN loss (182) and mTORC1 activation (183). Consistent with canonical PI3K/AKT signaling, downstream AKT activation also confers resistance to BYL719 as well as pan-PI3K inhibitors (178).

The AKT1/2/3 inhibitor MK-2206 has also entered clinical trials (184,185). In phase I studies, 42% of ER+ breast cancer patients benefited from combined MK-2206 and endocrine therapy (anastrozole and/or fulvestrant) treatment. As anticipated, *PIK3CA* mutation status did not correlate with response to MK-2206. MK-2206 in combination with endocrine therapy mainly stabilized tumors rather than inducing apoptosis (185). Based on the LTED models described above, Jansen *et al.* postulate that MK-2206 may have greater efficacy in the setting of endocrine-resistance ER+ breast cancer with PI3K pathway activation (186). Combination therapy and patient stratification will likely be required to improve patient response to PI3K/AKT inhibitors.

Cell cycle activation

Functional genetic screens have enabled unbiased characterization of resistance to tamoxifen and estrogen deprivation (187-194). Kinome-wide siRNA screening identified CDK4 as a key vulnerability in the estrogen-independent growth of LTED cells. Mechanistically, Miller *et al.* found that LTED MCF7 and HCC-1428 cells retain a functional ER that signals through the CDK4/RB/E2F pathway to enable hormone-independent growth. Under estrogen-deprived conditions, fulvestrant-mediated destabilization of ER results in downregulation of two E2F family members (E2F1 and E2F2) that bind RB and in reduced expression of many E2F target genes. Similarly, treatment of estrogen-deprived MCF7 breast cancer xenografts with fulvestrant lowers E2F1 and E2F2 protein levels. Since estrogen has previously been shown to stimulate E2F1 expression (195), ER likely regulates E2F expression (194). Notably, these LTED cells are also sensitive to the small molecule CDK4/6 inhibitor, PD 0332991. Thus, in the absence of ligand, ER can promote E2F1 and E2F2 expression, potentially explaining the dependency of LTED on CDK4.

Since ER-directed therapies arrest sensitive cells in G1 (196), numerous studies have similarly implicated aberrant cell cycle activation in endocrine resistance (193). Whereas antiestrogen treatment downregulates cyclin D1 levels in sensitive cells (197), cyclin D1 overexpression drives S phase progression and resistance to fulvestrant *in vitro* (198,199). Cyclin D1 can also function as an ER coactivator and drive hormone-independent transcription of ER target genes (84,85). Cyclin D1-CDK4/6 complexes phosphorylate RB, which helps activate CDK2 by upregulating cyclin E2 and sequestering negative regulators of CDK2, such as p21 (198,200). Knockdown of p21 and p27 similarly activates CDK2 and renders cells insensitive to tamoxifen, fulvestrant or estrogen depletion (201). Since CDK4/6 and CDK2 activity ultimately impinges on RB, RB loss also bypasses cell cycle arrest mediated by fulvestrant or estrogen deprivation (202). Furthermore, high Ki67 staining, a marker of proliferation, after short-term anastrozole and/or tamoxifen treatment effectively predicts

resistance to endocrine therapy (203). Thus, cell cycle deregulation is a hallmark of endocrine resistance.

CDK4/6 inhibitors in ER+ breast cancer

Given the intricate link between the ER, cell cycle and the dependency of breast cancers on CDK4 described above, the recent development of highly specific CDK4/6 inhibitors is a breakthrough in treatment for patients with advanced ER+ breast cancer. Previous generations of cell cycle inhibitors promiscuously targeted multiple CDKs and faltered in the clinic due to toxicity (204). Third generation cell cycle inhibitors, such as palbociclib (PD 0332991), abemaciclib (LY2835219) and ribociclib (LEE011) are ATP-competitive and highly selective for CDK4/6 (5,7,8). As discussed below, preclinical characterization of CDK4/6 inhibitors has led to a new standard of care in ER+ breast cancer. Palbociclib in combination with endocrine therapy has been FDA-approved for metastatic ER+ breast cancer in the first- and second-line settings.

Preclinical data

In preclinical models, palbociclib, abemaciclib and ribociclib inhibit CDK4/6 at nanomolar concentrations and arrest cells in G1 by decreasing RB phosphorylation at serine 780 and 807/811 (6-8,205-208). Structurally, palbociclib is a pyridopyrimidine derivative with selectivity for CDK4 and CDK6 (**Fig. 1.4 and Table 1.1**); among the 36 kinases profiled, CDK4 and CDK6 were the only kinases that palbociclib inhibited in the nanomolar range (6). Ribociclib is a pyrrolo-pyrimidine derivative and has the highest CDK4/6 selectivity among the three inhibitors (8). In contrast, abemaciclib is the most structurally distinct CDK4/6 inhibitor and was optimized from a 2-Anilino-2,4-Pyrimidine-[5-Benzimidazole] scaffold (7). Notably, abemaciclib has nearly seven times higher affinity for CDK4 than CDK6 (209). Abemaciclib is also uniquely able to

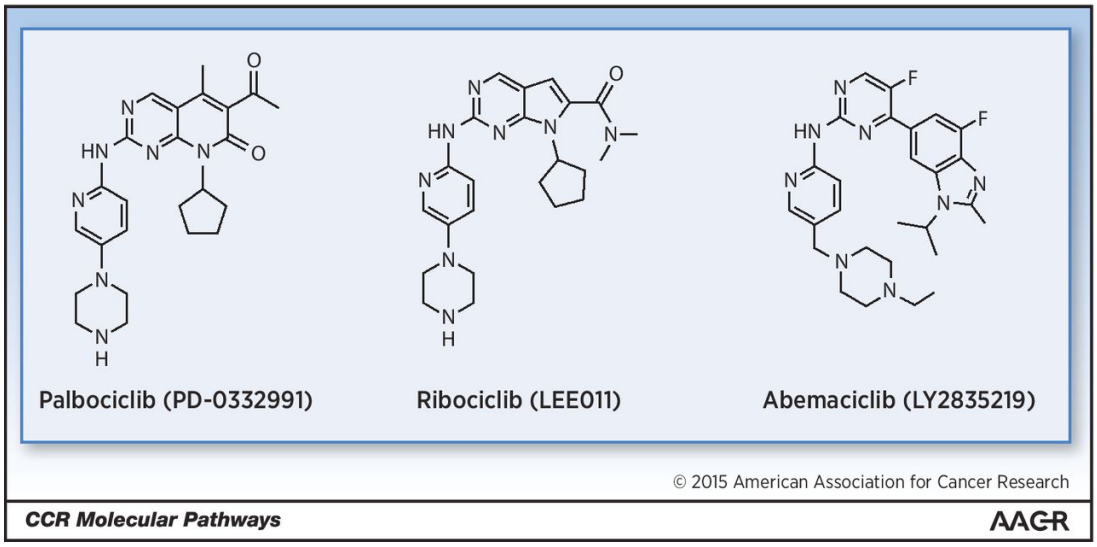

Figure 1.4. Chemical structures of CDK4/6 inhibitors. Figure from VanArsdale *et al.* (210).

Table 1.1. Kinase inhibition by CDK4/6 inhibitors. The concentration needed for half of the maximum inhibition (IC_{50}) of each kinase is indicated. Modified from O'Leary *et al.* to include non-CDKs (7,208).

Kinase	Palbociclib	Ribociclib	Abemaciclib
CDK4	9-11 nM	10nM	2nM
CDK6	15nM	39nM	5nM
CDK1	>10 μM	>100 μM	>1 μM
CDK2	>10 μM	>50 μM	>500nM
CDK5	>10 μM	ND	ND
CDK7	ND	ND	300nM
CDK9	ND	ND	57nM
DYRK1A	2 μM	ND	ND
PIM1	ND	ND	50nM
PIM2	ND	ND	3.4μM
DYRK2	ND	ND	61nM

cross the blood-brain-barrier (211). In addition to targeting CDK4 and CDK6, abemaciclib is active at micromolar concentrations against CDK2, CDK7, CDK9 and PIM1/2 (**Table 1.1**). CDK7 and CDK9 are transcriptional CDKs that phosphorylate the C-terminal domain of RNA polymerase II to enhance processivity (212,213). In particular, inhibitors that target CDK9, such as flavopiridol, may decrease expression of the anti-apoptotic protein myeloid cell leukemia sequence-1 (MCL-1) and are clinically active in chronic lymphocytic leukemia (214-216). We have previously shown that PIM kinases can drive resistance to BYL719 by re-activating AKT target proteins (178). As discussed below, abemaciclib's off-target activity may be clinically relevant.

RB proficiency and ER positivity are currently the best predictors of sensitivity to CDK4/6 inhibition in breast cancer (4,217-219). As RB is the main target of CDK4/6, inhibitor-mediated G1 cell cycle arrest requires a functional RB. Notably, RB is intact in nearly 90% of primary ER+ breast cancers (55). In Finn *et al.*'s characterization of 47 breast cancer cell lines, ER+ luminal cells were the most responsive to palbociclib (4). Furthermore, microarray analysis of breast cancer cell lines correlated sensitivity with high RB and cyclin D1 expression and low levels of p16. Similarly, RB expression and low p16 expression correlates with palbociclib sensitivity in glioblastoma (220,221), ovarian (221) and renal carcinoma cells (222).

Although CDK4/6 inhibitor monotherapy induced tumor regression in a few *in vivo* tumor models, these inhibitors are generally cytostatic and responses are short-lived. For example, despite an initial decrease in tumor burden in the first 10-20 days of palbociclib treatment, colo-205 colorectal cell xenografts rapidly progressed on therapy (6). Primary CDK4-amplified liposarcoma xenografts had mixed responses to ribociclib treatment; tumor growth was durably reduced in one model, while ribociclib treatment was cytostatic for two other xenografts (207). Ribociclib only delayed tumor progression of neuroblastoma cells *in vivo (206).* Abemaciclib

also suppressed growth of colo-205 colorectal cells and acute myeloid leukemia cells *in vivo* without tumor regression; tumors subsequently relapsed after twenty days of treatment (7).

Given the short-lived responses with single agent treatment, numerous groups have investigated combinatorial treatments with CDK4/6 inhibitors in breast cancer. Palbociclib synergizes with tamoxifen to reduce growth of ER+ breast cancer cells (4). Consistent with these observations, letrozole and palbociclib durably suppressed the growth of ER+ breast cancer patient-derived xenografts better than either single agent (223). Mechanistically, combined estrogen deprivation and CDK4/6 inhibition significantly reduced RB phosphorylation and E2F1 expression. Furthermore, co-treatment lowered the levels of forkhead box M1 (FOXM1) transcription factor compared to each treatment alone (223). FOXM1 is a CDK4/6 target gene whose activation promotes S phase progression. Downregulation of FOXM1 expression with combined letrozole and palbociclib treatment results in senescence (224). Abemaciclib also synergized with anti-HER2 to inhibit the proliferation of trastuzumab-resistant cells; when combined with HER2 inhibition, abemaciclib enhanced suppression of mTORC1 targets in HER2+ cells (225). As previously mentioned, CDK4/6 activity confers resistance to PI3K inhibition (179). Ribociclib re-sensitizes BYL719-refractory breast cancer cells to PI3K inhibition (179).

Combination therapy with CDK4/6 inhibitors has also been investigated in other tumor types. Dual CDK4/6 and MEK inhibition was required for tumor regression in mouse models of *NRAS*-mutant melanoma (226). Similarly, combined MEK and CDK4/6 inhibition was superior to each single agent in suppressing the growth of patient-derived *KRAS*-mutant colorectal cancer xenografts (227). Whereas palbociclib alone induced a G1 cell cycle arrest but not apoptosis in multiple myeloma cells, co-treatment with either dexamethasone (corticosteroid) (228) or bortezomib (proteasomal inhibitor) effectively kills cells (229). Abemaciclib also enhanced the antitumor activity of the chemotherapeutic agent temozolomide in a xenograft

model of intracranial glioblastoma (211). Thus, CDK4/6 inhibitors are most efficacious when used in combination.

Clinical trials with CDK4/6 inhibitors in breast cancer

Palbociclib is the most clinically advanced CDK4/6 inhibitor in ER+ breast cancer. As a single agent, the clinical benefit rate (complete response (CR) + partial response (PR) + stable disease (SD) $\geq$ 6 months) for palbociclib was 21% in ER+/HER2-/RB+ breast cancer patients (230). This phase II study also found that palbociclib was more efficacious in patients who had previously been treated with more than two lines of endocrine therapy. The PALOMA-1 phase II randomized study enrolled ER+, HER2- metastatic breast cancer patients who had no prior systemic treatment for advanced disease (231). Patients received either 2.5mg letrozole daily or 2.5mg letrozole continuous daily plus 125mg palbociclib. Palbociclib was given on a 3-weeks-on 1-week-off schedule. PALOMA-1 was originally designed to include two cohorts of patients; patients with ER+, HER2- negative breast cancer were admitted in cohort 1, while in cohort 2, only ER+, HER2- tumors with cyclin D1 gene (*CCND1*) amplification and/or p16 gene (*CDKN2A*) loss were enrolled. When an unplanned interim analysis of cohort 1 revealed that these biomarkers were not prognostic, the investigators stopped enrolling patients in cohort 2 and combined the results from both cohorts in their final analysis. In PALOMA-1, ER+ breast cancer patients with advanced disease had a 20.2 month increase in median progression-free survival (PFS) when given palbociclib in combination with letrozole compared to 10.2 months with letrozole alone (231). 42% of patients showed a PR to the combination and 1% had a CR for a total objective response rate of 43%. The clinical benefit rate was 81% for the combination compared to 58% on letrozole alone. Neutropenia was the predominant palbociclib-associated toxicity; 54% of patients had grade 3-4 neutropenia in the palbociclib group compared to letrozole monotherapy. Based on the significant improvement in PFS, palbociclib was approved

in February 2015 for first-line treatment of ER+, HER2- metastatic breast cancer in combination with letrozole (232).

In PALOMA-1, patients receiving fulvestrant and palbociclib had greater instances of neutropenia (62% grade 3 or 4 neutropenia on the combination vs. 0.6% for fulvestrant alone). Combination treatment was also associated with higher rates of leukopenia (25.2 vs. 0.6%). For patients who progressed on prior endocrine therapy, fulvestrant and palboiclcib significantly increased PFS (9.2 months on the combination vs. 3.8 months on fulvestrant alone) in PALOMA-3, a phase III clinical trial (233). In PALOMA-3, patients received 125mg palbociclib (for 3 weeks followed by a 1 week holiday) and fulvestrant (500mg biweekly for the first three treatments and then every 28 days) or fulvestrant plus placebo. Retrospective analysis of PALOMA-3 indicated that *PIK3CA* mutations do not stratify patient response to fulvestrant and palbociclib (234). In February 2016, palbociclib in combination with fulvestrant received FDA approval for the treatment of patients with advanced ER+/HER2- breast cancer who progressed on prior endocrine therapy (235). Additional clinical trials combining palbociclib with drugs targeting HER2, PI3K and mTOR are ongoing in breast cancer (**Table 1.2).**

Ribociclib's clinical activity in breast cancer mirrors that of palbociclib. A phase I clinical trial evaluated ribociclib monotherapy in RB+ cancer patients or patients with a tumor type known to have CDK4/6 pathway activation (236). 2.3% (3/132) of patients showed a PR and 14% of patients had SD for more than 6 months. In this study, only one of the twenty breast cancer patients had a PR; the patient had ER+, *CCND1*-amplified and *PIK3CA*-mutant breast cancer. Due to toxicity observed with continuous dosing, the investigators established the following dosing schedule: 600mg ribociclib daily for 3-weeks-on and 1-week-off (236). Ribociclib in combination with letrozole was also investigated in a phase III clinical trial as first-line treatment for postmenopausal women with ER+, HER2- breast cancer (237). Patients either received 600mg ribociclib (daily 3-weeks-on, 1-week-off) and 2.5mg letrozole daily or continuous letrozole and placebo. The median PFS at 18 months was 63% for patients treated

Table 1.2. Palbociclib clinical trials in breast cancer.

ClinicalTrial.gov Identifier	Therapy	Setting and Biomarker	Phase	Target
NCT01037790	Palbociclib	HER2+/-, ER+/- Advanced breast cancer	II	CDK4/6
	Palbociclib	any alteration in G1/S checkpoint; RB positive	II	CDK4/6
NCT01684215	Palbociclib	Advanced ER+, HER2- Japanese women	I/II	CDK4/6
NCT02549430	Palbociclib	Advanced ER+ HER2-	II	CDK4/6
NCT00721409	Palbociclib + Letrozole	Advanced ER+, HER2-	I/II	CDK4/6 + aromatase
NCT01684215	Palbociclib + Letrozole	Advanced ER+, HER2- Japanese women	I/II	CDK4/6 + aromatase
NCT01709370	Palbociclib + Letrozole	Neoadjuvant ER+, HER2-	II	CDK4/6 + aromatase
NCT01723774	Palbociclib + Anastrozole + Goserelin	Neoadjuvant ER+, HER2- Stage 2/3	II	CDK4/6 + aromatase + ovary
NCT01740427	Palbociclib + Letrozole (Paloma-2)	Advanced ER+, HER2-	III	CDK4/6 + Aromatase
NCT01864746	Palbociclib + endocrine therapy (PENELOPE-B)	ER+, HER2+ relapsed on chemotherapy + surgery	III	CDK4/6 + hormonal therapy
NCT02040857	Palbociclib + Tamoxifen or AI	Advanced ER+, HER2-	II	CDK4/6 + ER/aromatase
NCT02296801	Palbociclib + Letrozole	Primary ER+, HER2- neoadjuvant	II	CDK4/6 + aromatase
NCT02297438	Palbociclib + Letrozole (PALOMA-4)	Advanced ER+, HER2- Asian women	III	CDK4/6 + aromatase
NCT02400567	Palbociclib + Letrozole vs. chemotherapy (NeoPAL)	Neoadjuvant ER+, HER2- Stage II-IIIA PAM 50 ROR-defined Low or Intermediate Risk Luminal	II	CDK4/6 + aromatase
NCT02491983	Palbociclib + Fulvestrant or Letrozole	Advanced, ER+, HER2-	II	CDK4/6 + ER or aromatase
NCT02499146	Palbociclib + Letrozole	Advanced ER+, HER2- Chinese women	I	CDK4/6 + aromatase
NCT02549430	Palbociclib + Anastrozole/ Letrozole/ Exemestane/ Fulvestrant (TREnd)	Advanced ER+, HER2-	II	CDK4/6 + aromatase/ER
NCT02592083	Tamoxifen/aromatase inhibitor/aromatase inhibitor + Goserelin + Palbociclib (PREDIX LumA)	Low ki67 early stage ER+, HER2- after endocrine therapy	II	ER/aromatase/aromatase +ovary + CDK4/6
NCT02592746	Palbociclib, Lupron + Exemestane	Advanced ER+, HER2+	II	CDK4/6, ovary + aromatase
NCT02668666	Palbociclib + Tamoxifen	Advanced ER+, HER2-	II	CDK4/6 + ER
NCT02917005	Palbociclib, Exemestane + Goserelin (FATIMA)	Advanced ER+, HER2+	II	CDK4/6, aromatase + ovary
NCT02536742	Palbociclib + Fulvestrant	Advanced ER+, HER2-	II	CDK4/6 + ER
NCT02448420	Palbociclib + Trastuzumab + /- Letrozole	Advanced HER2+	II	CDK4/6 + HER2 + /- aromatase
NCT02530424	Palbociclib + Trastuzumab + Pertuzumab + Fulvestrant	Neoadjuvant ER+, HER2+	II	CDK4/6 + HER2 + HER2 + ER
NCT02907918	Palbociclib, Letrozole + Trastuzumab (PALTAN)+Goserelin	Neoadjuvant ER+, HER2-	II	CDK4/6, aromatase + HER2
NCT02774681	Palbociclib + Trastuzumab if HER2+	Advanced HER2+ with brain metastasis	II	CDK4/6 + HER2
NCT03054363	Palbociclib + Tucantinib + Letrozole	Advanced ER+, HER2+	I/II	CDK4/6 + HER2 + aromatase
NCT02389842	Palbociclib + Taselisib / Pictilisib (PIPA)	Advanced ER+, HER2-	I	CDK4/6 + PI3K
NCT02389842	Palbociclib, Fulvestrant + Taselisib / Pictilisib (PIPA)	Advanced ER+, HER2- + PIK3CA mutant	I	CDK4/6, ER + PI3K
NCT02599714	Palbociclib + Fulvestrant + AZD2014	Advanced ER+, HER2-	I/II	CDK4/6 + ER + mTORC1/2
NCT02626507	Palbociclib + Fulvestrant + Gedatolisib +Zoladex	Neoadjuvant Advanced ER+, HER2-	I	CDK4/6 + ER + PI3K/MTOR + ovary
NCT02684032	Palbociclib + Gedatolisib + Letrozole/Fulvestrant	Advanced ER+, HER2-	IB	CDK4/6 + PI3K/mTOR + aromatase/ER
NCT02603679	Palbociclib + Tamoxifen followed by Paclitaxel (Predix LumB)	Neoadjuvant ER+, HER2-	II	CDK4/6 followed by chemotherapy
	Palbociclib + AI followed by Paclitaxel	Neoadjuvant ER+, HER2-	II	CDK4/6 + aromatase followed by chemotherapy
	Palbociclib + Goserelin + aromatase inhibitor followed by Paclitaxel	Neoadjuvant ER+, HER2-	II	CDK4/6 + ovary + aromatase followed by chemotherapy
NCT01320592	Palbociclib + Paclitaxel	Advanced RB-expressing	I	CDK4/6 + chemotherapy
NCT02605486	Palbociclib + Bicalutamide	Triple negative androgen receptor positive breast cancer	I/II	CDK4/6 + androgen receptor
NCT02624973	Palbociclib + treatment depending on sequencing (PETREMAC)	Treatment based on ER, HER2, p53 status	II	CDK4/6 + various

Table 1.3. Ribociclib clinical trials in breast cancer.

ClinicalTrial.gov Identifier	Therapy	Setting and Biomarker	Phase	Target
NCT02187783	Ribociclib (SIGNATURE)	Advanced ER+, HER2- pretreated; CDK4 amp/mutation, CDK6 amp/ mutation, CCND1 amp, CCND3 amp, or CDKN2A	II	CDK4/6
NCT02632045	Ribociclib + Fulvestrant	Advanced ER+, HER2- relapsed on CDK4/6 + AI	II	CDK4/6 + ER
NCT02422615	Ribociclib + Fulvestrant (MONALEESA-3)	Advanced ER+, HER2- men and women	III	CDK4/6 + ER
NCT01958021	Ribociclib + Letrozole (MONALEESA-2)	Advanced ER+, HER2- first line	III	CDK4/6 + aromatase
NCT02941926	Ribociclib, Letrozole (+ Goserelin if needed) COMPLEEMENT-1	Advanced ER+, HER2- women + men	III	CDK4/6, aromatase (+ ovary)
NCT02586675	Ribociclib + Tamoxifen + Goserelin	Advanced ER+, HER2-	I	CDK4/6 + ER + ovary
NCT02734615	Ribociclib + LSZ102	Advanced ER+, HER2-	I	CDK4/6 + ER
NCT02333370	Ribociclib + Hormonal therapy + Goserelin	Advanced ER+, HER2-	I	CDK4/6 + aromatase/ER
NCT02712723	Ribociclib + Letrozole (FELINE)	Neoadjuvant ER+, HER2-	II	CDK4/6 + aromatase
NCT02278120	Ribociclib, Tamoxifen + Goserelin/AI+Goserelin MONALEESA-7	Advanced ER+, HER2-	III	CDK4/6, ER + ovary/aromatase+ovary
NCT02154776	Ribociclib, Buparlisib + Letrozole (LeeBLet)	Advanced ER+, HER2-	I	CDK4/6, pan-PI3K + aromatase
NCT01872260	Ribociclib, Letrozole + Alpelisib	Advanced ER+, HER2-	I	CDK4/6, aromatase + PI3Kα
NCT02088684	Ribociclib, Fulvestrant + Alpelisib/Buparlisib	Advanced ER+, HER2-	I/II	CDK4/6, ER + PI3Kα/pan-PI3K
NCT01857193	Ribociclib, Everolimus + Exemestane	Advanced ER+, HER2-	I	CDK4/6, MTOR + aromatase
NCT02732119	Ribociclib, Everolimus + Exemestane (TRINITI-1)	Advanced ER+HER2-	I/II	CDK4/6, MTOR + aromatase
NCT02657343	Ribociclib + T-DM1/Trastuzumab	Advanced HER2+	Ib/II	CDK4/6 + HER2
NCT02754011	Ribociclib + Capecitabine (GEP14-LEECAP)	HER2- Previously Treated With Anthracyclines and Taxanes	I	CDK4/6 + chemotherapy
NCT02599363	Ribociclib + Paclitaxel	Advanced RB+	I	CDK4/6 + chemotherapy
NCT03056755	Alpelisib + Fulvestrant/Letrozole (BYLIEVE)	Advanced ER+, HER2- PIK3CA mutant relapsed on CDK4/6i + AI/Fulvestrant	II	PI3Kα + ER/aromatase

Table 1.4. Abemaciclib clinical trials in breast cancer.

ClinicalTrial.gov Identifier	Therapy	Setting and Biomarker	Phase	Target
NCT02831530	Abemaciclib (ABC-POP)	Early stage neoadjuvant HR+ HER2+/-	II	CDK4/6
NCT02102490	Abemaciclib (MONARCH 1)	Advanced HR+, HER2- previously treated	II	CDK4/6
NCT02308020	Abemaciclib	Advanced HR+ breast cancer with brain metastasis	II	CDK4/6
NCT02246621	Abemaciclib + Letrozole/Anastrozole (MONARCH 3)	Advanced HR+, HER2-	III	CDK4/6 + aromatase
NCT02246621	Abemaciclib + Letrozole/Anastrozole (MONARCH 3)	Advanced HR+, HER2-	III	CDK4/6 + aromatase
NCT02107703	Abemaciclib + Fulvestrant	Advanced HR+, HER2-	III	CDK4/6 + ER
NCT02747004	Abemaciclib + Tamoxifen + loperamide (nextMONARCH 1)	Advanced HR+, HER2- previously treated	II	CDK4/6 + ER + diarrhea
NCT02763566	Abemaciclib + AI (Letrozole/Anastrozole)	Advanced HR+, HER2-	III	CDK4/6 + aromatase
	Abemaciclib + Fulvestrant	Advanced HR+, HER2-	III	CDK4/6 + ER + diarrhea
NCT02441946	Abemaciclib + Loperamide + Anastrozole	Advanced HR+, HER2-	II	CDK4/6 + diarrhea + aromatase
NCT02246621	Abemaciclib + Letrozole/Anastrozole (MONARCH 3)	Advanced HR+, HER2-	III	CDK4/6 + aromatase
NCT02675231	Abemaciclib + Trastuzumab + Fulvestrant	Advanced HR+, HER2+ previously treated with two anti-HER2 therapies	II	CDK4/6 + HER2 + ER
	Abemaciclib + Trastuzumab	Advanced HR+, HER2+ previously treated with two anti-HER2 therapies	II	CDK4/6 + HER2
NCT02057133	Abemaciclib + various AI/PI3K pathway inhibitors/SERD	Advanced HR+, HER2-	IB	CDK4/6 + various
NCT02779751	Abemaciclib + pembrolizumab	Advanced HR+, HER2-	I	CDK4/6 + PD-1

with the combination compared to 42.2% of patients on letrozole alone. The overall response rate (complete response and partial response) was 40.7% for patients treated with ribociclib and letrozole compared to 27.5% for patients receiving letrozole and placebo. As with palbociclib treatment, ribociclib-associated toxicity included neutropenia, nausea and fatigue. On March 13, 2017, the FDA approved ribociclib for front-line treatment of ER+, HER2- breast cancer patients in combination with aromatase inhibition.

Triple combination therapy with ribociclib, letrozole/fulvestrant and PI3K pathway inhibition is also being investigated in ER+, HER2- patients (**Table 1.3**). In preclinical models, BYL719 (alpelisib, alpha-specific PI3K inhibitor) or BKM120 (buparlisib, pan-PI3K inhibitor) enhanced the sensitivity of ER+ breast cancer mouse xenografts to ribociclib and hormonal therapy (238). No toxicity was observed with the triplet. There is also a phase Ib/II clinical trial evaluating ribociclib, exemestane and everolimus in a cohort of heavily pre-treated ER+, HER2- metastatic breast cancer patients (239). Many of the patients had progressed on CDK4/6 inhibitors or PI3K/AKT/mTOR inhibitors prior to joining the study. At the interim analysis in March 2015, 1 of the 55 evaluated patients had a CR, 2 with a confirmed PR and 26 with stable disease. While not statistically significant, the investigators noted that patients with *CCND1*-amplified tumors tended to stay on treatment longer. These findings suggest that ribociclib triple combination therapy with anti-estrogen and PI3K/mTOR inhibitors is tolerated and clinically active in ER+, HER2- patients who have progressed on other therapies.

Unlike palbociclib and ribociclib, abemaciclib has potent single agent activity against ER+/HER2- metastatic breast cancers (240-244). Phase I abemaciclib dose escalation studies revealed that the predominant dose-limiting toxicity was fatigue and continuous dosing was well-tolerated. Abemaciclib also has high blood-brain barrier permeability (244). Furthermore, ER positivity was associated with breast cancer response to abemaciclib, while p53 DNA-binding domain mutations were more prevalent in resistant patients (244). In a phase II clinical trial (MONARCH-1), abemaciclib was assessed in 132 ER+/HER2- patients given 200mg

abemaciclib twice daily and continuously with no drug holiday (241). Patients enrolled in the study were heavily pretreated with a median of 3 lines of prior treatment including endocrine therapy and chemotherapy. Interim analysis at 8 months of treatment revealed that 17% of patients had a CR or PR on abemaciclib and the clinical benefit rate was 42.4% with 5.7 months PFS (241). Hematologic toxicity was less prevalent with abemaciclib treatment (26.9% Grade 3-4) compared to palbociclib monotherapy (51% Grade 3-4) (230). The main abemaciclib treatment-associated toxicities were diarrhea (19.7%) and fatigue (12.0%). Differences in the toxicity profile of abemaciclib compared to other CDK4/6 inhibitors may be attributed to its higher affinity for CDK4 over CDK6 and/or its off-target activity for other kinases (10). Knockout of CDK6 in mice specifically results in impaired thymic development and prevents Notch/AKT-mediated lymphomagenesis (245). Thus, abemaciclib's lower affinity for CDK6 may result in fewer instances of neutropenia. Abemaciclib is also being explored in combination with HER2-directed therapies and with immunotherapy in breast cancer (**Table 1.4**).

Resistance to CDK4/6 inhibition

Numerous studies suggest that cells can proliferate in the absence of CDK4/6. Although embryonic knockout of CDK4 and CDK6 causes severe anemia and is ultimately lethal, CDK4/CDK6 double knockout mouse embryonic fibroblasts become immortalized when cultured *in vitro* (246). Serum stimulation initiated S phase in CDK4/6-null cells, suggesting that cells can compensate for CDK4/6 loss. Furthermore, triple-negative RB-null breast cancer cells are intrinsically resistant to palbociclib treatment (4). As described below, various groups have also chronically cultured RB+ ER+ breast cancer cells in the presence of CDK4/6 inhibitors to generate models of acquired resistance (247-249).

Studies of resistance to CDK4/6 inhibitors have mainly focused on cell cycle genes. Intrinsic resistance is associated with loss of RB expression (4,218). RB loss has also been

observed in ER+ T47D cells with acquired resistance to palbociclib (248). Consistent with RB's mechanism of action, overexpression of E2F prevents palbociclib-induced cell cycle arrest in Hs578t cells (219). CDK6 amplification maintains RB phosphorylation and bypasses abemaciclib inhibition in ER+ breast cancer cells (249). CDK2 activation has also emerged as a key bypass mechanism for CDK4/6 inhibition. Exogenous expression of CDK2's cognate cyclins (E1 or E2) renders ER+ breast cancer cells insensitive to palbociclib treatment (250). Cyclin E1 amplification was detected in palbociclib-cultured to resistance ER+ MCF7 cells and CDK2 knockdown re-sensitizes resistant cells to CDK4/6 inhibition (248). Cyclin E1-CDK2 complexes phosphorylate RB on several residues (251) and CDK2 can interact with cyclin D1 to phosphorylate RB (34,248). Thus, RB inactivation, either by genetic loss or phosphorylation enables escape from CDK4/6 inhibition.

Given the prevalence of *PIK3CA* mutations (142) and PI3K pathway activation in endocrine resistance (156,159), CDK4/6 and PI3K combination therapy has also been investigated in ER+ breast cancer (179,247,248). Dual inhibition of CDK4/6 and PI3K is synergistic and prevents the development of resistance in ER+ breast cancer cells (247,248). Whereas single agent ribociclib only delayed tumor progression in an ER+ patient-derived breast cancer xenograft, co-treatment with BYL719 durably suppressed tumor growth (248). ER+ breast cancer cells that have acquired resistance to palbociclib, however, are less amenable to dual CDK4/6 and PI3K blockade; unlike parental cells, resistant cells continued to enter S phase despite combined GDC-0941 (pan-PI3K inhibitor) and palbociclib treatment (248). Thus, PI3K inhibition may not be efficacious in the setting of acquired resistance to CDK4/6 inhibition.

Precision medicine for metastatic ER+ breast cancer

Molecular subtyping of primary breast cancers has dramatically improved patient outcomes and fostered the development of targeted therapies. Since combined CDK4/6 inhibition and endocrine therapy is the new standard of care in metastatic ER+ breast cancer, we similarly must understand the underlying determinants of response and resistance. As summarized below, current use of CDK4/6 inhibitors is limited by a lack of clinical biomarkers and by a need to understand resistance to combination treatment.

Despite strong preclinical studies, clinical biomarkers of response are scarce. For example, loss of p16 expression or *CCND1* expression predicts sensitivity to palbociclib *in vitro* (4), but these genes were not prognostic in patients (230,252). Similarly, *PIK3CA* mutations have no prognostic value in determining patient outcomes with palbociclib or abemaciclib treatment (234,244). ER positivity is currently the best predictor of sensitivity to CDK4/6 inhibition, but many patients present with intrinsic resistance or relapse on therapy.

One potential limitation of current preclinical CDK4/6 inhibitor studies is the presence of estrogen in normal growth media. While many *in vitro* characterizations of resistance were conducted with estrogen-replete media, CDK4/6 inhibitors are only approved for use in combination with endocrine therapy (237,252,253). Thus, clinically relevant mechanisms must confer resistance to combination treatment. Furthermore, it is unclear whether resistance mechanisms may differ between CDK4/6 inhibitors.

To uncover markers of response and resistance to CDK4/6 inhibition, we leveraged sequencing data, large-scale screens and cultured to resistance cell models. The first project in this dissertation investigated whether *ESR1*-mutant breast cancer cells that are dependent on ER signaling require CDK4/6. Next, near genome-wide screens were conducted to identify mechanisms of resistance to CDK4/6 inhibition alone and in combination with estrogen deprivation. By coupling *in vitro* studies with clinical sequencing information, we seek to improve the efficacy and durability of CDK4/6 inhibitors in the treatment of metastatic ER+ breast cancer.

CHAPTER 2

ER-MUTANT BREAST CANCER CELLS ARE SENSITIVE TO CDK4/6 INHIBITION

Attributions

All the experiments and analyses in this chapter were performed by Flora Luo. Dr. Peter Choi kindly provided the lentiCRISPR v2-control guide and the digested lentiCRISPR vector for cloning of RB CRISPR guides.

Abstract

Highly specific cyclin-dependent kinase 4/6 (CDK4/6) inhibitors are a recent breakthrough in treatment for metastatic breast cancers that express the estrogen receptor (ER). CDK4/6 inhibitors, such as palbociclib, decrease phosphorylation of the retinoblastoma protein (RB1, hereafter RB) and prevent cell cycle progression from growth phase 1 (G1) to the DNA synthesis (S) phase of the cell cycle. Palbociclib, however, is only approved in combination with hormonal therapy, such as estrogen deprivation. Approximately 20% of metastatic breast cancer patients harbor an activating mutation in the ligand-binding domain (LBD) of the gene encoding the ER, *ESR1*, which confers resistance to estrogen deprivation. It is unclear whether tumors harboring endocrine treatment-associated *ESR1* mutations will also respond to CDK4/6 inhibition under estrogen-deprived conditions. Therefore, we sought to determine whether ligand-independent growth of ER-mutant breast cancer cells requires CDK4/6. We observed that cells expressing ER mutants are sensitive to CDK4/6 inhibition. Mechanistically, ER LBD mutants upregulate key mediators of the G1/S cell cycle transition, such as cyclin D1. Furthermore, the sensitivity of ER-mutant breast cancer cells to CDK4/6 inhibition requires RB. While cells expressing RB respond to CDK4/6 inhibition, knockout of RB via CRISPRs renders ER-mutant breast cancer cells resistant to combined estrogen deprivation and CDK4/6 inhibition.

Our studies suggest that tumors harboring *ESR1 LBD* mutations and an intact RB will respond to CDK4/6 inhibition and hormonal therapy.

Introduction

Estrogen receptor α (ER) is expressed in about 70% breast cancers. Since ER+ breast cancers are highly dependent on estrogen, aromatase inhibitors that prevent estrogen production are a mainstay of treatment for postmenopausal women (91-93). About 20-30% of breast cancers, however, are intrinsically resistant to aromatase inhibition and acquired resistance often develops (254,255). Many advanced breast cancers that acquire resistance to aromatase inhibitors are ER+ and ER-dependent; treatment with the ER destabilizer, fulvestrant, has a clinical benefit rate of 35% (255). Thus, ER remains active in many advanced hormone-independent breast cancers. As resistance to fulvestrant invariably develops, novel treatment strategies are needed for ER+ breast cancer patients who have relapsed on prior endocrine therapy.

Chronic culturing of ER+ breast cancer cells under estrogen-deprived conditions (charcoal-stripped serum media, CSS) has enabled *in vitro* characterization of hormone-resistant clones. Long term estrogen deprived cells (LTED) not only retain a functional ER but also are dependent on the ER for growth in CSS (194). Furthermore, LTED are dependent on cyclin dependent kinase 4 (CDK4) and are sensitive to a CDK4/6 inhibitor (194). While cyclin D1 activates CDK4/6, CDK4/6 inhibitors such as p16 prevent phosphorylation of the retinoblastoma protein RB and induce a G1 cell cycle arrest. Palbociclib is currently the most clinically advanced small molecule CDK4/6 inhibitor. While palbociclib in combination with hormonal therapy has been FDA-approved for patients who have relapsed on prior endocrine therapy (256), markers of sensitivity have been scarce.

In recent years, sequencing of metastatic ER+ breast cancers revealed activating ligand-binding domain (LBD) mutations in the gene encoding the ER, *ESR1* (110,112-114). Functionally, the mutants constitutively activate the ER and promote ligand-independent expression of ER target genes (110,112). These variants also promote estrogen-independent growth of breast cancer cells either *in vivo* (110) or *in vitro* (110,112,113). ER destabilizers like fulvestrant inhibit the activity of the ER mutants and impair cell growth of mutant cells, but the concentration of fulvestrant needed to inhibit ER activity by 50% (IC_{50}) is two to fourfold higher for the mutants compared to wild-type ER (112). Acquired resistance also limits the efficacy of fulvestrant. Non-hormonal therapies are needed to treat *ESR1*-mutant patients. Since LTED ER+ breast cancer cells are dependent on CDK4 for survival (194), we reasoned that cells expressing a constitutively active ER mutant would also respond to the CDK4/6 inhibition.

Results

ER LBD mutants upregulate cyclin D1.

Using site-directed mutagenesis, we generated six ER LBD point mutants (Y537C/N/S, D538G, S463P and L536Q) that were identified in advanced metastatic breast cancer samples (110,112-114). To determine whether these constructs are constitutively active, we infected T47D breast cancer cells with lentivirus encoding wild-type (WT) or mutant ER. We then cultured cells in estrogen-rich fetal bovine serum media (FBS) or in charcoal-stripped serum media (CSS) to mimic estrogen-deprivation. Although T47D cells are ER+, they have low viability under estrogen-deprived conditions (GFP CSS, **Fig. 2.1A**) Overexpression of ER^{WT} increased estrogen-independent growth by 15% compared to control GFP (**Fig. 2.1A**), consistent with *ESR1* amplification in long-term estrogen-deprived breast cancer cultures (113). Cells expressing each of the six LBD mutants had significantly higher viability in CSS media

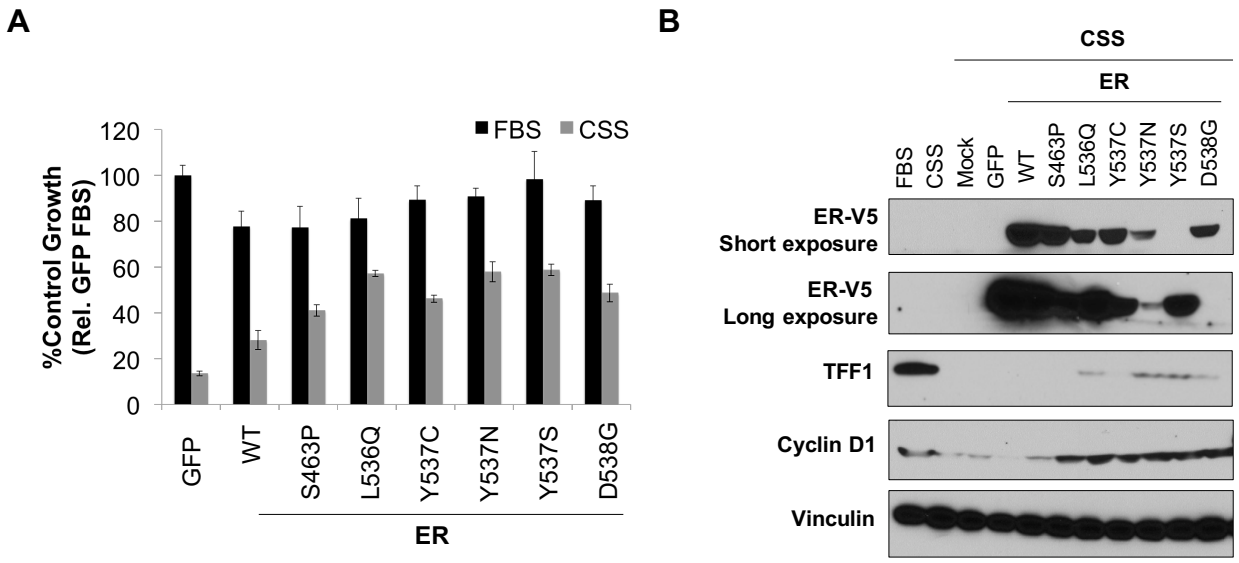

Figure 2.1. ER LBD mutants are constitutively active. (A) T47D cells were infected with lentivirus encoding indicated constructs in 96-well format and grown in either FBS or CSS media. The % viability (determined by the MTS assay) relative to GFP FBS for 3 replicates is shown +/- STDEV after 6-day treatment. **(B)** Western blot analysis of T47D cells infected with indicated constructs and grown in estrogen-deprived CSS media for four days.

compared to ER^{WT} control ($p<0.01$ for all mutants except S463P, $p<0.05$). Similarly, LBD mutant cells had 3-4 fold higher viability in CSS media compared to GFP controls (**Fig. 2.1A**). Thus, as previously reported, ER LBD mutants confer resistance to estrogen deprivation (110-114).

Mechanistically, estrogen upregulates cyclin D1 expression to drive cell cycle progression (257-259). Since the LBD mutations constitutively activate the ER (110,112-114), we also assessed whether the LBD mutants induce cyclin D1 expression under estrogen-deprived conditions. Despite the slight increase in viability induced by exogenous ER, ER^{WT} is unable to promote robust expression of downstream target genes like cyclin D1 and/or trefoil factor 1 (TFF1) in CSS media (**Fig. 2.1B**). In comparison, all mutant ERs upregulate cyclin D1 and to varying degrees TFF1 under estrogen deprivation (**Fig. 2.1B**). Given that cyclin D1 stimulates CDK4/6 activity, these results suggest that CDK4/6 is active in cells with mutant ER.

Breast cancer cells expressing ER mutants are sensitive to CDK4/6 inhibition.

Next, we investigated whether cells expressing ER LBD mutants respond to CDK4/6 inhibition. ER+ T47D cells were infected in a 96-well format with lentivirus encoding control GFP, ER^{WT} or one of the six LBD mutants. Cells were subsequently treated with palbociclib in estrogen-replete media containing fetal bovine serum (FBS) or in estrogen-deprived CSS media. Cell viability via MTS assay was determined after 6 days. Under normal cell culture conditions in FBS media, parental T47D cells are sensitive to CDK4/6 inhibition (4). Similarly, all cells regardless of mutation status were sensitive to CDK4/6 inhibition in estrogen-replete media (**Fig. 2.2**). However, under estrogen-deprived conditions, both parental and ER^{WT} cells were not further sensitized to palbociclib, while palbociclib reduced the viability of mutant cells in a dose-dependent manner (**Fig. 2.2**).

To assess whether palbociclib induces cell cycle arrest in cells with mutant ER under estrogen-deprived conditions, we also analyzed treated cells by western blot and cell cycle

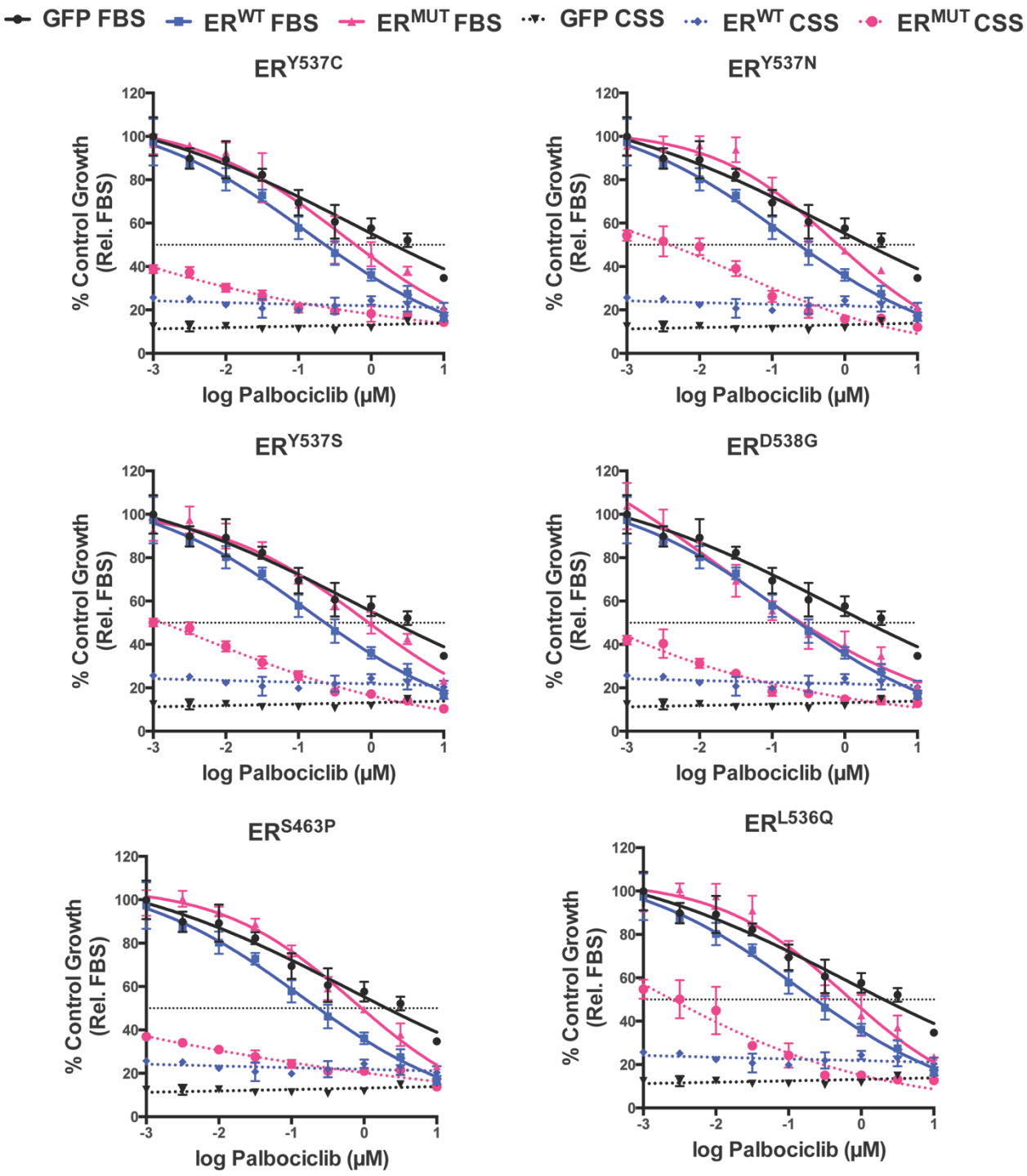

Figure 2.2. Estrogen-independent growth of *ER*-mutant breast cancer cells is dependent on CDK4/6. T47D cells were infected with virus encoding indicated ER mutant and treated with palbociclib in FBS or CSS media for six days. Average viability relative to FBS (accessed by MTS assay) for 3 replicates +/- SD is shown. For clarity, the results for each mutant are graphed separately; GFP and ESR1WT dose response curves are the same across all panels. analysis. When control (GFP and ER^{WT}) cells are grown without estrogen, the ER is inactive.

Therefore, in estrogen-depleted CSS media, control GFP and ER^{WT} cells downregulate ER target genes such as cyclin D1 and E2F1 (**Fig. 2.3A**). CSS treatment also reduces RB phosphorylation in control GFP-expressing cells compared to parental cells growing in FBS media. These biochemical changes result in a G1 cell cycle arrest as measured by propidium iodide staining (**Fig. 2.3B**); only 5% of parental cells are actively replicating (in S phase) in CSS media compared to 29% in FBS media. In contrast, ER^{Y537N}, ER^{Y537S} and ER^{D538G} upregulate cyclin D1 and E2F1 (**Fig. 2.3A**) and promote RB phosphorylation (**Fig. 2.3A**). RB inactivation leads to S phase progression under estrogen-deprived conditions (11% of ER^{Y537N} and 13% of ER^{Y537S} cells are in S phase compared to 8% of ER^{WT} cells and 3% of GFP cells) (**Fig. 2.3B**). These results suggest that ER LBD mutants drive S phase progression under estrogen-deprived conditions.

Treatment with the CDK4/6 inhibitor palbociclib, however, reduces RB phosphorylation and E2F1 expression in ER^{Y537N} and ER^{Y537S} cells, which results in a G1 cell cycle arrest (**Fig. 2.3A** and **2.3B**). These results suggest that ER mutants upregulate modulators of the cell cycle under estrogen-deprived conditions, conferring resistance to estrogen deprivation, but also sensitivity to inhibitors of the cell cycle, such as the CDK4/6 inhibitor palbociclib.

CDK6 activation confers resistance to CDK4/6 inhibitors.

Since amplification or mutation of the drug target often confers resistance to small molecule inhibitors (260,261), we assessed whether constitutive expression of CDK6 and its binding partner cyclin D1 drives resistance to palbociclib. CDK6 and cyclin D1 increased the dose of palbociclib at which 50% viability was achieved (GI_{50}) by nearly 10-fold compared to GFP controls (**Fig. 2.4A**). Whereas CSS and palbociclib reduce RB phosphorylation in control GFP cells, co-expression of CDK6 and cyclin D1 maintains RB phosphorylation under combination treatment (**Fig. 2.4B**). To determine whether CDK6 inactivation is required to

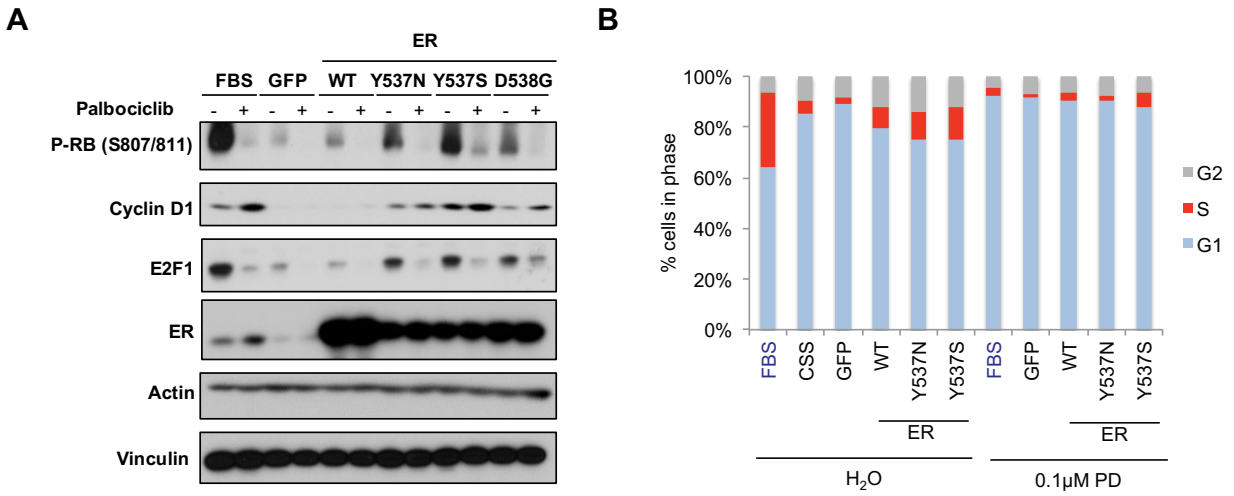

Figure 2.3. Palbociclib induces a G1 cell cycle arrest in hormone-independent ER-mutant cells. (A) Western blot analysis of cells in grown in FBS or CSS media for at least four days. Cells were then treated with +/-0.1μM palbociclib (PD) for 24 hours. **(B)** Cell cycle analysis of T47D cells treated as in (A). Cells were grown in CSS media unless otherwise noted. Cells were stained with propidium iodide and indicated cell cycle phases were analyzed by flow cytometry.

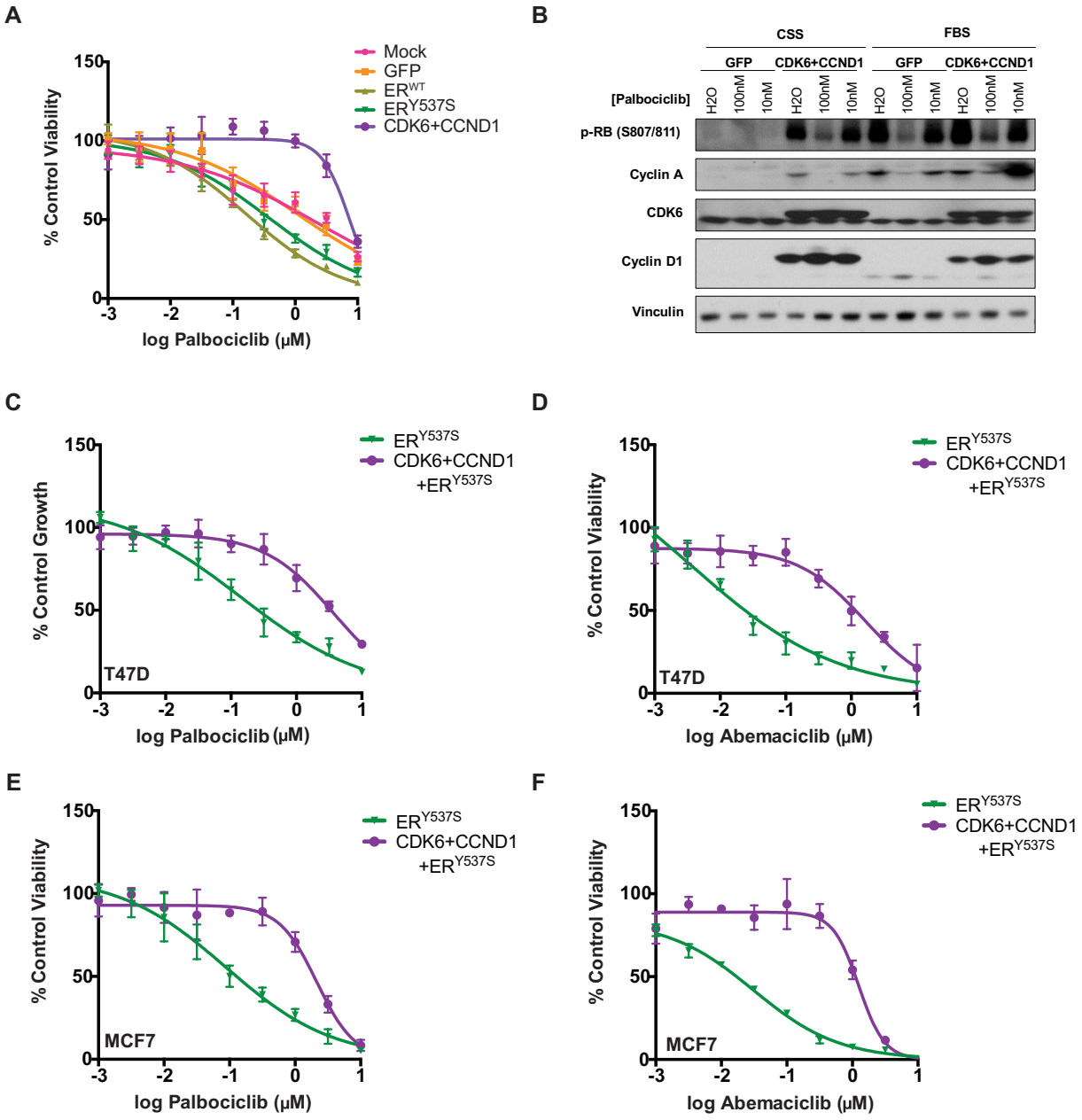

Figure 2.4. Overexpression of CDK6 and cyclin D1 drives resistance to CDK4/6 inhibitors. **(A)** T47D were infected at in 96-well format and subsequently treated with indicated palbociclib concentrations in FBS media. % viability +/- SD as measured by MTS relative to vehicle control for five replicates is shown. **(B)** Immunoblot analysis of ORF-expressing T47D cells following overnight treatment with palbociclib in FBS or CSS media. **(C-F)** T47D or MCF7 cells were treated as in (A). Results for 3-5 replicates +/-SD shown.

sensitize cells with mutant ER to palbociclib, we co-expressed CDK6 and cyclin D1 in ER^{Y537S} cells. Exogenous CDK6 and cyclin D1 expression significantly shifted the palbociclib GI_{50} of ER^{Y537S} cells by 10-fold (**Fig. 2.4C**). This effect was neither drug-specific nor cell-line specific as similar results were observed with another CDK4/6 inhibitor (abemaciclib, **Fig. 2.4D**) and in MCF7 cells (**Fig. 2.4E-2.4F**). Since upregulation of active CDK6-cyclin D1 complexes bypasses CDK4/6 inhibition, these data suggest that ER LBD mutants act upstream of CDK6 to drive proliferation.

RB is required for cells with mutant ER to respond to CDK4/6 inhibition.

To investigate whether RB is the only pocket protein required for the response of ER-mutant breast cancer cells to CDK4/6 inhibition, we generated RB knockout cells via CRISPR technology (**Fig. 2.5A**). Cells were subsequently infected with lentivirus encoding GFP, ER^{WT} or mutant ER (**Fig. 2.5B**). In both estrogen-replete and estrogen-deprived media (FBS and CSS respectively), ER^{Y537N} and ER^{Y537S} cells with intact RB are sensitive to CDK4/6 inhibition (**Fig. 2.5C-2.5D**). In GFP control cells, RB loss confers a small but reproducible viability advantage in CSS media compared to cells expressing RB (increase of 10-20% in viability for GFP RB null cells compared to GFP cells expressing RB, **Fig. 2.5D**). Furthermore, palbociclib has little effect on the viability of cells that have lost RB, regardless of ER mutation status (**Fig. 2.5D**). Even at 3μM palbociclib in CSS, the viability of ER^{Y537N} RB-null cells is twice that of mutant cells with intact RB. Similarly, RB loss increased the viability of ER^{Y537S} cells by 1.8-2.2 times in 3μM palbociclib. Thus, CDK4/6 inhibitors are only effective against ER-mutant cells when RB is intact.

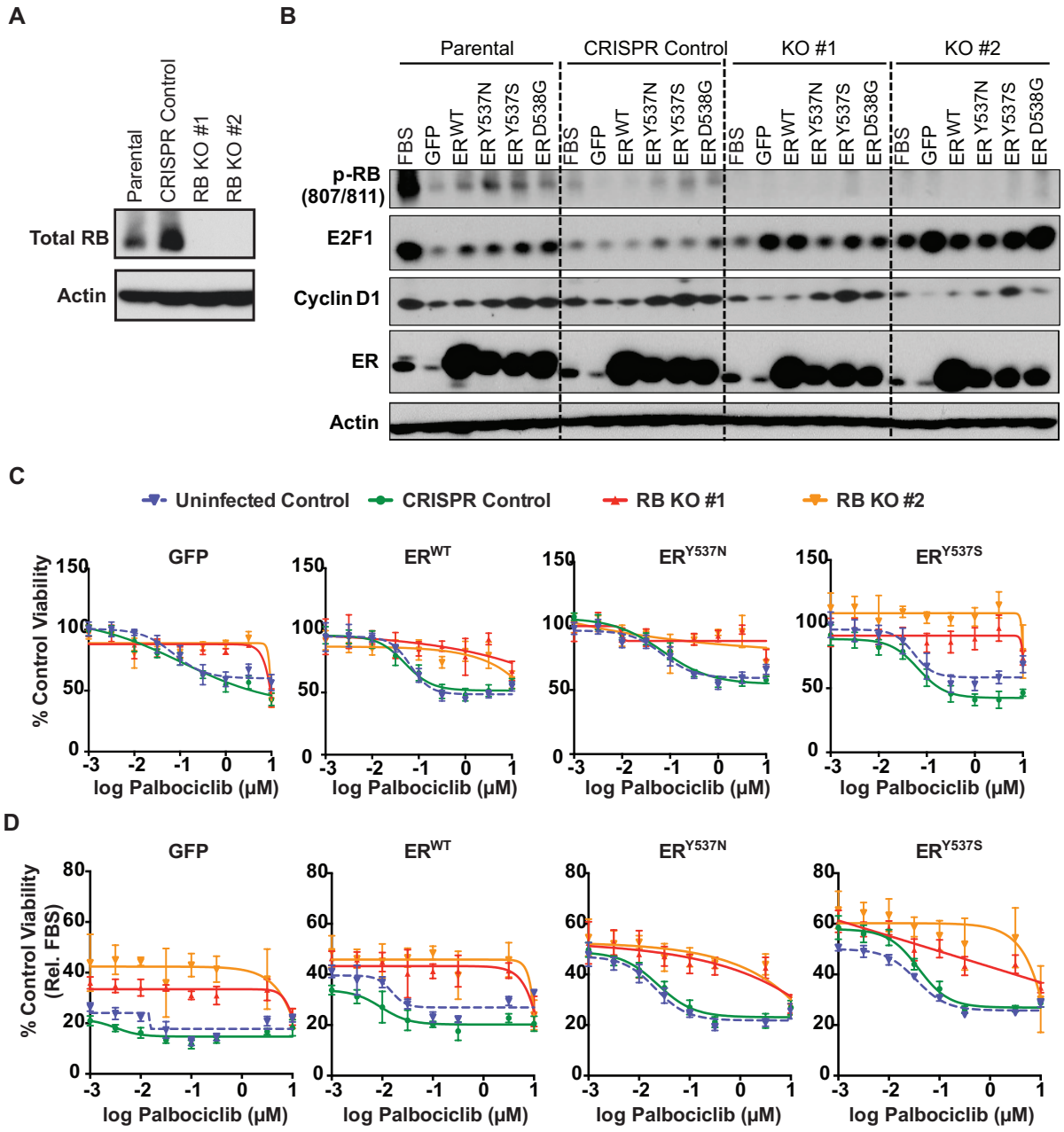

Figure 2.5. Knockout (KO) of RB confers resistance to CDK4/6 inhibition in cells with a ligand-independent ER. **(A)** Western blot analysis of T47D cells expressing control or RB CRISPRs. Cells were grown in full serum (FBS containing media). **(B)** Western blot analysis of T47D+/-RB cells infected with indicated constructs and grown in estrogen-deprived CSS media for five days. Cells grown in FBS media are shown as controls. Lysates for parental T47D cells are same as in Fig, 1B and shown for reference. **(C)** T47D cells +/-RB were infected with indicated constructs in 96 well format with virus and treated with increasing concentrations of palbociclib in FBS media for 6 days. The average viability (by MTS) relative to vehicle control is shown for 6 replicates +/- SD. **(D)** Same as in (C) except cells were grown in CSS media. Average viability relative to FBS vehicle control for six replicates is shown.

Discussion

Our results indicate that ER LBD mutations enable estrogen-independent growth by driving cell cycle progression into S phase. These results are consistent with ER's known effects on the cell cycle (257-259). Under estrogen-deprived conditions, we found that ER-mutant breast cancer cells upregulate cyclin D1 expression and have high RB phoshorylation **(Fig. 2.3A)**. Since RB is a direct target of CDK4/6, these results suggest that CDK4/6 may be active, which may render these cells sensitive to CDK4/6 inhibition. Indeed, in estrogen-deprived CSS media, palbociclib reduced the viability of ER-mutant cells (**Fig. 2.2**). This decrease in viability corresponded to a G1 cell cycle arrest and decrease in RB phosphorylation phoshorylation **(Fig. 2.3B)**. Interestingly, we found that wild-type and mutant ER potentially further sensitizes cells to CDK4/6 inhibition. For example, when we expressed ER^{WT} or mutant ER, there was a small but reproducible decrease in GI_{50} compared to cells expressing control GFP (**Fig. 2.2** and **Fig. 2.4A).** These results are consistent with *in vitro* (4) and clinical findings (252) in which ER positivity is currently the best predictor of sensitivity to CDK4/6 inhibition.

Dr. Rinath Jeselsohn and Wardell *et al.* similarly found that ER-mutant breast cancer cells are sensitive to dual ER and CDK4/6 inhibition; ER-mutant cells were sensitive to the combination of an ER degrader (like fulvestrant or bazedoxifene) and palbociclib (262). In phase 3 clinical trials, fulvestrant and palbociclib increased progression-free survival of *ESR1*-mutant patients from 3.6 months on fulvestrant alone to 9.4 months (263). Thus, *ESR1*-mutant patients will likely benefit from CDK4/6 inhibition combined with hormonal therapy.

ESR1 mutations are predominantly found in endocrine-resistant tumors and are largely absent from treatment-naïve samples (257-259,263). Since heavily pre-treated metastatic tumors may harbor additional mutations that cause cross-resistance to CDK4/6 inhibition, we also investigated resistance in the setting of ER-mutant breast cancer. Overexpression of CDK6 and cyclin D1 increased the GI_{50} of cells expressing ER^{Y537S} **(Fig. 2.4C-F)**. RB loss has

been associated with clinical resistance to the ER modulator tamoxifen (264). Similarly, RB loss increases the viability of ER+ breast cancer cells in estrogen-deprived CSS media and renders cells with mutant ER cross-resistant to palbociclib (**Fig. 2.5D)**.

Since RB is intact in 90% of treatment naïve ER+ breast cancer patients, patients in PALOMA-1 were not screened for RB loss (252). Data is emerging that genetic alterations in RB may be more prevalent in the metastatic setting (265). Our findings suggest that RB inactivation through increased in CDK6 activity or by genetic RB loss may render ER-mutant cells insensitive to CDK4/6 inhibition. Therefore, an RB inactivation signature may be helpful in stratifying patient response to CDK4/6 inhibition.

Materials and Methods

Cell lines and inhibitors

T47D and MCF7 breast cancer cells were obtained from lab stocks purchased from ATCC. Cells were passaged no more than 10 times after each thaw to prevent genetic drift. Cells were maintained in RPMI-1640 media + 10% heat-inactivated FBS (Gemini bioproducts). Compounds include: palbociclib and abemaciclib (Selleck). For experiments with CSS, cells were grown in phenol-red free RPMI-1640 media with 10% charcoal-stripped serum (Life Technologies).

Plasmids, cloning and site-directed mutagenesis of *ESR1*

Wild-type *ESR1* in both pDONR223 and pLX_304 vectors were obtained from the Broad Institute's Genetic Perturbation Platform (GPP). The pLX_304 vector is V5 tagged, confers blasticidin resistance and drives expression from a CMV promoter. Mutations were generated in the pDNOR223 vector with the Quikchange Lightning mutagenesis kit (Agilent) according to manufacturer's instructions.

The following primers were used for mutagenesis:

Y537N: Forward: 5'-cgtggtgcccctcaatgacctgctgct-3'

Reverse: 5'-agcagcaggtcattgaggggcaccacg-3'

Y537S: Forward: 5'-acgtggtgcccctcagtgacctgctgctgg-3'

Reverse: 5'-ccagcagcaggtcactgaggggcaccacgt-3'

Y537C: Forward: 5'- aagaacgtggtgcccctctgtgacctgctg-3'

Reverse: 5'-cagcaggtcacagaggggcaccacgttctt-3'

S463P: Forward: 5'-gagtgtacacatttctgcccagcaccctgaagtc-3'

Reverse: 5'- gacttcagggtgctgggcagaaatgtgtacactc-3'

L536Q: Forward: 5'- agaacgtggtgccccagtatgacctgctgctg-3'

Reverse: 5'-cagcagcaggtcatactggggcaccacgttct-3'

Sanger sequencing was used to confirm mutations. Open reading frames were then cloned into the pLX_304 vector with the Gateway LR clonase II system (Invitrogen). GFP (pDNOR223, gift from Dr. Chengyin Min), CDK6 (pDNOR223, Broad Institute GPP) and cyclin D1 (pDNOR221, Harvard PlasmID) were similarly cloned into the pLX_304 vector. All expression constructs are V5-tagged. Infected cells were selected with 35μg/ml blasticidin.

Cell viability assays

1.3-2x10^3 cells were plated in 96 well plates. The next day, cells were infected with 1:4-1:10 dilution of lentivirus encoding ORF of interest and 4 μg or 8μg polybrene. Mock transfected cells were only incubated with polybrene. Lentivirus was produced in 293T cells as previously described (266). For infection, plates were spun for 30 minutes at 2250rpm and 30^{o}C and the media was replaced the next day. The media was changed again and cells were treated with compounds in either FBS or CSS media. In parallel, cells were infected on a separate 96-well plate to assess infection efficiency (with 35 μg/ml blasticidin). After 6 days of treatment, media

was changed to DMEM (with phenol red) + 10% FBS and cell viability was assessed with the CellTiter96 Aqueous MTS assay (Promega) assay according to manufacturer's instructions.

Cell Cycle Analysis

Treated cells were trypsinized, resuspended in 70% ethanol in PBS and fixed for at least 24 hours. Pellets were washed in PBS and stained with 200µl propidium iodide (PI)/tritonX-100 solution (PBS with 0.1% TritonX-100, 0.2mg/ml RNase A and 20µg/ml PI) for 30 minutes at room temperature in the dark. 300 µl was added after the incubation and flow cytometry was performed with BD LSRFortessa at 605nm wavelength. ModFit software was used to analyze the percentage of cells in S phase from FCS files.

Western blot

After indicated treatment, cells were washed with PBS and lysed with RIPA buffer (SIGMA) containing a protease inhibitor cocktail (cOmplete, EDTA-free, SIGMA Aldrich) and phosphatase inhibitors (PhosSTOP, SIGMA). After protein concentrations were determined with the Bio-Rad protein assay and normalized, lysates were resolved with SDS-PAGE protein gels and transferred onto PVDF membranes. All antibodies were from Cell Signaling Technologies, except CDK6 (C-21, sc-177) and cyclin A (sc-596).

CRISPR constructs

Detailed protcol for cloning of CRISPR guides may be found here: https://www.addgene.org/static/data/plasmids/52/52961/52961-attachment_B3xTwla0bkYD.pdf
The following guides were cloned into the LentiCRISPRv2 vector (Feng Zhang lab, Addgene):
hDummy (HGLibA_14098, control): ATCGTTTCCGCTTAACGGCG
RB (HGLibB_41361): AACATCTAATGGACTTCCAG
RB (HGLibB_41363): AGTCCAAGAGAATTCATAAA

CHAPTER 3

SYSTEMATIC FUNCTIONAL MAPPING OF RESISTANCE TO CDK4/6 INHIBITION IN ER+ BREAST CANCER

Attributions

This chapter is based on a manuscript in preparation with the following authorship:

Flora Luo[1,2], Seth Wander[1,2], Joseph Geradts[3], Glenn Cowley[2], Federica Piccioni[2], Sasha Pantel[2], Cory Johannessen[2], Nikhil Wagle[1,2], and Levi Garraway[1,2].

1) Dana-Farber Cancer Institute, Harvard Medical School, Boston, MA 02115
2) The Broad Institute of Harvard and MIT, Cambridge, MA 02142
3) Brigham and Women's Hospital, Boston, MA 02115

All the experiments and analyses in this chapter were performed by Flora Luo except as follows:

Glenn Cowley and the Genetic Perturbation Platform at the Broad Institute sequenced the primary screens, performed quality control and data deconvolution. Secondary screens were conducted by Sasha Pantel and Federica Piccioni in the Genetic Perturbation Platform. Cory Johannessen performed initial analysis of secondary screen. Clinical information was provided by Seth Wander and Nikhil Wagle. Joseph Geradts analyzed the immunohistochemistry stains.

Abstract

Cyclin-dependent kinase 4/6 (CDK4/6) inhibitors in combination with hormonal therapy is the new standard of care for advanced ER+ breast cancer patients. Despite this advancement, some patients present with intrinsic resistance, while others progress after a variable period of clinical benefit. We utilized large-scale pooled expression screens to identify genes whose upregulation drive resistance to CDK4/6 inhibition alone and combined with estrogen deprivation. Activation of the serine/threonine kinase AKT emerged as a key node of resistance

across all treatment conditions. Mechanistically, AKT stabilized expression of the CDK activator cyclin D1 and maintained RB phosphorylation, which was abrogated by either AKT or mTOR inhibition. Targeting of AKT or its downstream effector mTOR suppressed AKT-mediated resistance. Activating mutations in *AKT1* were also associated with resistance in patient biopsies. Our study offers new insights into the landscape of resistance to CDK4/6 inhibition and nominates novel combination therapies.

Introduction

The recent clinical development of highly specific cyclin dependent kinase 4/6 (CDK4/6) inhibitors (253,267,268) is an exciting breakthrough for ER+ breast cancer patients. CDK4/6 inhibitors, such as palbociclib, abemaciclib and ribociclib, prevent phosphorylation of the retinoblastoma protein RB and block G1-S cell cycle transition (4,7). Although palbociclib in combination with the aromatase inhibitor letrozole is approved as first-line therapy for patients with metastatic ER+ breast cancer, about 15% of patients derive no clinical benefit (253). For patients who have relapsed on prior hormonal therapy, the clinical benefit rate of palbociclib in combination with the ER degrader fulvestrant was only 34% (256). Furthermore, acquired resistance is also a common issue for targeted therapies.

Preclinical investigations have identified several mechanisms of resistance to CDK4/6 inhibition in ER+ breast cancer. Cultured to resistance models and other *in vitro* studies suggest that RB loss (219,248), cyclin E1/2 expression (248,250), FOXM1 stabilization (224), PDK1 activity (247) or CDK6 amplification (249) can bypass CDK4/6 inhibition. Many of these mechanisms converge on RB either by genetic loss or inactivation by phosphorylation. Cells overexpressing CDK6 maintain RB phosphorylation despite CDK4/6 inhibition (249). Cyclin E1 activates CDK2, which can phosphorylate RB on several residues (251). Since CDK2 can also interact with cyclin D1, CDK2 activation has emerged as a potential node of resistance to

CDK4/6 inhibition (248). The current standard of care, however, is combined CDK4/6 inhibition with hormonal therapy. Since most *in vitro* studies with CDK4/6 inhibitors were conducted in estrogen-rich media with fetal bovine serum (FBS), the spectrum of resistance to combination therapy remains unclear.

Clinical biomarkers of response and resistance to CDK4/6 inhibition have also been scarce. While elevated expression of the CDK4/6 activator cyclin D1 and low expression of the CDK4/6 inhibitor p16 predicted sensitivity of ER+ breast cancers *in vitro* (4), these biomarkers were not clinically useful (252). The *PIK3CA* oncogene, which encodes PI3K, is mutated in ~30% of breast cancers. PI3K's main downstream effector protein kinase B (AKT) drives the cell cycle by promoting cyclin D1 stability and inactivating the CDK2 inhibitors p21/p27 (269). AKT activation is also a major node of endocrine resistance (193). *PIK3CA* mutations, however, do not predict resistance to palbociclib and fulvestrant (234). The use of systematic functional screens allows for unbiased characterization of resistance to targeted therapies. Therefore, we conducted expression screens to identify the landscape of resistance to CDK4/6 inhibition alone and in combination with estrogen deprivation.

Results

Near genome-wide open reading frame (ORF) screens identify mechanisms of resistance to estrogen deprivation, CDK4/6 inhibition and the combination.

To determine the landscape of resistance to CDK4/6 inhibition, we conducted five large-scale genome-wide open reading frame (ORF) screens with palbociclib and abemaciclib. ER+ T47D breast cancer cells were infected with the Broad Institute's 17,255 barcoded ORF library, which encodes ~14,000 genes. Cells were subsequently selected with puromycin and a sample was collected to determine ORF representation at this "early time point". Then, cells were

cultivated in the presence of 1) 10% full serum media (FBS) + 1μM palbociclib, 2) FBS+ 0.3μM abemaciclib, 3) 10% charcoal-stripped serum media (CSS) to mimic estrogen-deprivation 4) CSS+0.1μM palbociclib or 5) CSS+ 0.03μM abemaciclib (**Fig. 3.1A**). "Late time point" genomic DNA was isolated on day 28 for all FBS arms or day 31 for all CSS treatment arms **(Fig. 3.2A-B)** and massively parallel sequencing was performed on three replicates per treatment. There were at least 20 million sequencing reads per replicate, corresponding to at least 1000 reads per ORF (**Fig. 3.2C**).

To determine relative ORF abundance at each time point and for each replicate, a log normalized score was generated. Most ORFs in the library were well-represented at the early time point; the log normalized score for 95% of ORFs were within two standard deviations of the mean (**Fig. 3.2D**). R squared value analysis shows high correlation between replicates (**Fig. 3.2E**) with the lowest R-squared value being 0.78. To determine whether a given ORF was enriched during drug treatment, we calculated the log fold change (LFC) of normalized reads at the late time point versus the early time point. ORFs with a median LFC greater than 2 (corresponding to a z-score of greater than 3) were nominated as candidate resistance hits (**Fig. 3.1B; Tables 3.1-3.5**). Some genes in the library were encoded by multiple ORFs; for example, EGFR ORFs encoding different oncogenic alterations were included in the collection. Gene ontology-guided annotation of our candidate resistance genes indicates that a variety of protein classes may confer resistance to CDK4/6 inhibition. The highest scoring resistance ORFs across multiple treatment arms encoded receptor tyrosine kinases, serine/threonine kinases, GTPases, non-receptor kinases and cyclin-dependent kinases (**Fig. 3.3**).

Our screens nominated known resistance pathways to hormonal therapy. For example, the receptor tyrosine kinase EGFR is a known mediator of resistance to endocrine therapy (270,271). Multiple constitutively active EGFR ORFs conferred resistance to estrogen deprivation (CSS) (**Fig. 3.1B and Table 3.3**). Previously, MCF7 mouse xenografts resistant to

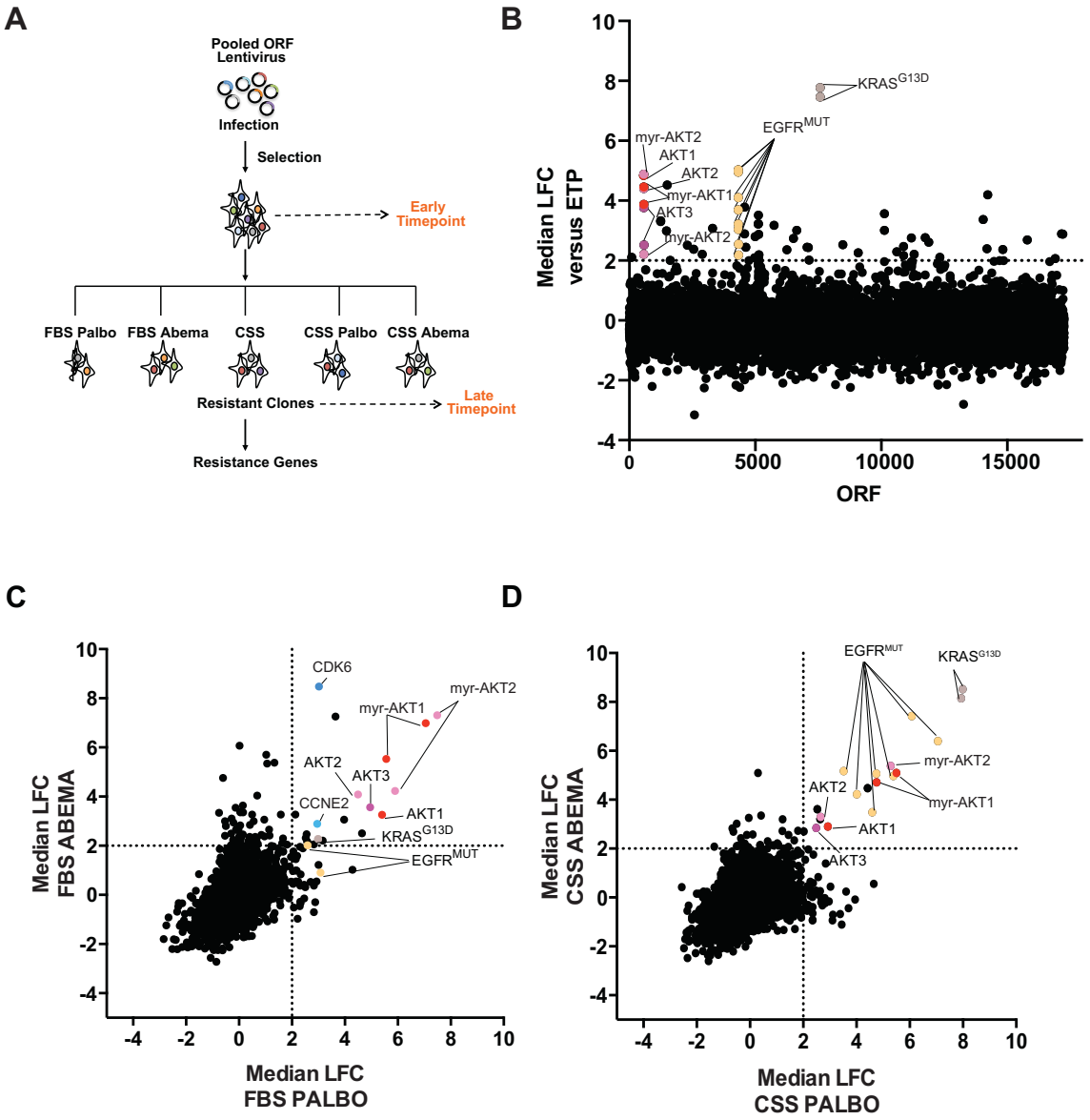

Figure 3.1. Large-scale resistance screens implicate novel mediators of resistance to CDK4/6 inhibition. (A) Overview of screens. **(B)** ORFs at the end of the screen with median log fold change (LFC) greater than 2 were nominated as candidate resistance hits (red). Results for CSS treatment shown. **(C-D)** Comparison of ORF median LFC in indicated treatments. CCNE2 ORF encodes a N-terminally truncated lower molecular weight (LMW) isoform of cyclin E2.

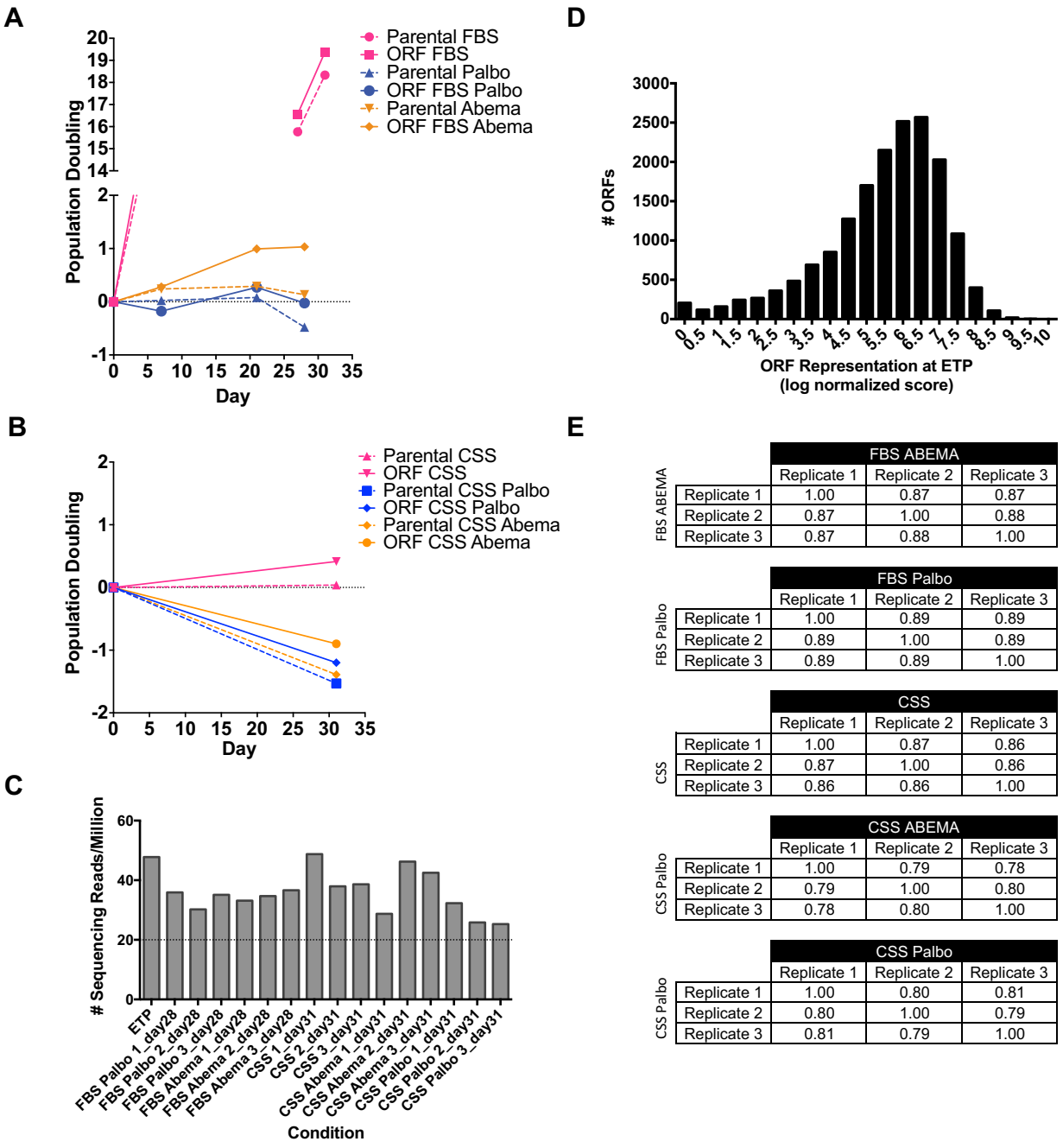

FBS ABEMA	Replicate 1	Replicate 2	Replicate 3
Replicate 1	1.00	0.87	0.87
Replicate 2	0.87	1.00	0.88
Replicate 3	0.87	0.88	1.00

FBS Palbo	Replicate 1	Replicate 2	Replicate 3
Replicate 1	1.00	0.89	0.89
Replicate 2	0.89	1.00	0.89
Replicate 3	0.89	0.89	1.00

CSS	Replicate 1	Replicate 2	Replicate 3
Replicate 1	1.00	0.87	0.86
Replicate 2	0.87	1.00	0.86
Replicate 3	0.86	0.86	1.00

CSS Palbo	Replicate 1	Replicate 2	Replicate 3
Replicate 1	1.00	0.79	0.78
Replicate 2	0.79	1.00	0.80
Replicate 3	0.78	0.80	1.00

CSS Palbo	Replicate 1	Replicate 2	Replicate 3
Replicate 1	1.00	0.80	0.81
Replicate 2	0.80	1.00	0.79
Replicate 3	0.81	0.79	1.00

Figure 3.2. Population doubling and quality metrics for primary screen. (A) Growth of control parental and ORF-infected cells cultured in FBS media +/- palbociclib (palbo) or abemaciclib (abema). Data represent 3 replicates per ORF-infected screening arm. Parental cells were passaged as controls. Early time point = day 0 and late time point = day cells were harvested (day 28). Y-axis split to show population doublings for ORF-infected cells. **(B)** As in (A) except in CSS media. Late time point = day 31. **(C)** Number of sequencing reads per million for each treatment replicate in the screen. A sequencing depth of 20 million reads ensures 1000 reads/ORF. **(D)** Distribution of log normalized score (relative sequencing reads) for ORFs at early time point (ETP). **(E)** R squared correlation analysis of ORF representation at the end of the screen (late time point) between the replicates in each condition.

Table 3.1. The top genes from FBS palbociclib primary screen with LFC >2.

Rank	Construct ID	ORF	Median LFC	Z score
1	TRCN0000489868	MYR-AKT2	7.486	17.997
2	TRCN0000489962	MYR-AKT1	7.055	16.973
3	TRCN0000488903	AKT2	5.895	14.221
4	TRCN0000488923	MYR-AKT1	5.559	13.425
5	TRCN0000491814	AKT1	5.404	13.057
6	TRCN0000487677	AKT3	4.953	11.986
7	TRCN0000478789	PDGFRB	4.647	11.261
8	TRCN0000488553	MYR-AKT2	4.497	10.906
9	TRCN0000465580	EIF4B	4.285	10.401
10	TRCN0000489669	AKT3	3.970	9.654
11	TRCN0000488053	ERBB2	3.650	8.895
12	TRCN0000470972	FBXO5	3.164	7.743
13	TRCN0000488391	EGFR (del746-750)	3.076	7.534
14	TRCN0000488331	CDK6	3.022	7.406
15	TRCN0000488644	PRKCZ	3.004	7.363
16	TRCN0000489180	KRAS (G13D)	2.990	7.329
17	TRCN0000474343	CCNE2 (truncated)	2.957	7.252
18	TRCN0000491946	LASP1	2.933	7.194
19	TRCN0000476130	IRX2	2.881	7.071
20	TRCN0000488169	KRAS (G13D)	2.832	6.954
21	TRCN0000466700	KIAA0922	2.831	6.952
22	TRCN0000471795	LMAN2L	2.827	6.942
23	TRCN0000479090	CYP19A1	2.702	6.647
24	TRCN0000488513	ERBB2	2.595	6.392
25	TRCN0000491390	EGFR (L858R)	2.586	6.372
26	TRCN0000478714	MAG	2.572	6.337
27	TRCN0000469110	PDGFRB	2.553	6.292
28	TRCN0000468173	RRN3	2.522	6.219
29	TRCN0000467027	PDIA3	2.503	6.174
30	TRCN0000470693	Pid1	2.464	6.082
31	TRCN0000489684	MED20	2.462	6.076
32	TRCN0000478339	ZNF677	2.416	5.967
33	TRCN0000477690	PCDHGB2	2.333	5.770
34	TRCN0000469616	CDK5RAP1	2.326	5.755
35	TRCN0000489702	HRAS	2.313	5.724
36	TRCN0000491754	C22orf23	2.312	5.720
37	TRCN0000467007	CSF1R	2.302	5.697
38	TRCN0000481566	AGPAT2	2.294	5.677
39	TRCN0000489003	PRKCZ	2.235	5.539
40	TRCN0000481318	SIGLEC10	2.214	5.487
41	TRCN0000468162	FGFR1OP	2.195	5.443
42	TRCN0000477926	SEMG2	2.182	5.414
43	TRCN0000465329	KLHDC3	2.151	5.340
44	TRCN0000471519	SGK223	2.146	5.326
45	TRCN0000470716	ZBTB48	2.143	5.320
46	TRCN0000491535	NTRK3	2.126	5.279
47	TRCN0000472750	SSX3	2.071	5.148
48	TRCN0000473787	INSRR	2.054	5.108
49	TRCN0000471836	KCNAB3	2.049	5.097
50	TRCN0000472712	DLX5	2.036	5.067

Table 3.2. The top genes from FBS abemaciclib primary screen with LFC >2.

Rank	Construct ID	ORF	Median LFC	Z score
1	TRCN0000488331	CDK6	8.474	17.686
2	TRCN0000489868	MYR-AKT2	7.313	15.313
3	TRCN0000488053	ERBB2	7.259	15.202
4	TRCN0000489962	MYR-AKT1	6.986	14.644
5	TRCN0000478845	SLC27A6	6.074	12.777
6	TRCN0000467546	CDK6	5.703	12.019
7	TRCN0000488923	MYR-AKT1	5.530	11.665
8	TRCN0000488060	CSF1R	5.383	11.364
9	TRCN0000481165	CDK6	5.344	11.284
10	TRCN0000488860	P2RY8	4.758	10.085
11	TRCN0000488903	AKT2	4.227	9.000
12	TRCN0000488553	MYR-AKT2	4.089	8.717
13	TRCN0000487698	MAP2K2	4.044	8.625
14	TRCN0000488109	CDK2	3.633	7.784
15	TRCN0000487677	AKT3	3.566	7.648
16	TRCN0000466529	SURF1	3.545	7.603
17	TRCN0000478920	METTL10	3.387	7.282
18	TRCN0000473629	SLC25A35	3.360	7.225
19	TRCN0000470056	CRHBP	3.356	7.217
20	TRCN0000479914	LMNA	3.343	7.191
21	TRCN0000491535	NTRK3	3.269	7.040
22	TRCN0000489478	NTRK3	3.269	7.040
23	TRCN0000476037	PRIMPOL	3.265	7.031
24	TRCN0000491814	AKT1	3.258	7.017
25	TRCN0000473786	FGFR3	3.110	6.713
26	TRCN0000489669	AKT3	3.066	6.624
27	TRCN0000488483	FGFR4	3.062	6.616
28	TRCN0000467572	OSGIN1	2.998	6.485
29	TRCN0000477178	RNASE13	2.996	6.481
30	TRCN0000477570	SPAG11B	2.944	6.375
31	TRCN0000474343	CCNE2 (truncated)	2.894	6.273
32	TRCN0000480935	TMEM151A	2.842	6.165
33	TRCN0000481444	ALPL	2.828	6.137
34	TRCN0000466624	SMARCAL1	2.805	6.090
35	TRCN0000473256	NXNL1	2.775	6.030
36	TRCN0000491475	PDGFRA	2.660	5.794
37	TRCN0000476560	NAP1L2	2.658	5.790
38	TRCN0000489508	CHRM5	2.650	5.774
39	TRCN0000489947	GHRHR	2.635	5.743
40	TRCN0000478789	PDGFRB	2.504	5.475
41	TRCN0000465390	SHC1	2.498	5.462
42	TRCN0000469110	PDGFRB	2.468	5.402
43	TRCN0000469209	SERPINB4	2.459	5.382
44	TRCN0000469646	EIF2S2	2.441	5.346
45	TRCN0000480014	AXL	2.413	5.288
46	TRCN0000474290	PHKB	2.409	5.279
47	TRCN0000468273	BBS4	2.375	5.211
48	TRCN0000478241	LOC105375356	2.366	5.192
49	TRCN0000478978	KARS	2.358	5.176
50	TRCN0000488545	STRADB	2.358	5.175

Table 3.2 (Continued).

51	TRCN0000468622	FGF10	2.357	5.173
52	TRCN0000468173	RRN3	2.314	5.086
53	TRCN0000469894	C6orf118	2.296	5.048
54	TRCN0000489180	KRAS (G13D)	2.267	4.990
55	TRCN0000466716	NLK	2.261	4.977
56	TRCN0000477967	TSPAN15	2.244	4.943
57	TRCN0000465556	NO_MATCH_72	2.231	4.915
58	TRCN0000478604	NLK	2.228	4.910
59	TRCN0000465244	NCOA4	2.214	4.882
60	TRCN0000470972	FBXO5	2.209	4.872
61	TRCN0000477770	FGF3	2.201	4.855
62	TRCN0000477932	CHRNA7	2.194	4.840
63	TRCN0000467886	CCDC40	2.189	4.831
64	TRCN0000478714	MAG	2.181	4.813
65	TRCN0000488513	ERBB2	2.118	4.685
66	TRCN0000467170	CDK5R1	2.104	4.657
67	TRCN0000489667	EPHB1	2.071	4.588
68	TRCN0000470492	ZNF85	2.064	4.574
69	TRCN0000488169	KRAS (G13D)	2.053	4.552
70	TRCN0000466845	MMD	2.050	4.546
71	TRCN0000468084	PAPOLB	2.028	4.501
72	TRCN0000469396	LGALS3BP	2.021	4.487
73	TRCN0000491390	EGFR (L858R)	2.019	4.482
74	TRCN0000477556	FAM98A	2.015	4.473
75	TRCN0000479136	SMCO3	2.003	4.449

Table 3.3. The top genes from CSS primary screen ranked with LFC >2.

Rank	Construct ID	ORF	Median LFC	Z score
1	TRCN0000489180	KRAS (G13D)	7.770	16.091
2	TRCN0000488169	KRAS (G13D)	7.465	15.476
3	TRCN0000491390	EGFR (L858R)	5.030	10.558
4	TRCN0000488391	EGFR (del746-750)	4.953	10.402
5	TRCN0000489868	MYR-AKT2	4.886	10.266
6	TRCN0000491814	AKT1	4.842	10.178
7	TRCN0000471040	BRMS1L	4.526	9.541
8	TRCN0000489962	MYR-AKT1	4.452	9.391
9	TRCN0000488903	AKT2	4.410	9.306
10	TRCN0000488838	SRC	4.195	8.872
11	TRCN0000489511	EGFR (T790M, L858R)	4.100	8.680
12	TRCN0000488923	MYR-AKT1	3.873	8.222
13	TRCN0000488053	ERBB2	3.779	8.032
14	TRCN0000487677	AKT3	3.764	8.002
15	TRCN0000489590	EGFR (L858R)	3.687	7.846
16	TRCN0000489478	NTRK3	3.566	7.601
17	TRCN0000479562	FGF8	3.514	7.497
18	TRCN0000476238	SOHLH1	3.369	7.203
19	TRCN0000489649	AXL	3.328	7.121
20	TRCN0000480014	AXL	3.300	7.065
21	TRCN0000474663	FGF6	3.228	6.920
22	TRCN0000489889	EGFR (T790M, L858R)	3.217	6.896
23	TRCN0000467429	FGF17	3.215	6.893
24	TRCN0000478834	GNE	3.176	6.815
25	TRCN0000488060	CSF1R	3.074	6.607
26	TRCN0000489095	EGFR (del747-748, A750P)	3.040	6.540
27	TRCN0000491535	NTRK3	3.011	6.481
28	TRCN0000489702	HRAS	3.005	6.468
29	TRCN0000491583	BRAF	2.995	6.448
30	TRCN0000478339	ZNF677	2.893	6.243
31	TRCN0000488513	ERBB2	2.889	6.235
32	TRCN0000471939	ZNF816-ZNF321P	2.885	6.225
33	TRCN0000491431	FGFR2	2.873	6.203
34	TRCN0000479278	FBXL4	2.799	6.053
35	TRCN0000469241	PRKAG1	2.764	5.981
36	TRCN0000489909	PIM1	2.753	5.961
37	TRCN0000465566	HLA-G	2.735	5.923
38	TRCN0000469184	TSPAN8	2.686	5.825
39	TRCN0000470818	PRRC1	2.612	5.675
40	TRCN0000491764	EGFR (del752-759)	2.548	5.546
41	TRCN0000488247	MAPK9	2.526	5.501
42	TRCN0000489669	AKT3	2.521	5.491
43	TRCN0000470181	CCND3	2.509	5.467
44	TRCN0000469110	PDGFRB	2.469	5.385
45	TRCN0000470220	INS	2.448	5.345
46	TRCN0000489098	ESR1	2.445	5.338
47	TRCN0000466535	IQCH	2.432	5.312
48	TRCN0000487888	SPPL3	2.397	5.241
49	TRCN0000488331	CDK6	2.376	5.199
50	TRCN0000475133	TBK1	2.372	5.190

Table 3.3 (Continued).

51	TRCN0000487994	HAS1	2.357	5.160
52	TRCN0000472315	PACSIN1	2.293	5.030
53	TRCN0000488816	MSX1	2.259	4.963
54	TRCN0000489661	PLCB2	2.208	4.860
55	TRCN0000488553	MYR-AKT2	2.207	4.857
56	TRCN0000466139	CLCN6	2.207	4.856
57	TRCN0000488483	FGFR4	2.191	4.825
58	TRCN0000487903	EGFR (T790M)	2.186	4.814
59	TRCN0000478789	PDGFRB	2.167	4.777
60	TRCN0000471615	RASAL3	2.107	4.656
61	TRCN0000471114	ABL2	2.104	4.649
62	TRCN0000469346	FASTKD3	2.087	4.615
63	TRCN0000465402	FGFR2	2.085	4.611
64	TRCN0000473799	ZNF132	2.065	4.571
65	TRCN0000466060	IRF9	2.011	4.462
66	TRCN0000471675	C12orf60	2.003	4.445
67	TRCN0000492076	FGFR2	2.002	4.444

Table 3.4. The top genes from CSS palbociclib primary screen with LFC >2.

Rank	Construct ID	ORF	Median LFC	Z score
1	TRCN0000489180	KRAS (G13D)	7.994	16.232
2	TRCN0000488169	KRAS (G13D)	7.932	16.109
3	TRCN0000491390	EGFR (L858R)	7.059	14.399
4	TRCN0000488391	EGFR (del746-750)	6.073	12.465
5	TRCN0000489962	MYR-AKT1	5.501	11.345
6	TRCN0000489095	EGFR (del747-748, A750P)	5.381	11.109
7	TRCN0000489868	MYR-AKT2	5.286	10.923
8	TRCN0000488923	MYR-AKT1	4.758	9.889
9	TRCN0000489590	EGFR (L858R)	4.752	9.877
10	TRCN0000489718	FGFR2	4.646	9.669
11	TRCN0000489889	EGFR (T790M, L858R)	4.589	9.557
12	TRCN0000488838	SRC (Y530F)	4.420	9.227
13	TRCN0000489511	EGFR (T790M, L858R)	4.013	8.427
14	TRCN0000492150	HSP90AB1	3.949	8.303
15	TRCN0000465780	RPS27	3.696	7.808
16	TRCN0000474959	TLE2	3.612	7.642
17	TRCN0000491764	EGFR (del752-759)	3.523	7.468
18	TRCN0000479295	NEK5	3.448	7.320
19	TRCN0000473088	42249	3.384	7.195
20	TRCN0000471533	AMPD2	3.111	6.661
21	TRCN0000467580	DENND5A	3.101	6.640
22	TRCN0000491744	ERN1	3.025	6.492
23	TRCN0000468708	ABI3BP	2.968	6.381
24	TRCN0000491814	AKT1	2.922	6.290
25	TRCN0000471040	BRMS1L	2.843	6.135
26	TRCN0000488247	MAPK9	2.824	6.098
27	TRCN0000488904	GRK5	2.811	6.073
28	TRCN0000470562	CBR4	2.719	5.892
29	TRCN0000480149	DCAF12L1	2.674	5.805
30	TRCN0000468821	TRPV5	2.668	5.793
31	TRCN0000488903	AKT2	2.651	5.759
32	TRCN0000481233	NECAB3	2.639	5.735
33	TRCN0000467429	FGF17	2.633	5.724
34	TRCN0000481145	STAU2	2.564	5.588
35	TRCN0000476741	TXNDC16	2.553	5.567
36	TRCN0000479562	FGF8	2.533	5.527
37	TRCN0000487677	AKT3	2.488	5.439
38	TRCN0000477999	ZNF326	2.478	5.420
39	TRCN0000469243	CASC4	2.380	5.227
40	TRCN0000468135	FADS1	2.371	5.210
41	TRCN0000467183	PSTPIP1	2.357	5.182
42	TRCN0000466730	C14orf39	2.357	5.182
43	TRCN0000472441	PALM2	2.354	5.177
44	TRCN0000474191	TLK2	2.350	5.168
45	TRCN0000489656	P2RY4	2.347	5.163
46	TRCN0000479687	UBE2G1	2.278	5.027
47	TRCN0000472583	MCMDC2	2.264	5.001
48	TRCN0000466279	TFIP11	2.263	4.998
49	TRCN0000474774	OR2J2	2.208	4.891
50	TRCN0000487996	NUP37	2.194	4.864

Table 3.4 (Continued).

51	TRCN0000471177	TUBGCP4	2.185	4.846
52	TRCN0000481487	SLC47A1	2.152	4.782
53	TRCN0000476045	DRD3	2.151	4.779
54	TRCN0000469506	POLD4	2.096	4.670
55	TRCN0000471268	KERA	2.074	4.628
56	TRCN0000465344	HN1	2.049	4.579
57	TRCN0000488553	MYR-AKT2	2.028	4.537
58	TRCN0000475762	SCIMP	2.019	4.519
59	TRCN0000472957	ARSI	2.006	4.495
60	TRCN0000470871	ICAM1	2.001	4.485

Table 3.5. The top genes from CSS abemaciclib primary screen with LFC>2.

Rank	Construct ID	ORF	Median LFC	Z score
1	TRCN0000489180	KRAS (G13D)	8.514	16.593
2	TRCN0000488169	KRAS (G13D)	8.145	15.903
3	TRCN0000488391	EGFR (del746-750)	7.436	14.577
4	TRCN0000491390	EGFR (L858R)	6.749	13.294
5	TRCN0000491764	EGFR (del752-759)	5.899	11.706
6	TRCN0000489590	EGFR (L858R)	5.427	10.824
7	TRCN0000489868	MYR-AKT2	5.351	10.682
8	TRCN0000489962	MYR-AKT1	5.346	10.671
9	TRCN0000489095	EGFR (del747-748, A750P)	5.261	10.514
10	TRCN0000471427	GPR39	5.170	10.343
11	TRCN0000472567	UPP2	4.829	9.707
12	TRCN0000488923	MYR-AKT1	4.644	9.361
13	TRCN0000488094	MAP3K5	4.455	9.007
14	TRCN0000471114	ABL2	4.399	8.903
15	TRCN0000488838	SRC (Y530F)	4.389	8.885
16	TRCN0000489770	HDAC6	4.304	8.726
17	TRCN0000489511	EGFR (T790M, L858R)	4.098	8.340
18	TRCN0000465231	CDK17	3.644	7.492
19	TRCN0000481279	TEKT1	3.632	7.470
20	TRCN0000488087	PNLIP	3.604	7.417
21	TRCN0000477168	FKTN	3.597	7.404
22	TRCN0000488903	AKT2	3.451	7.131
23	TRCN0000479562	FGF8	3.411	7.056
24	TRCN0000487996	NUP37	3.400	7.037
25	TRCN0000470048	METTL13	3.294	6.837
26	TRCN0000489889	EGFR (T790M, L858R)	3.286	6.824
27	TRCN0000479976	LOC440570	3.247	6.749
28	TRCN0000476985	CCNA2	3.230	6.717
29	TRCN0000467429	FGF17	3.111	6.496
30	TRCN0000488553	MYR-AKT2	3.061	6.401
31	TRCN0000480037	ROCK2	3.018	6.323
32	TRCN0000491451	RIPPLY1	2.998	6.285
33	TRCN0000491814	AKT1	2.909	6.118
34	TRCN0000469243	CASC4	2.846	6.001
35	TRCN0000474663	FGF6	2.825	5.961
36	TRCN0000466060	IRF9	2.769	5.857
37	TRCN0000487677	AKT3	2.622	5.583
38	TRCN0000488060	CSF1R	2.612	5.563
39	TRCN0000480539	CFHR3	2.607	5.554
40	TRCN0000474337	NR1D2	2.607	5.553
41	TRCN0000471268	KERA	2.569	5.482
42	TRCN0000475501	APOF	2.549	5.446
43	TRCN0000476122	RHPN1	2.544	5.436
44	TRCN0000480581	SARS2	2.543	5.434
45	TRCN0000475289	STK3	2.454	5.269
46	TRCN0000468878	GALNS	2.419	5.202
47	TRCN0000471564	DHRS7B	2.403	5.173
48	TRCN0000473795	DGKB	2.396	5.159
49	TRCN0000488307	GPR37	2.378	5.125
50	TRCN0000470349	IL2RB	2.325	5.027

Table 3.5 (Continued).

51	TRCN0000489702	HRAS	2.285	4.952
52	TRCN0000476328	CATSPERB	2.268	4.920
53	TRCN0000473969	POLA2	2.260	4.906
54	TRCN0000467277	LRRC8B	2.223	4.837
55	TRCN0000491725	PTPN18	2.192	4.778
56	TRCN0000489909	PIM1	2.177	4.751
57	TRCN0000488331	CDK6	2.106	4.618
58	TRCN0000489478	NTRK3	2.070	4.551
59	TRCN0000488486	CAMK2B	2.068	4.547
60	TRCN0000474662	GABRQ	2.062	4.536
61	TRCN0000487903	EGFR (T790M)	2.056	4.525
62	TRCN0000473419	MPC2	2.036	4.486

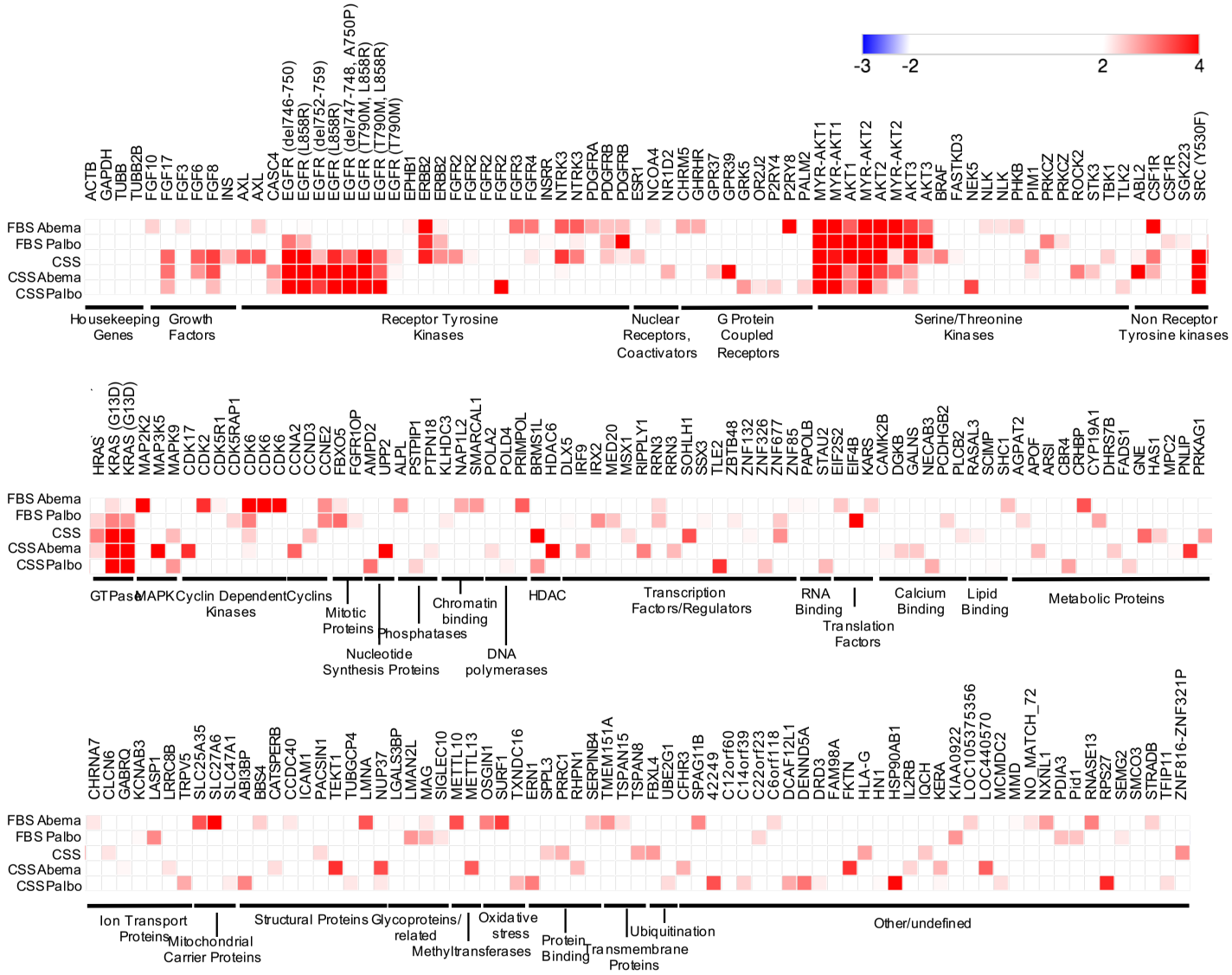

Figure 3.3. Candidate resistance ORFs span diverse gene categories. Heat map generated with Morpheus software comparing median LFC of ORF representation at the end of the screen versus the early time point for all treatments. Gene ontology guided categorization of ORFs shown below. Deepest red color indicates LFC $\geq$ 4.

tamoxifen (a canonical selective ER modulator) responded to the receptor tyrosine kinase inhibitor gefinitib (171). Gefinitib targets the EGFR growth factor receptors. These results have prompted clinical investigation of combining EGFR pathway inhibitors with endocrine therapy

Previously characterized cell cycle genes such as CDK6 (249) and CCNE2 (250) also scored in the FBS CDK inhibitor arms of the screen (**Fig. 3.1C**). CDK6 was the top resistance driver under FBS abemaciclib treatment and validated in short-term dose response studies (**Fig. 3.4A-B**). While largely absent from normal breast tissue, lower molecular weight (LMW) isoforms of cyclin E1 are specifically generated in breast cancer cells and are associated with poor prognosis (272-275). LMW cyclin E1 proteins have previously been shown to constitutively activate CDK2 and drive S phase progression (276). In our screen and validation studies, expression of an N-terminally truncated cyclin E2 ORF confers resistance to palbociclib and abemaciclib in FBS media **(Table 3.1-3.2 and Fig. 3.4 C-D**)**.** These findings are consistent with CDK2 activation driving resistance to palbociclib in full serum (219,277).

AKT confers resistance to CDK4/6 inhibition.

To identify nodes of resistance to CDK4/6 inhibition, we compared resistance profiles for palbociclib and abemaciclib as single agents in FBS and in combination with estrogen deprivation (CSS). Members of the protein kinase b (AKT) family (AKT1, AKT2 and AKT3) were consistently nominated as resistance genes across all treatments in our screen (**Fig. 3.1C** and **Fig. 3.1D**). In many instances, both constitutively active (myristolated) and wild-type ORFs encoding the same AKT family member also score. AKT is a serine/threonine kinase that acts downstream of receptor tyrosine kinases to promote cell cycle progression and survival (278). KRAS and EGFR mutants, which have previously been shown to upregulate AKT activity (279,280) also conferred resistance to combined estrogen deprivation and CDK4/6 inhibition. Secondary screens were conducted in T47D cells with FBS, FBS+1 μM palbociclib, CSS and

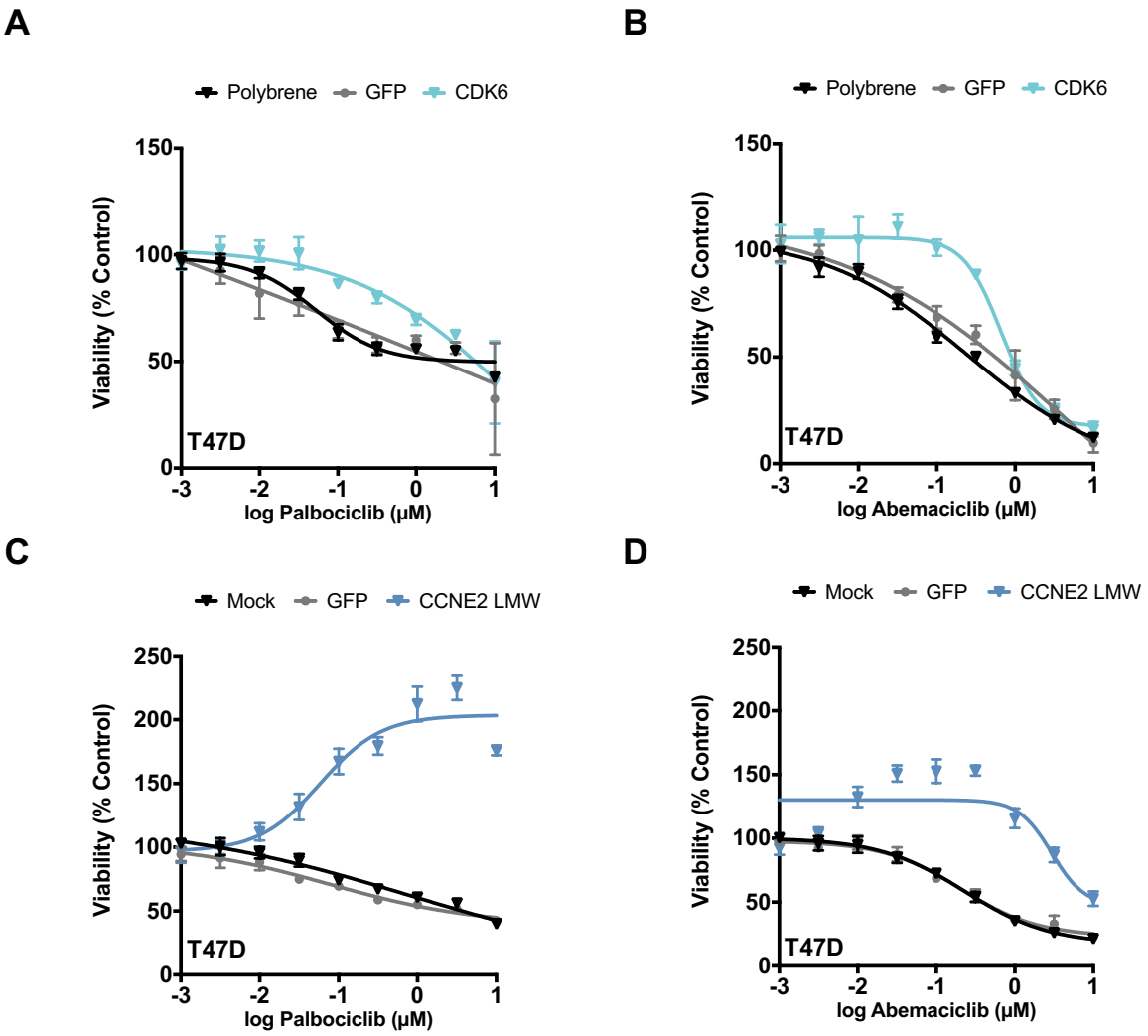

Figure 3.4. Validation of cell cycle genes. (A-D) T47D Cells were plated in 96-well format, infected with lentivirus encoding indicated ORFs and grown in FBS with increasing concentrations of CDK4/6 inhibitor. Viability was measured with the WST-1 assay 6 days after treatment. Mean viability +/- SD for 3 (A, B, and D) or 6 (C) replicates is shown. CCNE2 lower molecular weight (LMW) ORF encodes N-terminally truncated CCNE2 protein. GFP used in CCNE2 LMW studies is in pLX307 vector (same as pLX317 except no barcode).

CSS + 1 μM palbociclib and lasted two weeks. ORFs encoding all three AKT isoforms, activated EGFR and activated KRAS did not confer a growth advantage in FBS media but were once again enriched (with a z-score greater than 3) under palbociclib treatment (**Fig. 3.5A-3.5D**). AKT activation (indicated by phosphorylation at serine 473 and threonine 308 has been associated with hormone refractory ER+ breast cancer (156,159) and 3-5% of breast cancers harbor the activating E17K mutation in AKT1 (281). Therefore, we investigated AKT activation as a node of resistance to CDK4/6 inhibition.

To determine the generalizability of our findings, we generated dose response curves for cells expressing AKT1, AKT2 and activated EGFR ($EGFR^{L858R}$) with palbociclib and abemaciclib. In estrogen-rich FBS media, AKT1 and AKT2 consistently shifted the GI_{50} of three ER+ breast cancer cell lines (T47D, MCF7 and ZR-75-1) by 10-fold relative to controls (**Fig. 3.6A**-**3.6B**). As in the primary screen, $EGFR^{L858R}$ cells were comparatively less resistant to CDK4/6 inhibition in FBS media (**Fig. 3.6A**-**3.6B**). Addition of a src myristolation sequence to AKT targets AKT to the plasma membrane and renders AKT constitutively active (282). Myristolated AKT1 (myr-AKT) also conferred resistance to CDK4/6 inhibition in FBS media **(Fig. 3.6C)**. Thus, expression of wild-type AKT1/2 or myr-AKT sufficiently drives resistance to CDK4/6 inhibitor monotherapy.Since CDK4/6 inhibitors are only FDA-approved in combination with endocrine therapy (232,252,256), clinically relevant genes must confer resistance to combination therapy. While myr-AKT has a viability disadvantage in FBS media, the construct drives resistance to estrogen deprivation (CSS) (**Fig. 3.6D**). Similar results were observed in the secondary screens in which myr-AKT ORFs were relatively depleted in FBS media but enriched in CSS media (**Fig. 3.5A** and **3.5C**). Constitutive AKT signaling may be lethal in the absence of a selection pressure. Myr-AKT increased the viability of T47D and MCF7 cells 2-3 fold in CSS media relative to controls (**Fig. 3.6D**). To determine whether constitutive activation of AKT renders cells insensitive to combination therapy, we also treated myr-AKT cells with palbociclib in CSS media. Myr-AKT conferred resistance to CDK4/6 inhibition even in CSS (**Fig. 3.6E**). Similarly,

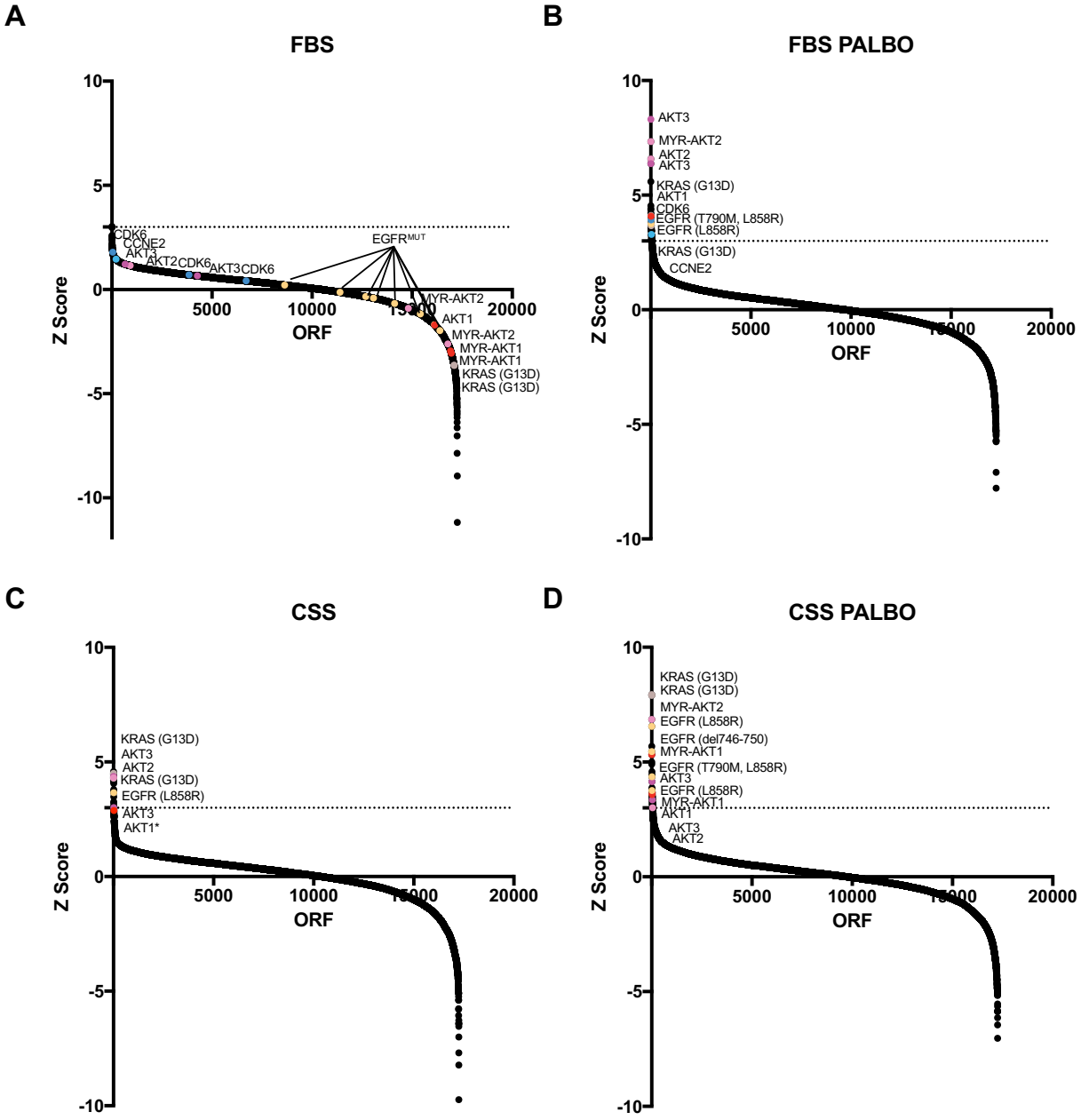

Figure 3.5. Secondary screens. (A-D) Z score distribution of median LFC for ORFs in each screening arm of secondary screens. ORFs corresponding to candidate resistance genes from primary screen are highlighted. Dotted line indicates z=3. In CSS treatment, AKT1 ORF had a z score of 2.89 and noted with * (just under the cut-off).

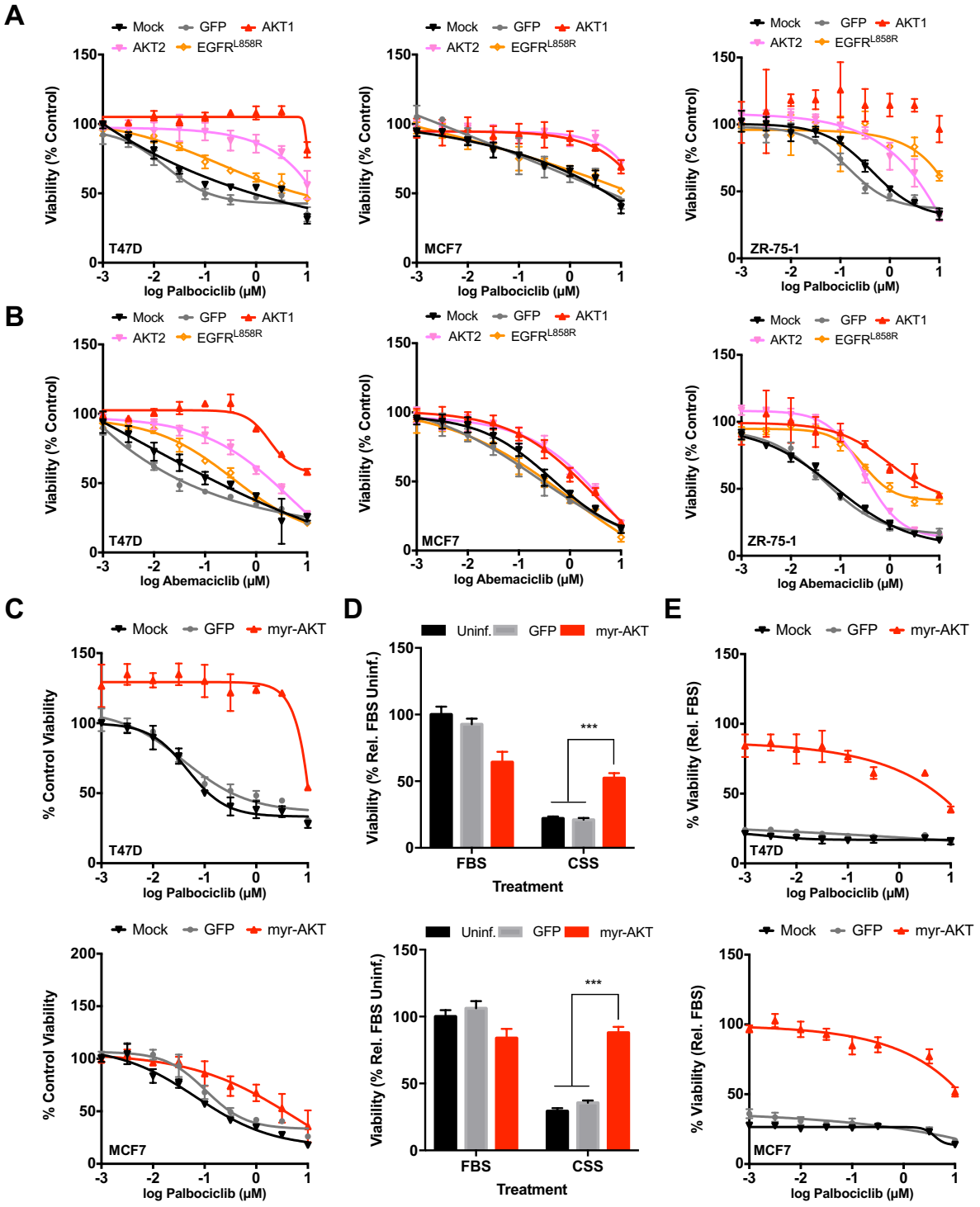

Figure 3.6. AKT mediates resistance to CDK4/6 inhibition. (A-C) Cells were seeded in 96-well plates, infected with ORF-encoding lentivirus and treated with CDK4/6 inhibitor in FBS media for 6 days. Mean viability relative to vehicle treatment +/- SD, n = 3. **(D-E)** Cells were similarly infected, switched to CSS media to remove residual estrogen and treated for six days in FBS or CSS media +/- palbociclib. Uninf. = uninfected cells. ***P<0.001. In (D), viability is relative to uninf. FBS, n = 6. In (E), values are relative to each ORF's viability in FBS, n = 3.

AKT1, AKT2 and EGFR^{L858R} drive estrogen- and CDK4/6-independent growth (**Fig. 3.7A-3.7B**). Thus, activated AKT sufficiently bypasses dual CDK4/6 inhibition and estrogen deprivation.

AKT activation maintains RB phosphorylation to prevent CDK4/6 inhibitor-mediated G1 cell cycle arrest.

Resistance to targeted agents often involves re-engagement of the targeted pathway. For example, PIM1 mediates resistance to PI3K inhibition by phosphorylating downstream targets of AKT (178). Furthermore, re-activation of the MAPK pathway confers resistance to RAF or MEK inhibitors in *BRAF*-mutant melanoma (283,284). Since palbociclib and abemaciclib induce a G1/S cell cycle arrest by preventing RB phosphorylation (4,6,7,285), we next assessed whether AKT-mediated resistance modulated RB phosphorylation. T47D cells expressing AKT1, AKT2, or activated EGFR were first grown in CSS media to remove residual estrogen and subsequently co-treated with 100nM palbociclib or 30nM abemaciclib for 48 hours. Treatment with either CDK4/6 inhibitor significantly decreased RB phosphorylation in control GFP-expressing cells. In contrast, AKT1-, AKT2- and EGFR^{L858R}-expression sustained RB phosphorylation despite CDK4/6 inhibitor treatment (**Fig. 3.7C-3.7D**). These data suggest that cells with activated AKT can inactivate RB to bypass CDK4/6 inhibition.

Mechanistically, AKT can induce S phase by promoting cyclin D1 stability (134,286,287). Expression of AKT1, AKT2, or EGFR^{L858R} maintained AKT phosphorylation at serine 473 in cells cultured in CSS and palbociclib or abemaciclib. We also observed GSK3β phosphorylation at serine 9, a downstream target of AKT. Phosphorylation of GSK3β by AKT inactivates GSK3β, so GSK3β can no longer target cyclin D1 for degradation, resulting in stabilized cyclin D1 levels (**Fig. 3.7C-3.7D**). These biochemical changes are accompanied by S phase progression. Under CSS and palbociclib treatment, only 1.8% of parental and 3% of GFP-expressing cells are in S phase (**Fig. 3.7E**). In contrast, 9.2%, 5.4% and 7.1% of AKT1-, AKT2- or EGFR^{L858R} – expressing cells parental cells respectively are in S phase under CSS and palbociclib treatment.

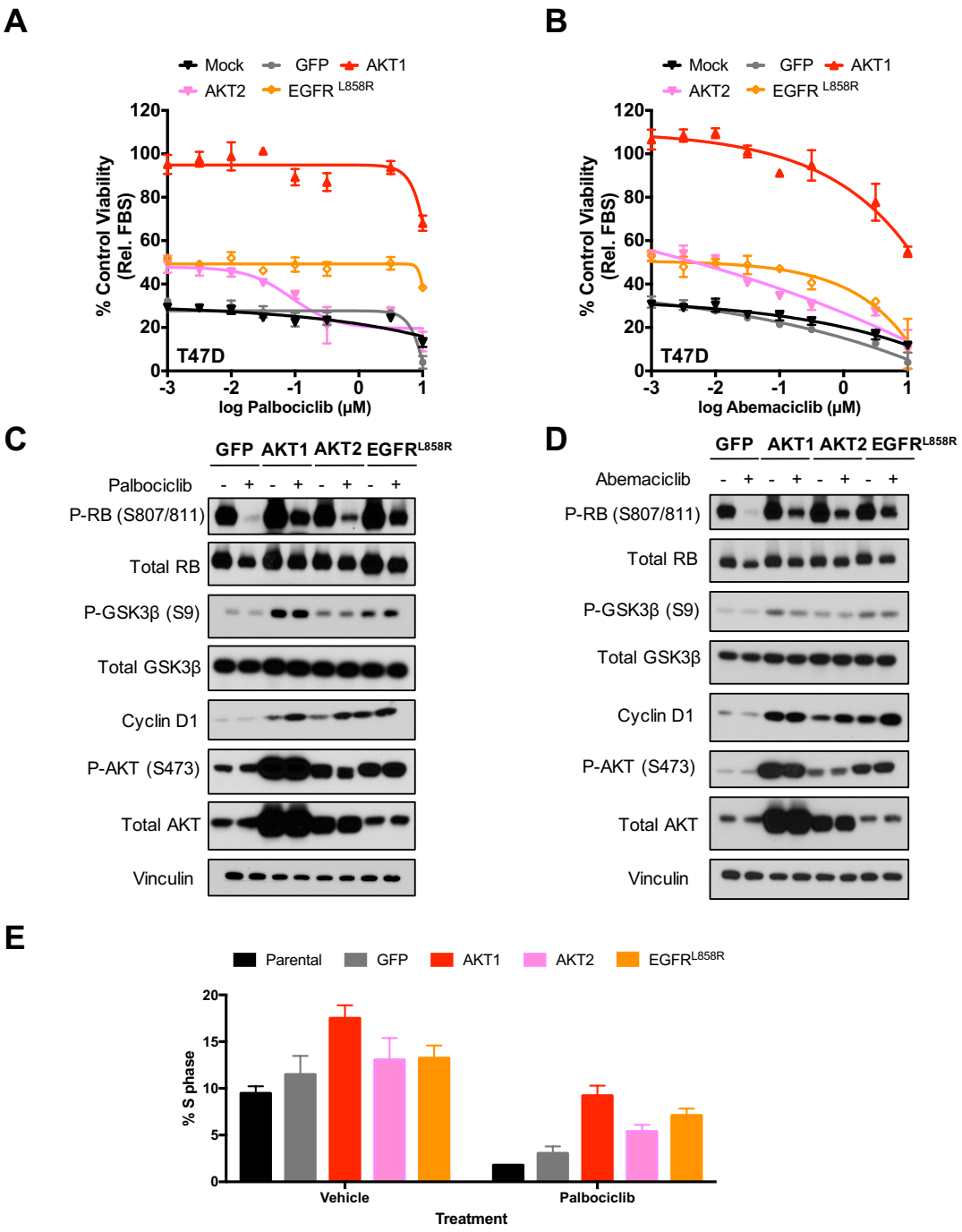

Figure 3.7. AKT drives S phase despite CDK4/6 inhibition and estrogen deprivation. (A-B) Cells were spin-infected with virus, switched to CSS media and then treated with inhibitor for 6 days. Mean viability +/- SD relative to each ORF's growth in FBS media, n=3. **(C-D)** ORF-infected T47D cells were plated and grown in CSS media for two days followed by treatment with 100nM palbociclib or 30nM abemaciclib in CSS media for 48 hours. Cell lysates were analyzed by western blot. **(E)** Cells were treated as in (C-D), fixed and stained with propidium iodide for cell cycle analysis. Mean +/- SD. Representative of N=2. **See also Figure 3.8D.**

Notably, the extent of AKT phosphorylation at serine 473 correlated with RB phosphorylation at serine 807/811 under CDK4/6 inhibitor treatment and with the extent of the rescue. AKT1 expression induced the highest pathway activation (AKT phosphorylation, cyclin D1 expression and RB phosphorylation) (**Fig. 3.7C-3.7D**) and produced the greatest resistance to CDK4/6 inhibition in CSS (**Fig. 3.7A-3.7B**). These results raise the possibility that AKT-mediated resistance to CDK4/6 may be due in part to stabilization of cyclin D1.

AKT pathway inhibition sensitizes cells with activated AKT to CDK4/6 inhibition.

To determine whether the observed effects were on target, we also treated cells with MK-2206, an AKT inhibitor (288). Triple combination treatment (with CSS, CDK4/6 inhibitor and MK-2206) reduced AKT-mediated resistance. MK-2206 sensitized cells with activated AKT to palbociclib treatment (**Fig. 3.8A**). When used with palbociclib or abemaciclib under estrogen-deprived conditions, MK-2206 decreased RB phosphorylation and counteracted cyclin D1 stabilization in cells expressing AKT1, AKT2 and to a lesser extent $EGFR^{L858R}$ (**Fig. 3.8B**). AKT can also promote cell cycle progression by phosphorylating the cell cycle inhibitor p21 (289,290). Phosphorylation by AKT at threonine 145, has also been reported to sequester p21 in the cytoplasm (289) and disrupt its interaction with CDK2 (150). We also observed AKT-dependent phosphorylation of p21 at threonine 145; in cells with activated AKT, p21 phosphorylation is diminished with MK-2206 treatment (**Fig. 3.8B**). Thus, AKT likely activates CDK2 to promote RB phosphorylation and bypass of CDK4/6 inhibition. Cells with activated AKT also maintained CDK2 phosphorylation at threonine 160 under CDK4/6 inhibitor treatment, which is required for CDK2's kinase activity (**Fig. 3.8B**) (291). With triple combination therapy, however, CDK2 phosphorylation was reduced in AKT1- and AKT2-expressing cells (**Fig. 3.8B**), which corresponded to a greater suppression of S phase in AKT1- and AKT2-expressing cells compared to CDK4/6 inhibition (**Fig. 3.8C**). Consistent with the residual RB phosphorylation detected in $EGFR^{L858R}$ cells after treatment with CDK4/6, MK-2206 and CSS, there was a

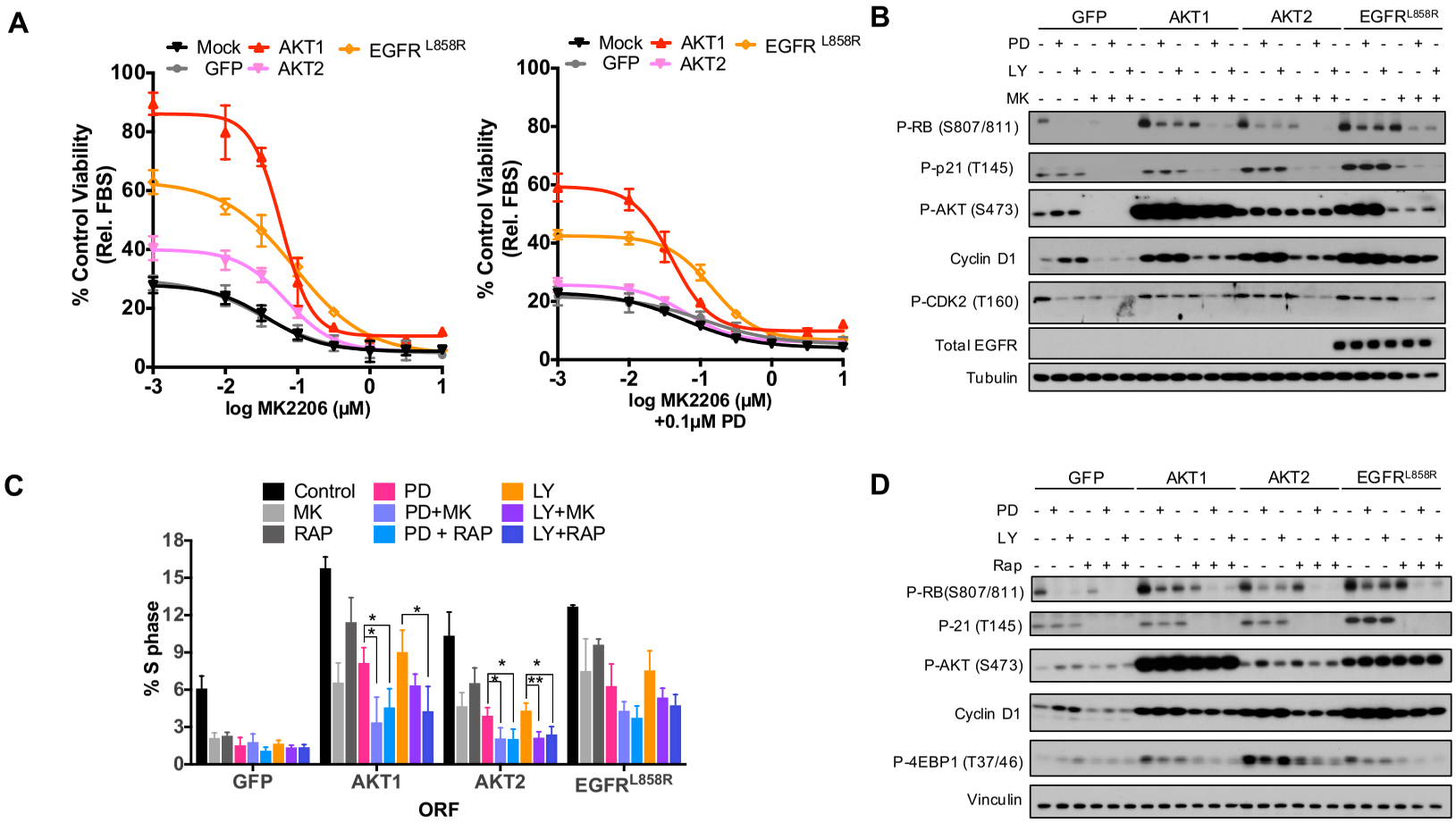

Figure 3.8. AKT-mediated resistance to CDK4/6 inhibition is mTOR-dependent. (A) T47D cells were infected in 96-well format, grown in CSS media (+/- 0.1μM PD) and treated with increasing concentrations of MK-2206. Viability was assessed with the WST-1 assay 6 days later. Mean viability relative to each ORF's viability in FBS +/- SD for 3 replicates is shown. **(B)** ORF-infected T47D cells were plated into 6-well plates and grown in CSS media for four days to remove residual estrogen. Cells were subsequently treated with 100nM palbociclib (PD). 30nM abemaciclib (LY) and/or 500nM MK-2206 (MK) in CSS media for 48 hours. Cell lysates were analyzed by western blot. **(C)** Cells were treated as in (B) +/-20nM rapamycin (Rap) and stained with propidium iodide for cell cycle analysis. Mean % cells in S phase +/- SD for 3 replicates is shown. For unpaired two tail t-test, *p<0.05, **p<0.01. **(D)** Cells were treated as in (C). Control, PD and LY lysates are the same as in (B); samples were obtained in parallel on the same day.

reduction in S phase with triple combination therapy compared to dual inhibition, but this was not statistically significant in $EGFR^{L858R}$ cells (**Fig. 3.8C**). Our results indicate that co-treatment with MK-2206 allows for palbociclib and abemaciclib to induce cell cycle arrest in AKT-activated cells under estrogen-deprived conditions.

Since mTOR is another key downstream effector of AKT signaling (292-294), we next investigated whether mTOR inhibition would counteract AKT-mediated resistance to palbociclib and abemaciclib. mTOR promotes cell growth through two distinct complexes, mTORC1 and mTORC2. AKT upregulates mTOR activity by phosphorylating and inactivating negative regulators of the mTORC1 complex (TSC1, TSC2 and PRAS40) (292-294). In contrast, rapamycin is a compound that interacts with FKBP12 to inhibit mTORC1 activity (295). As with MK-2206, rapamycin in combination with CDK4/6 inhibition reduced the percentage of AKT1- and AKT2-expressing cells in S phase compared to CDK4/6 inhibitor alone (**Fig. 3.8C**). Rapamycin co-treatment similarly decreased the percentage of $EGFR^{L858R}$ cells in S phase but the change was not significant. Suppression of S phase was reflected in a decrease in RB phosphorylation in all cells (**Fig. 3.8D**). Furthermore, rapamycin treatment also partially reduced cyclin D1 levels in resistant cells (**Fig. 3.8D**). These results suggest that AKT-mediated RB inactivation and subsequent S phase progression is mTOR-dependent.

To account for cell line-specific effects, we also overexpressed AKT1, AKT2 and activated EGFR in MCF7 cells. As observed with T47D cells, all three ORFs conferred resistance to combination treatment with CSS and palbociclib or abemaciclib (**Fig. 3.9A-3.9B**). AKT1 also maintained RB phosphorylation and stabilized cyclin D1 levels in MCF7 cells compared to GFP-expressing cells when treated with palbociclib in CSS (**Fig. 3.9C**). Co-treatment with MK-2206 reduced RB phosphorylation in resistant cells (**Fig. 3.9C**). AKT1 expression also increased levels of phospho-S6, a mTOR downstream effector. As previously observed, co-treatment with CSS, palbociclib and rapamycin decreased RB phosphorylation

Figure 3.9. Validation in MCF7 cells. (A-B) MCF7 cells were infected in 96-well format, grown in CSS media and treated with increasing concentrations of CDK4/6 inhibitor. Viability was assessed with the WST-1 assay 6 days later. Mean viability is relative to each ORF's viability in FBS +/- SD, n=3. **(C)** ORF-infected cells were grown in CSS media for two days to remove residual estrogen and then treated with 100nM palbociclib (PD), 250nM MK-2206 (MK) and/or 100nM rapamycin (rap) in CSS media for 48 hours. Western blot analysis shown. **(D)** Cells were treated as in (C) and stained with propidium iodide for cell cycle analysis. **(E)** As in (D) except with 30nM abemaciclib (LY), 500nM MK and 100nM everolimus (E). Mean +/- SD is shown. n=2 or 4 with *$p<0.05$ and **$p<0.01$ by unpaired two tail student t-test.

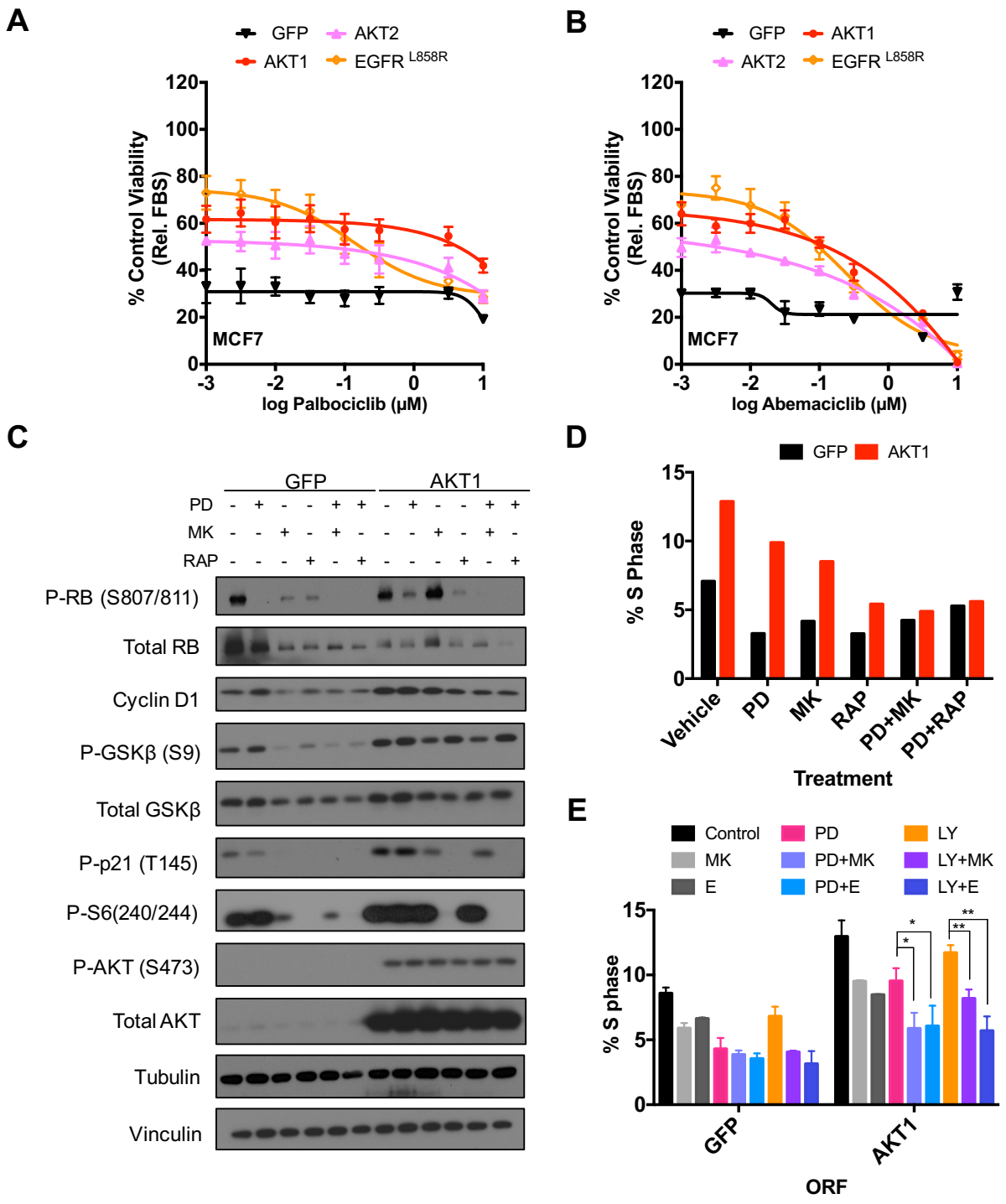

Figure 3.9 (Continued).

relative to CSS and palbociclib (**Fig. 3.9C**). Cell cycle analysis further confirmed that resistance to CDK4/6 inhibition in AKT1-expressing cells is AKT- and mTOR-dependent (**Fig. 3.9D-3.9E**). We also tested another mTOR inhibitor (everolimus) and observed a similar reduction in S phase when combined with CDK4/6 inhibitor treatment in cells overexpressing AKT1 (**Fig. 3.9E**). Thus, AKT activation maintains RB phosphorylation to bypass CDK4/6 inhibition in a mTOR-dependent manner.

Palbociclib- and abemaciclib-resistant cells respond to AKT inhibition.

To complement our screens, we have generated *in vitro* models of acquired resistance to palbociclib and abemaciclib. T47D cells were chronically cultured in the presence of 1μM or 0.3μM abemaciclib in FBS media until resistant populations emerged. Palbociclib-resistant ($Palbo^R$) cells were cross-resistant to abemaciclib (**Fig. 3.10A**). Similarly, abemaciclib-resistant ($Abema^R$) cells were insensitive to palbociclib (**Fig. 3.10B**). Whereas palbociclib and abemaciclib treatment decreased RB phosphorylation in parental cells, resistant cells maintained RB phosphorylation (**Fig. 3.10C**).

While resistant cells did not have higher AKT phosphorylation at serine 473 compared to parental cells, there was a small but reproducible decrease in AKT phosphorylation when cultured to resistance cells were grown in the absence of CDK4/6 inhibitor (vehicle only) (**Fig. 3.10C**). This reduction in AKT phosphorylation upon drug withdrawal is generally more pronounced when cells were plated in the absence of CDK4/6 inhibitor overnight prior to re-treatment. We also noticed that $Palbo^R$ and $Abema^R$ cells did not attach well at low density compared to parental cells when plated in the absence of CDK4/6 inhibitor. These results suggest that there is feedback regulation whereby cells with acquired resistance may be dependent on CDK4/6 inhibitor treatment to upregulate AKT phosphorylation. A recent publication showed that CDK4/6 inhibition induces AKT activation in ER-negative breast cancer

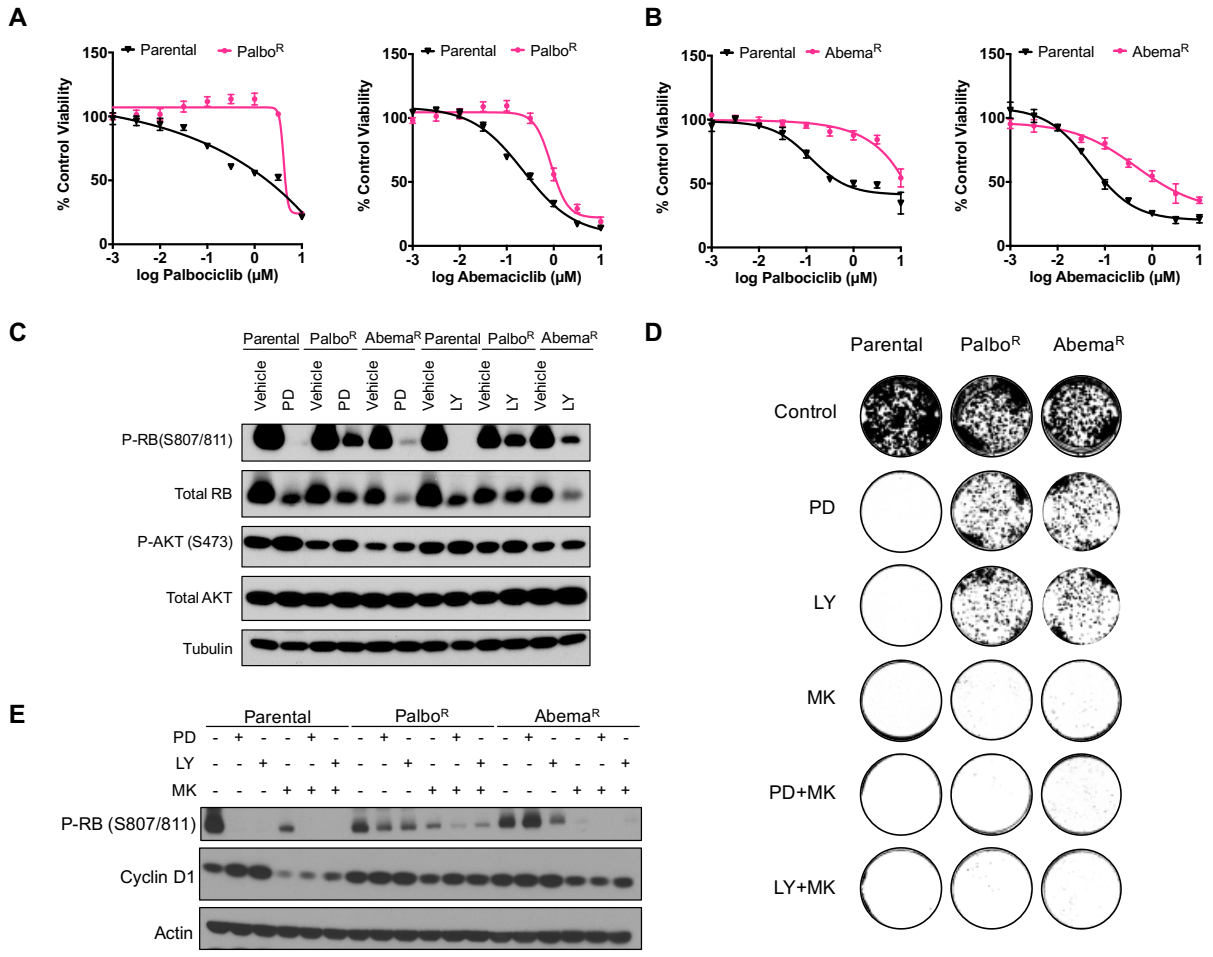

Figure 3.10. Cultured to resistance cells are sensitive to AKT inhibition. (A-B) Parental, palbociclib-resistant (Palbo^R) and abemaciclib-resistant (Abema^R) T47D cells were treated with CDK4/6 inhibitors for 6 days. Mean viability relative to vehicle control +/- SD with n= 3 or 6. **(C)** Immunoblot analysis of cells plated in the absence of CDK4/6 inhibitor and subsequently treated the next day with 1μM palbociclib (PD) or 0.3μM abemaciclib (LY) for 48 hours. **(D)** Cells were plated in native growing condition (with CDK4/6 inhibitor for resistant cells) overnight prior to drug treatment with 1μM PD, 0.3μM LY and/or 0.5μM MK-2206 (MK) for two weeks. Colonies were stained with crystal violet. Image representative of triple wells. All experiments in figure were conducted in FBS media. **(E)** Immunoblot analysis of cells treated as in (D) but lysates were taken 48 hours after drug treatment.

cells with intact RB (296). In these cells, palbociclib treatment relieves negative feedback regulation of hyperphosphorylated RB on mTORC2, which promotes AKT phosphorylation at serine 473 (296). To determine whether AKT inhibition may sensitize cells to CDK4/6 inhibition, we treated cultured to resistance cells with MK-2206 and palbociclib. Palbo^{R} and Abema^{R} cells were sensitive to MK-2206 monotherapy in colony formation assays (**Fig. 3.10D**), but combined MK-2206 and CDK4/6 inhibition induced the greatest suppression of RB phosphorylation and prevented growth of resistant cells (**Fig. 3.10D and 3.10E**). Ribociclib cultured to resistance cells are similarly sensitive to AKT inhibition (247). Thus, breast cancer cells with acquired resistance to CDK4/6 inhibition respond to AKT inhibition.

Activating mutations in AKT1 but not PIK3CA are associated with acquired resistance to CDK4/6 inhibition in breast tumor biopsies.

Consistent with findings from the PALOMA-3 clinical trial (234), ORFs encoding oncogenic *PIK3CA* point mutants generally showed low enrichment and did not drive resistance to CDK4/6 inhibition in the primary screen (**Fig. 3.11**). The highest median LFC enrichment for all *PIK3CA* ORFs was 2.07 under CSS abemaciclib treatment (H1047Y mutant, **Fig. 3.11**), whereas ORFs encoding wild-type or myristolated AKT consistently scored with a median LFC enrichment between 2.9 and 7. T47D and MCF7 cells also harbor *PIK3CA* mutations, but are sensitive to CDK4/6 inhibition. Preliminary analysis of breast cancer biopsies from the Center for Cancer Precision Medicine further indicates that *PIK3CA* mutations do not stratify patient response to palbociclib and aromatase inhibitor therapy. Both sensitive and resistant samples harbor *PIK3CA* mutations (Seth Wander and Nikhil Wagle, unpublished data). In contrast to *PIK3CA*, ORFs encoding AKT1 and AKT2 were highly enriched under palbociclib and abemaciclib treatment (**Fig. 3.11**). Furthermore, only wild-type AKT1 and AKT2 constructs that did not express a V5 tag were nominated as resistance drivers. The V5 tag likely disrupts

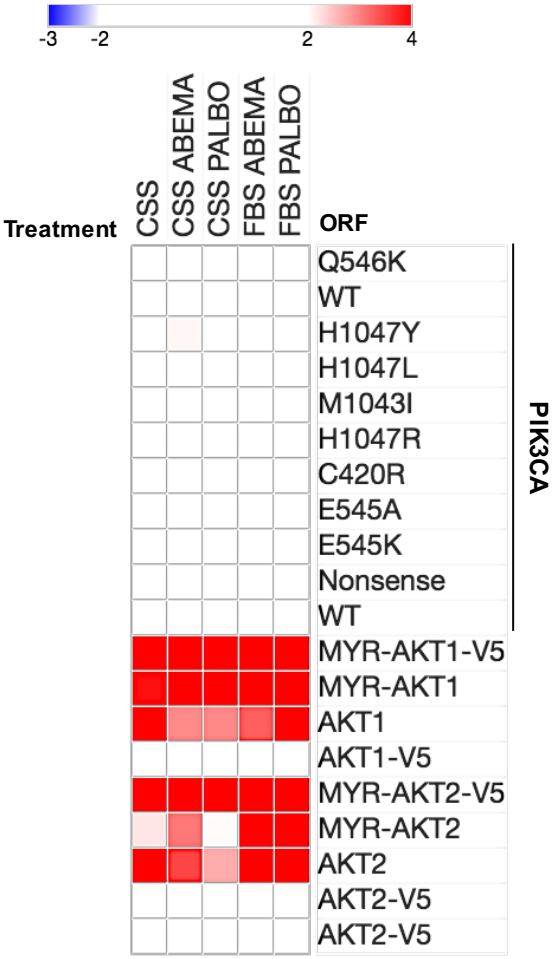

Figure 3.11. Enrichment of PIK3CA- and AKT-encoding ORFs from the primary screen. Heat map of median LFC enrichment for each ORF in the primary screen. Red color indicates median LFC $\geq$ 4. Figure generated with Morpheus software from the Broad Institute.

protein function. Therefore, our screening data and follow-up studies indicate that AKT activation not oncogenic *PIK3CA* mutations sufficiently drives resistance to CDK4/6 inhibition.

Next, we assessed the clinical relevance of AKT activation in biopsies from metastatic breast cancer patients. Targeted genomic sequencing (OncoPanel) and whole exome sequencing (WES) were performed on more than 150 patients with metastatic breast cancer at the Dana-Farber Cancer Institute (297,298). Samples were filtered to identify *AKT*-mutant breast cancer patients, who received CDK4/6 inhibitor therapy (see also Materials and Methods). Pleckstrin homology (PH) domain mutations in *AKT1* were identified in three ER+ breast cancer patients following clinical progression on various CDK4/6 inhibitors (**Figs. 3.12**-**3.14**). The three *AKT1* mutations were: W80R (patient 1, **Fig. 3.12**), a canonical E17K activating mutation (patient 2, **Fig. 3.13**), and L52H (patient 3, **Fig. 3.14**). While the exact W80R and L52H variants have not been previously characterized, mutation of each of the three residues is predicted to disrupt the interaction between the PH and kinase domain of AKT and have been shown to activate AKT (299). Furthermore, these mutations are predicted to be deleterious via COSMIC database. A full list of all mutations detected by OncoPanel for each of the three patients is provided (**Table 3.6**). Immunohistochemistry staining is currently available only for biopsies following progression on CDK4/6 inhibitor but pre-treatment stains are underway.

Patient 1 was originally diagnosed with a locally advanced ER+/HER2- breast cancer at the age of 41 years old (**Fig. 3.12A**). Targeted sequencing of a biopsy obtained at the time of her diagnosis revealed a rare but oncogenic N345K mutation in *PIK3CA* (300) but no mutations in AKT1. The patient received two lines of adjuvant treatment and subsequently progressed with metastatic disease. In the third-line metastatic setting, the patient received fulvestrant and ribociclib and responded for one year before acquiring resistance. Another biopsy was taken approximately 6-12 months after ribociclib therapy. Sequencing of this post-treatment biopsy revealed both the initial *PIK3CA* mutation and a missense W80R mutation in *AKT1* (**Fig. 3.12A**).

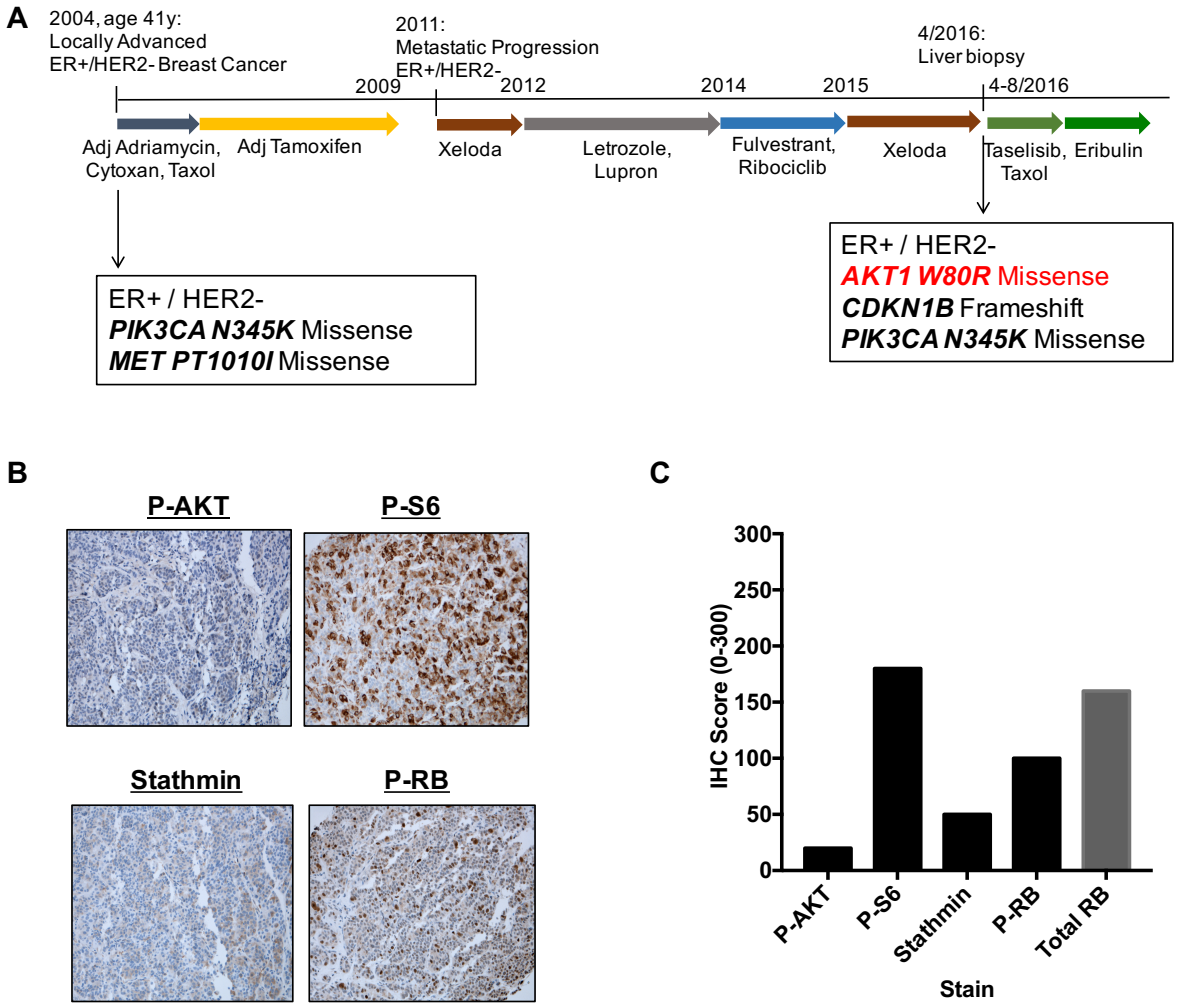

Figure 3.12. Clinical summary for patient 1. (A) Each of the patient's treatments are indicated by a multi-colored arrow with the associated regimen listed below. The length of each arrow is proportional to the duration on therapy. Biopsies are indicated by perpendicular arrows with associated targeted sequencing results for cancer-associated mutations by OncoPanel. **(B)** Representative photomicrographs are included for the IHC stain of post CDK4/6 inhibitor treatment biopsy specimens included for p-AKT (S473), p-S6 (235/236), stathmin and p-RB (S807/811). (All 200x magnification). **(C)** IHC quantification for p-AKT and related signaling molecules from (B). IHC score for total RB also shown. The IHC score is derived by multiplying the percent of tumor cells staining positive in a clinical specimen by the average intensity of the stain (graded 1-3; dynamic range 0-300).

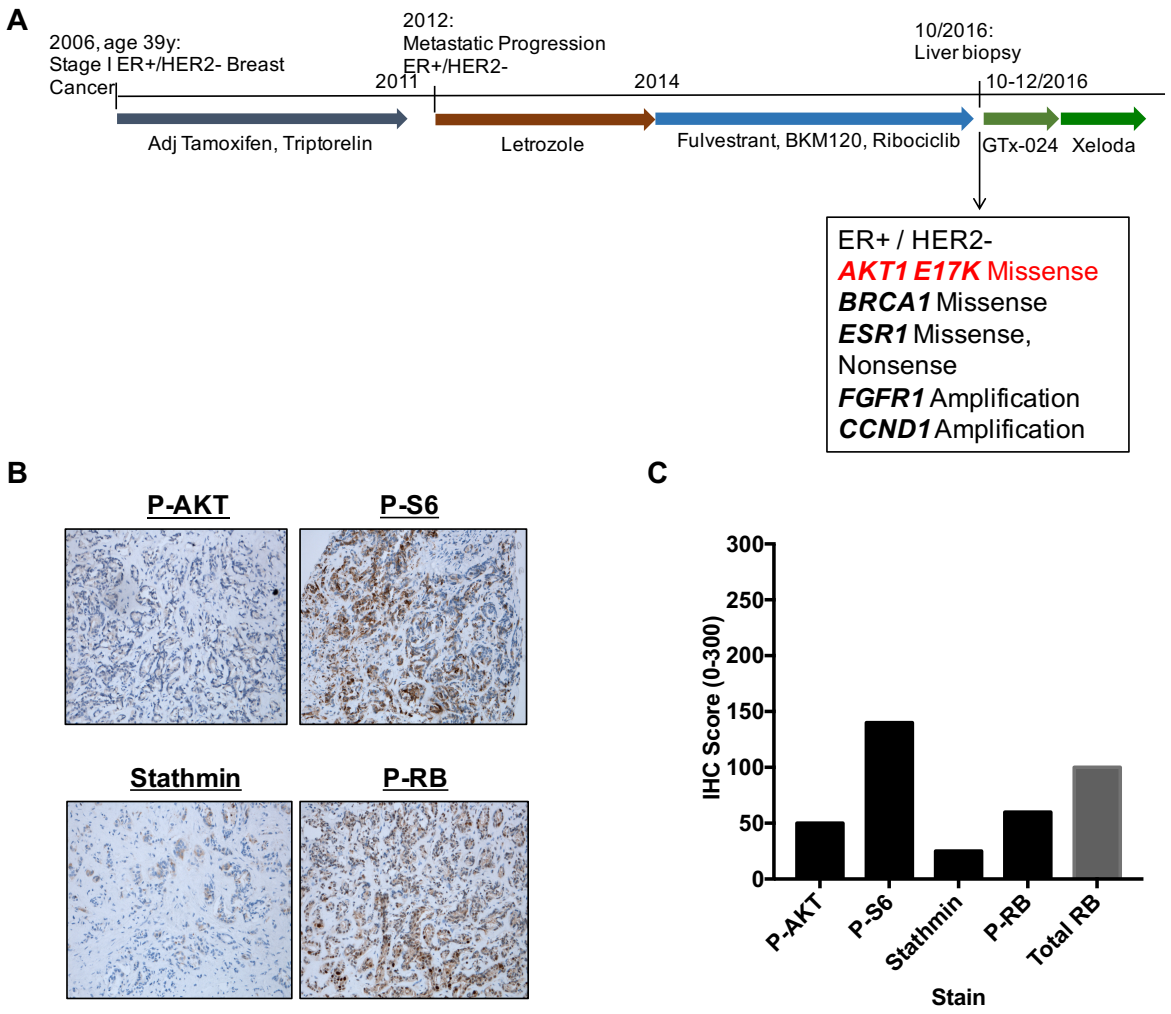

Figure 3.13. Clinical summary for patient 2. (A) Each of the patient's treatments are indicated by a multi-colored arrow with the associated regimen listed below. The length of each arrow is proportional to the duration on therapy. Biopsies are indicated by perpendicular arrows with associated targeted sequencing results for cancer-associated mutations by OncoPanel. **(B)** Representative photomicrographs are included for the IHC stain of post CDK4/6 inhibitor treatment biopsy specimens for p-AKT (S473), p-S6 (235/236), stathmin and p-RB (S807/811). (All 200x magnification). **(C)** IHC quantification for p-AKT and related signaling molecules from (B). IHC score for total RB also shown. The IHC score is derived by multiplying the percent of tumor cells staining positive in a clinical specimen by the average intensity of the stain (graded 1-3; dynamic range 0-300).

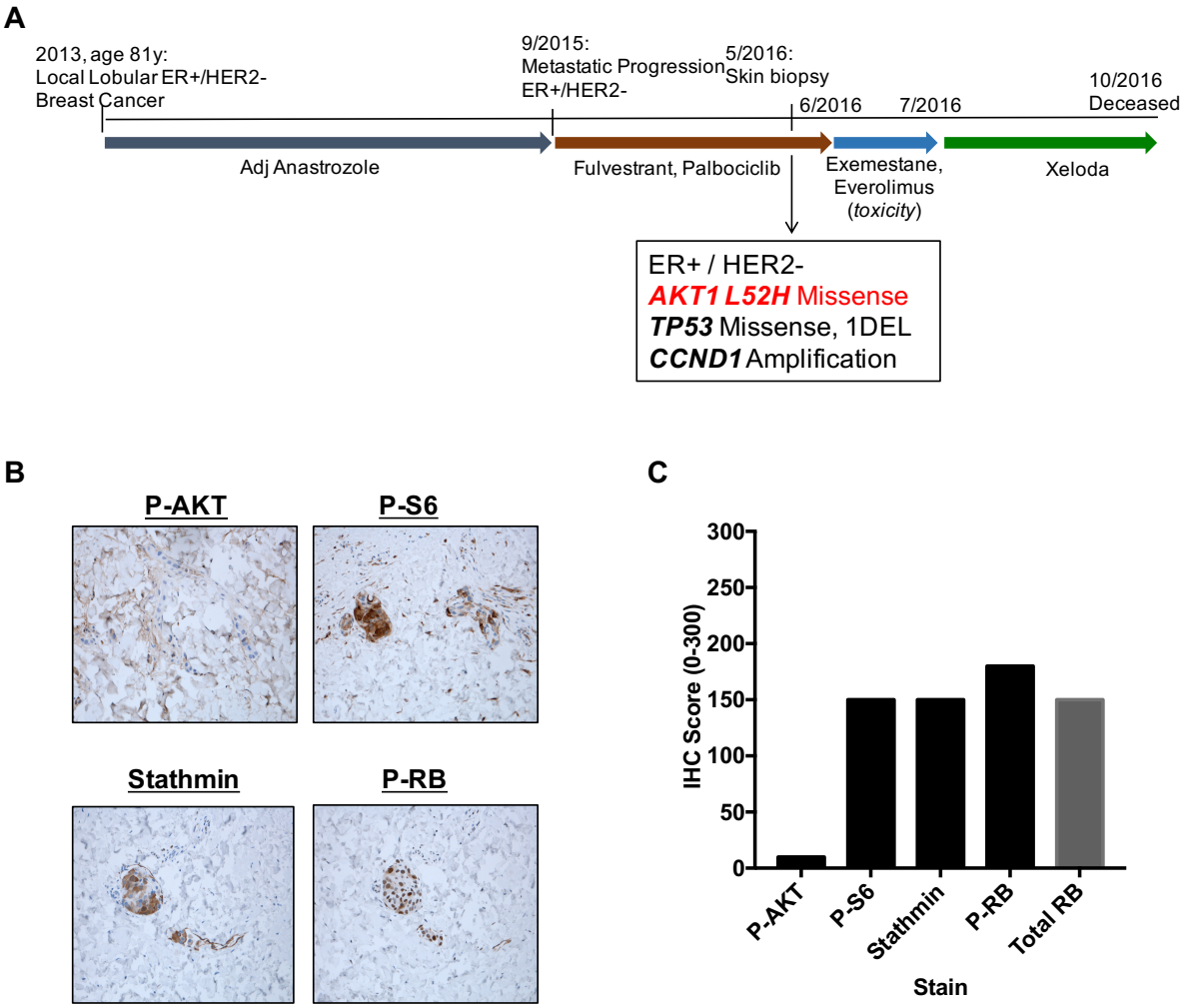

Figure 3.14. Clinical summary for patient 3. (A) Each of the patient's treatments are indicated by a multi-colored arrow with the associated regimen listed below. The length of each arrow is proportional to the duration on therapy. Biopsies are indicated by perpendicular arrows with associated targeted sequencing results for cancer-associated mutations by OncoPanel. **(B)** Representative photomicrographs are included for the IHC stain of post CDK4/6 inhibitor treatment biopsy specimens for p-AKT (S473), p-S6 (235/236), stathmin and p-RB (S807/811). (All 200x magnification). **(C)** IHC quantification for p-AKT and related signaling molecules from (B). IHC score for total RB also shown. The IHC score is derived by multiplying the percent of tumor cells staining positive in a clinical specimen by the average intensity of the stain (graded 1-3; dynamic range 0-300).

Table 3.6. Mutations detected by OncoPanel.

Patient #	Gene	Mutation Type	Mutation	Variant Allele Fraction	Coverage
1	AKT1	Missense	c.238T>C (p.W80R), exon 4	24.4604	139
1	ALOX12B	Missense	c.1148C>T (p.T383M), exon 9	25	168
1	ARID1B	Inframe_Ins	c.189_190insCAGCAG (p.Q62_Q63dup), exon 1	33.649289	211
1	CDKN1B	Frameshift	c.279_280insC (p.K96Qfs*29), exon 1	43.3006535	612
1	SYK	Missense	c.1897G>A (p.V633M), exon 14	48.954	239
1	MAP3K1	Frameshift	c.3369_3382delTGTCAATACAGAGC (p.V1124Qfs*5), exon 14	16.2376237	505
1	BUB1B	Missense	c.1826G>T (p.C609F), exon 15	48.125	480
1	PIK3CA	Missense	c.1035T>A (p.N345K), exon 5	37.3802	313
1	AKT3	LA			
1	ARID1A	1DEL			
1	ARID2	LA			
1	BAP1	1DEL			
1	BRCA2	1DEL			
1	CADM2	1DEL			
1	CARD11	LA			
1	CD58	1DEL			
1	CDC73	LA			
1	CDH1	1DEL			
1	CDK2	LA			
1	CDK4	LA			
1	CDK6	LA			
1	CDKN1B	LA			
1	CDKN2C	1DEL			
1	CHEK2	1DEL			
1	CIITA	LA			
1	CREBBP	LA			
1	CRKL	1DEL			
1	CRTC2	LA			
1	CSF3R	1DEL			
1	CUX1	LA			
1	CYLD	1DEL			
1	DDR2	LA			
1	DEPDC5	1DEL			
1	DIS3	1DEL			
1	EGFR	LA			
1	EP300	1DEL			
1	ERBB3	LA			
1	ERCC4	LA			
1	ERCC5	1DEL			
1	ETV1	LA			
1	ETV6	LA			
1	EWSR1	1DEL			
1	EXT1	LA			
1	FAM46C	1DEL			
1	FANCA	1DEL			
1	FGFR1	LA			
1	FH	LA			
1	FKBP9	LA			
1	FLT1	1DEL			
1	FLT3	1DEL			
1	FUS	LA			
1	GATA4	LA			
1	GLI1	LA			
1	GLI3	LA			
1	GSTM5	1DEL			
1	H3F3A	LA			
1	ID3	1DEL			
1	IKZF1	LA			
1	KMT2D	LA			
1	KRAS	LA			
1	LMO3	LA			
1	MAPK1	1DEL			
1	MCL1	LA			
1	MDM2	LA			
1	MDM4	LA			

Table 3.6 (**Continued**).

1	MITF	1DEL			
1	MPL	1DEL			
1	MTOR	1DEL			
1	MUTYH	1DEL			
1	MYBL1	LA			
1	MYC	LA			
1	MYCL	1DEL			
1	MYCL1	1DEL			
1	NBN	LA			
1	NEGR1	1DEL			
1	NF2	1DEL			
1	NOTCH2	1DEL			
1	NPRL2	1DEL			
1	NPRL3	LA			
1	NRAS	1DEL			
1	NTRK1	LA			
1	PALB2	LA			
1	PBRM1	1DEL			
1	PIK3C2B	LA			
1	PMS2	LA			
1	PRAME	1DEL			
1	PRKCZ	1DEL			
1	PRKDC	LA			
1	PRPF40B	LA			
1	PTK2	LA			
1	PTPN11	LA			
1	RAD21	LA			
1	RB1	1DEL			
1	RBL2	1DEL			
1	RECQL4	LA			
1	RFWD2	LA			
1	SBDS	LA			
1	SDHB	1DEL			
1	SDHC	LA			
1	SMARCB1	1DEL			
1	SOCS1	LA			
1	STAT6	LA			
1	TSC2	LA			
1	WRN	LA			
1 Archival	PIK3CA	Missense	c.1035T>A (p.N345K), exon 5		
1 Archival	MET	Missense	c.3029C>T (p.Thr1010Ile), exon 13		
2	ARID1A	Inframe_Ins	c.246_247insGGCGGC (p.G81_G82dup), exon 1	63.63636	11
2	DDB2	Splice_Region	c.1235-8C>G ()	41.2371	97
2	FANCC	Missense	c.1213G>A (p.E405K), exon 13	36.1233	227
2	MLH3	Frameshift	c.1267_1270delCAGA (p.Q423Vfs*30), exon 2	44.26229	305
2	RAD50	Missense	c.1644A>T (p.K548N), exon 11	4.2945	163
2	RASA1	Splice_Region	c.3061-4C>G ()	5.9259	135
2	IKZF1	Missense	c.1554G>A (p.M518I), exon 8	31.3559	118
2	EGFR	Missense	c.347C>T (p.S116F), exon 3	35.443	237
2	AR	Inframe_Ins	c.170_171insGCA (p.L57_Q58insQ), exon 1	9.345795	107
2	ARID1A	Frameshift	c.1543_1544insA (p.P516Afs*107), exon 3	53.76884	199
2	SOS1	Missense	c.1084G>A (p.E362K), exon 10	7.563	119
2	TSHR	Missense	c.584A>C (p.Y195S), exon 8	7.1006	169
2	ESR1	Missense	c.1613A>G (p.D538G), exon 10	40.9574	188
2	JAK1	Frameshift	c.591delC (p.S198Hfs*5), exon 6	7.804878	205
2	RHBDF2	Splice_Acceptor	c.556-1G>T ()	40.9836	122
2	PIK3C2B	Nonsense	c.3511G>T (p.E1171*), exon 24	8.2192	365
2	FAN1	Missense	c.598G>C (p.E200Q), exon 2	14.5	200
2	SMAD4	Nonsense	c.865C>T (p.Q289*), exon 7	63.5071	211
2	ESR1	Nonsense	c.1123C>T (p.Q375*), exon 7	17.0492	305
2	BRCA1	Missense	c.5485G>A (p.E1829K), exon 23	26.9036	197
2	PIK3CA	Missense	c.3129G>T (p.M1043I), exon 21	31.1881	202
2	GNAS	Missense	c.394G>A (p.E132K), exon 1	13.1637	904
2	MAP2K4	Missense	c.415G>A (p.E139K), exon 4	12.3377	154
2	MUS81	Missense	c.1355C>T (p.S452L), exon 13	37.6712	292
2	RET	Missense	c.2650G>A (p.E884K), exon 15	27.3684	190

Table 3.6 (**Continued**).

2	RHBDF2	Missense	c.896T>A (p.M299K), exon 8	29.5082	183
2	RIF1	Missense	c.1208C>T (p.P403L), exon 12	48.3471	242
2	ARID1B	Missense	c.635C>T (p.S212F), exon 1	40.3846	52
2	AKT1	Missense	c.49G>A (p.E17K), exon 3	33.7838	148
2	CBFA2T3	Missense	c.488A>G (p.Q163R), exon 4	39.4737	190
2	XPO1	Missense	c.1528G>A (p.E510K), exon 14	7.1895	306
2	EPCAM	Missense	c.-349G>T (), exon 1	38.3333	60
2	RHBDF2	Missense	c.953G>A (p.R318Q), exon 8	29.8429	191
2	RHBDF2	Nonsense	c.892G>T (p.E298*), exon 8	29.1892	185
2	KMT2D	Missense	c.16343G>A (p.R5448Q), exon 52	38.7097	186
2	CDC73	Missense	c.1241C>T (p.P414L), exon 14	26.4925	268
2	CDKN2A	Missense	c.355G>A (p.E119K), exon 2	37.6471	170
2	AKT3	LA			
2	ARHGEF12	1DEL			
2	ARID1A	1DEL			
2	ATM	1DEL			
2	AURKA	LA			
2	B2M	1DEL			
2	BCL2	1DEL			
2	BLM	1DEL			
2	BUB1B	1DEL			
2	C1orf86	1DEL			
2	CBL	1DEL			
2	CCND1	HA			
2	CDC73	LA			
2	CDH4	LA			
2	CDKN2C	1DEL			
2	CHEK1	1DEL			
2	CREBBP	LA			
2	CSF3R	1DEL			
2	DDR2	LA			
2	EGLN1	LA			
2	EP300	1DEL			
2	EXO1	LA			
2	FAH	1DEL			
2	FAM46C	1DEL			
2	FAN1	1DEL			
2	FANCI	1DEL			
2	FGFR1	HA			
2	FH	LA			
2	FUS	LA			
2	GATA4	1DEL			
2	GATA6	1DEL			
2	GBA	LA			
2	GNAS	LA			
2	GREM1	1DEL			
2	H3F3A	LA			
2	HMBS	1DEL			
2	HRAS	LA			
2	ID3	1DEL			
2	IDH2	1DEL			
2	IGF1R	1DEL			
2	JAK1	1DEL			
2	KAT6A	LA			
2	KIF1B	1DEL			
2	KMT2A	1DEL			
2	MAFB	1DEL			
2	MAP2K1	1DEL			
2	MCL1	LA			
2	MDM4	LA			
2	MGA	1DEL			
2	MPL	1DEL			
2	MRE11A	1DEL			
2	MTOR	1DEL			
2	MUTYH	1DEL			
2	MYBL1	1DEL			

Table 3.6 (**Continued**).

2	MYCL	1DEL			
2	NEIL1	1DEL			
2	NEIL2	1DEL			
2	NKX3-1	1DEL			
2	NOTCH2	1DEL			
2	NRAS	1DEL			
2	NRG1	1DEL			
2	NTHL1	LA			
2	NTRK1	LA			
2	NTRK3	1DEL			
2	PIK3C2B	LA			
2	PML	1DEL			
2	PRKDC	1DEL			
2	PTK2B	1DEL			
2	PTPN14	LA			
2	PVRL4	LA			
2	RAD51	1DEL			
2	RBBP8	1DEL			
2	RIT1	LA			
2	SDHB	1DEL			
2	SDHC	LA			
2	SDHD	1DEL			
2	SETBP1	1DEL			
2	SLX4	LA			
2	SMAD2	1DEL			
2	SMAD4	1DEL			
2	SS18	1DEL			
2	TAL1	1DEL			
2	TP53BP1	1DEL			
2	TRAF7	LA			
2	TSC2	LA			
2	UBE2T	LA			
2	UROD	1DEL			
2	USP28	1DEL			
2	USP8	1DEL			
2	WHSC1L1	HA			
2	WRN	1DEL			
2	XRCC6	1DEL			
2	YAP1	1DEL			
2	ZNF217	HA			
3	NTRK2	Missense	c.1279G>A (p.G427S), exon 13	44.8052	308
3	CDK5	Missense	c.650G>A (p.R217Q), exon 9	15.5251	219
3	CDH1	Frameshift	c.2188_2191delTTTC (p.L731Gfs*38), exon 14	15	380
3	TP53	Missense	c.844C>T (p.R282W), exon 4	14.3813	299
3	DEPDC5	Splice_Region	c.3129-3C>T (), exon 0	14.2857	147
3	GLI2	Missense	c.2498G>A (p.R833H), exon 13	26.8293	82
3	AKT1	Missense	c.155T>A (p.L52H), exon 3	64.5514	457
3	RBL2	Missense	c.1015G>A (p.E339K), exon 8	13.1868	364
3	AKT1	LA			
3	ALOX12B	1DEL			
3	APC	1DEL			
3	ATM	1DEL			
3	AURKB	1DEL			
3	CADM2	LA			
3	CBL	1DEL			
3	CCND1	HA			
3	CIITA	1DEL			
3	CREBBP	1DEL			
3	DDB2	LA			
3	DIS3	1DEL			
3	EED	1DEL			
3	EPHA5	1DEL			
3	ERCC5	1DEL			
3	EXT2	LA			
3	FBXW7	1DEL			
3	KDM6B	1DEL			

Table 3.6 (**Continued**).

3	KDR	1DEL			
3	KIT	1DEL			
3	KMT2A	1DEL			
3	LMO2	LA			
3	MAP3K1	1DEL			
3	MEN1	1DEL			
3	MITF	LA			
3	NFKBIA	HA			
3	NPRL3	1DEL			
3	PDGFRA	1DEL			
3	PIK3R1	1DEL			
3	PRDM1	LA			
3	RB1	1DEL			
3	RBL2	1DEL			
3	RPL26	1DEL			
3	SDHA	LA			
3	SDHAF2	1DEL			
3	SDHD	1DEL			
3	SF1	1DEL			
3	SLITRK6	1DEL			
3	TERT	LA			
3	TET2	1DEL			
3	TP53	1DEL			
3	TSC2	1DEL			
3	WT1	LA			
3	XPC	LA			

Consistent with our *in vitro* findings, an activating *PIK3CA* mutation was not sufficient to confer resistance to CDK4/6 inhibition.

Immunohistochemistry (IHC) staining was performed on the acquired resistance biopsy from patient 1 to assess the extent of AKT pathway activation (**Fig. 3.12B-C**). Samples were stained for AKT phosphorylation at serine 473. Since IHC staining for AKT phosphorylation in archival tissue can be unreliable and it is unclear whether mutations in AKT1 may affect antibody binding, we also analyzed samples for activation of the AKT/mTOR downstream target, S6 ribosomal protein (S6) at serine 235/236. Stathmin was also used as a readout of PI3K pathway activation (301). For the various immunostains, each tumor specimen was reviewed and scored for both the proportion of tumor cells positive for the target protein (percent, 0-100) as well as the average staining intensity across all positive tumor cells (1-3+). These two scores were multiplied to create a dynamic "IHC score" (0-300). The post-treatment biopsy from patient 1 showed high levels of phosphorylated S6, elevated stathmin and some AKT phosphorylation (IHC scores of 180, 50 and 20 respectively) (**Fig. 3.12B-C**). Thus, AKT is likely active in this acquired resistance biopsy.

Our *in vitro* data suggests that AKT1 confers resistance to CDK4/6 inhibition by promoting RB phosphorylation. To determine whether RB was inactivated, samples were also stained for RB phosphorylation at serine 807/811. Notably, RB was expressed in sample 1 and was hyperphosphorylated (**Fig. 3.12B-C**). Thus, we detected an acquired $AKT1^{W80R}$ mutation in a patient after progression on ribociclib and fulvestrant therapy; consistent with AKT-mediated resistance, the biopsy had high S6 and RB phosphorylation.

To assess the generalizability of our findings, we conducted similar sequencing and IHC analyses for the other *AKT1*-mutant patients in our cohort. Patient 2 was diagnosed with early stage ER+/HER2- breast cancer at the age of 39 **(Fig. 3.13A)**. Following adjuvant tamoxifen and triptorelin therapy, the patient developed metastatic ER+/HER2- breast cancer five years later. The patient first received letrozole treatment for metastatic disease. Upon relapse, the

patient was treated with a triple combination of fulvestrant, BKM120 (PI3K inhibitor) and ribociclib for two years before progressing. Sequencing of a post-ribociclib biopsy revealed a canonical E17K mutation in *AKT1* as well as amplification of *CCND1 and FGFR1* (**Fig. 3.13A**). Since AKT is downstream of PI3K, members of our lab have previously found that AKT activation confers resistance to PI3K inhibition (178). Stathmin was detected in the biopsy from patient 2 but at low levels. While the significance of the *CCND1 and FGFR1* amplifications are unclear, IHC staining revealed high S6 and RB phosphorylation in the sample from patient 2 (**Fig. 3.13B-C)**. These data are consistent with AKT pathway activation and bypass of CDK4/6 inhibition.

Patient 3 was diagnosed with local lobular ER+/HER2- breast cancer at the age of 81. Following two years of adjuvant aromatase inhibitor therapy, the patient developed metastatic ER+ breast cancer. She was treated with fulvestrant and palbociclib in the first-line metastatic setting, with clinical benefit extending approximately 9 months (**Fig. 3.14A**). Immediately prior to overt disease progression, the patient had a skin punch biopsy from a metastatic lesion. Targeted sequencing of the patient's skin punch biopsy revealed an AKT^{L52H} missense mutation as well as a mutation in *TP53* and a *CCND1* amplification (**Fig. 3.14A**). As with the second patient discussed above, analysis of a pre-CDK4/6 inhibitor treatment biopsy from patient 3 is required to determine if the AKT^{L52H} mutation was acquired during CDK4/6 inhibitor treatment. Nevertheless, S6 phosphorylation, stathmin levels and phosphorylated RB levels were high in patient 3 following palbociclib treatment (IHC scores: 150-180) (**Fig. 3.14B-C**). Thus, *AKT1* mutations have been detected in 3 patients following progression on CDK4/6 inhibitor treatment.

Preliminary cohort analysis to identify patients with AKT pathway activation.

As we retrospectively identified several patients with mutant AKT, upregulated AKT signaling, and clinical resistance to CDK4/6 inhibitor therapy, we are working on determining whether the extent of AKT upregulation identified via immunohistochemistry might stratify

individuals across a larger cohort of ER+ metastatic patients. As a pilot effort, we selected 38 patients from our Dana Farber Cancer Institute-Cancer Center for Precision Medicine research cohort and obtained IHC for phosphorylated AKT, S6 and RB as well as total stathmin (**Fig. 3.15)**. Patients were then categorized by response to CDK4/6 inhibitor therapy into sensitive, resistant or unknown (see Materials and Methods). Although stathmin levels were variable, biopsies from all three samples have high S6 phosphorylation, which is indicative of AKT pathway activity (**Fig. 3.15)**. Consistent with AKT activation, these three biopsies also show high RB phosphorylation (**Fig. 3.15)**. Our preliminary patient data are consistent with the hypothesis that AKT activation drives resistance to CDK4/6 inhibition by inactivating RB.

Discussion

CDK4/6 inhibition in combination with hormonal therapy is the new standard of care for patients with metastatic ER+ breast cancer in both the first-line and second-line metastatic setting. Unfortunately, very few clinically relevant biomarkers have been identified for response to CDK4/6 inhibitors and patients are inevitably progressing on treatment. Furthermore, metastatic disease is quite heterogeneous and patients with advanced breast cancer often have a long treatment history. Therefore, effective treatment of patients with advanced breast cancer necessitates an understanding of drivers of resistance to CDK4/6 inhibition alone and in combination with endocrine therapy.

Large-scale expression screens enable unbiased mapping of the landscape of resistance to targeted therapies. Near genome-wide ORF screens have been employed in our lab to uncover PIM1 as a key mediator of resistance to PI3K inhibition (178) and to identify drivers of resistance to MAPK pathway inhibitors (302). In this study, we conducted five gain-of-function screens in pooled format to interrogate resistance to palbociclib and abemaciclib. Use

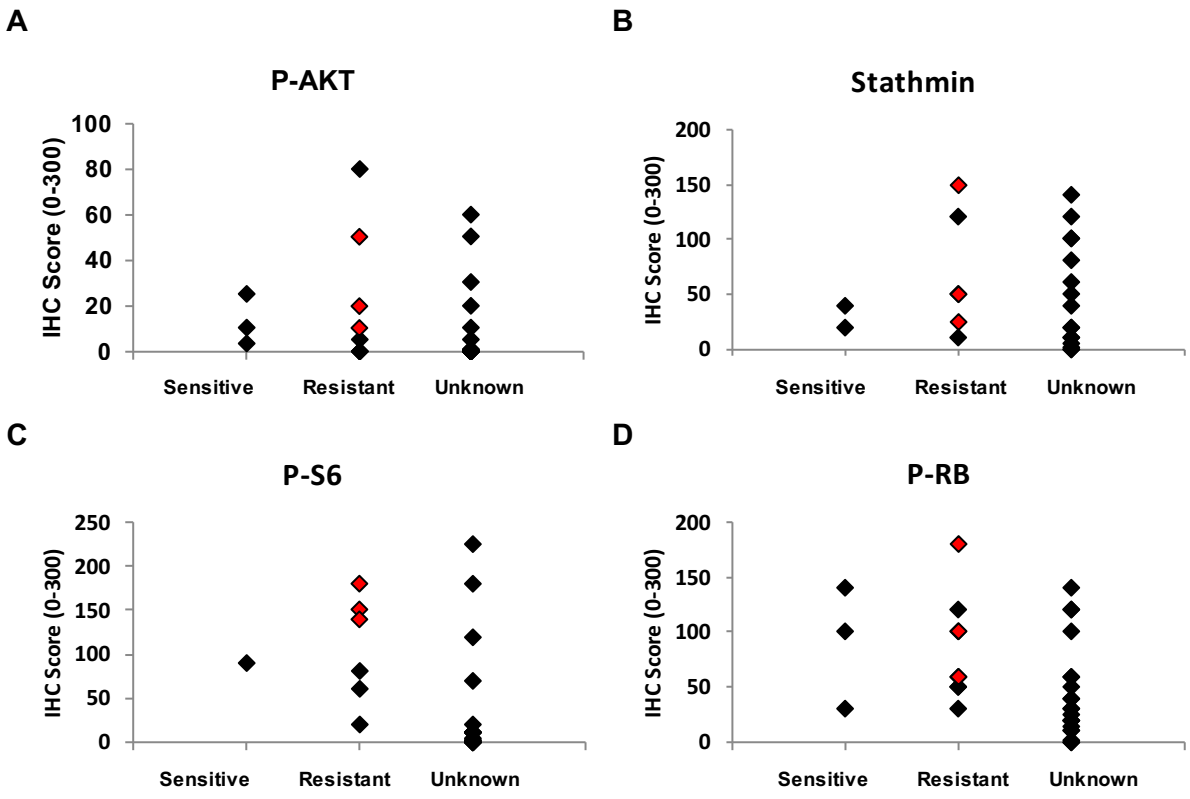

Figure 3.15. Assessment of AKT pathway signaling in clinical tumor specimens from ER+ metastatic breast cancer patients. (A-D) 38 pilot specimens were analyzed by IHC analysis. These results are demonstrated across the pilot cohort for each protein of interest. Each individual data point represents a single patient and stains are categorized by response to CDK 4/6 inhibitor therapy (sensitive, resistant or unknown). Samples with acquired resistance and known AKT mutation (patients 1-3) are highlighted in red.

of both FBS and CSS media in our screens was crucial to understanding resistance to CDK4/6 inhibitor monotherapy and in combination with estrogen deprivation.

Encouragingly, our screens identified known mechanisms of resistance to single agent CDK4/6 inhibition. For example, CDK6 amplification has been detected in models of acquired resistance to abemaciclib (249). Correspondingly, in our primary screens, CDK6 was the top resistance driver under abemaciclib treatment in FBS media and conferred resistance to palbociclib. Notably, ORFs encoding CDK4 were not enriched under any treatment condition in both primary and secondary screens. All three CDK4 constructs in the library, however, were well-represented at the early time point (with log normalized scores between 4.4-4.7) and at least one of the CDK4 constructs should be functional (one of the three ORFs encodes wild-type CDK4 without a V5 tag). Moreover, CDK4-amplified liposarcomas are sensitive to ribociclib (207). Therefore, our findings suggest that overexpression of CDK4 is not sufficient to drive resistance to palbociclib, abemaciclib or ribociclib. At least for abemaciclib, the differences in resistance phenotypes between CDK4 and CDK6 may be attributable to the compound's greater selectivity for CDK4 (7). These findings support CDK6 as a key driver of resistance and provide motivation for the development of more potent CDK6 inhibitors.

AKT emerged as a major node of resistance to CDK4/6 inhibition alone and in combination with estrogen deprivation. We found that upstream PI3K activation, however, cannot bypass the antiproliferative effects of CDK4/6 inhibition. Several lines of evidence support this finding. ORFs encoding constitutively active *PIK3CA* mutants were not highly enriched in our primary screens. Both T47D and MCF7 cells harbor activating *PIK3CA* mutations and respond to CDK4/6 inhibition. PI3K inhibition also failed to re-sensitize cells with acquired resistance to palbociclib (248). Furthermore, oncogenic *PIK3CA* mutations are not predictive of resistance to CDK4/6 inhibition and hormonal therapy (234). Since AKT validates as a strong mediator of resistance to palbociclib and abemaciclib in our studies, there is likely a disconnect between PI3K activation and AKT signaling. Our lab has previously found that many

PIK3CA-mutant cells have low AKT activation; in these cells, activated PI3K signals in an AKT-independent manner by activating PDK1 and its downstream target SGK3 (303). Despite harboring oncogenic mutations in *PIK3CA,* both T47D and MCF7 cells have low AKT phosphorylation. Thus, PI3K activation is not sufficient to upregulate AKT signaling and promote resistance to CDK4/6 inhibition in the ER+ breast cancer cell lines described here. Collectively, our data suggest that AKT activation and not PI3K is required to bypass CDK4/6 inhibition.

Our studies support an emerging hypothesis that CDK2 activity can phosphorylate and inactivate RB to bypass CDK4/6 inhibition (219,247,248). Mechanistically, we found that cells with activated AKT phosphorylate p21 at T145, which relieves CDK2 inhibition (150). Cells with activated AKT also maintained CDK2 phosphorylation at T160, which is required for CDK2 activity (291) and upregulated cyclin D1 levels. While some studies suggest that noncanonical interactions between cyclin D1 and CDK2 promote RB phosphorylation and bypass of CDK4/6 inhibition (247,248), other studies found that cyclin D1 is a marker of sensitivity to CDK4/6 inhibition in ER+ breast cancer (4). One possible explanation for the discrepancy is that there may be a difference between stabilization of cyclin D1 and simple overexpression. Notably, amplification of the gene encoding cyclin D1, *CCND1,* co-occurred with an *AKT1* mutation in two out of the three CDK4/6 inhibitor-resistant tumor biopsies in our study. An ORF encoding *CCND1*-V5 also did not score confer resistance to CDK4/6 inhibition in our screens. Thus, the level of cyclin D1 induced by *CCND1* gene expression may be sufficient to drive S phase progression, but render cells sensitive to CDK4/6 inhibitor. In contrast, a cyclin D1 T286A mutant, which cannot be phosphorylated by GSK3β and is not targeted for degradation, promotes CDK2 activation and enables RB phosphorylation at serine 807/811 (34). Thus, stabilization of cyclin D1 levels by AKT may activate CDK2 and confer resistance to CDK4/6 inhibition.

Correspondingly, we found that cyclin D1 protein levels were highly elevated in cells expressing the constitutively active *EGFR*^{L858R} mutant compared to GFP. EGFR^{L858R} expression also upregulated AKT phosphorylation as anticipated and conferred resistance to CDK4/6 inhibition. Triple combination therapy (MK-2206, CDK4/6 inhibitor and CSS) decreased the viability of *EGFR*^{L858R} and there was a trend towards significance in decreasing cell cycle progression relative to CDK4/6 and CSS doublet therapy. This reduction in S phase, however, was not statistically significant, suggesting that activated EGFR can drive resistance to CDK4/6 inhibition in an AKT-independent manner. Notably, *EGFR*^{L858R}-expressing cells maintained higher levels of cyclin D1 relative to AKT1- or AKT2-expressing cells under triple combination therapy. One potential explanation for this difference is that EGFR signaling activates the RAF-MEK-ERK MAPK pathway in addition to AKT (128); ERK2 activation in turn can phosphorylate and prevent cyclin D1 degradation (304). Our studies suggest that cyclin D1 stability modulates response to CDK4/6 inhibition. Additional studies are necessary to test this hypothesis.

The present study identified activating *AKT1* mutations in breast cancer patients with acquired resistance to CDK4/6 inhibition that are likely clinically relevant. Since CDK4/6 inhibitors have only recently received FDA approval (232,235), few clinical samples of acquired resistance have been reported. Previous publications have detected RB loss in patient-derived xenograft models of resistance to CDK4/6 inhibition (248,262). In contrast, RB remained intact in all three patient samples examined in this study. Since *AKT1* mutations co-occur with other alterations in the patient samples, a larger cohort of matched pre-treatment and post-relapse biopsies is needed to completely assess the significance of *AKT1* mutations. The three patient samples described in this study, however, support *in vitro* findings that AKT activation promotes RB phosphorylation to drive resistance to CDK4/6 inhibition. In this regard, all resistance genes characterized in this study also promote RB phosphorylation. Thus, as an alternative to RB loss, we find that a subset of ER+ breast cancer cells hyperphosphorylate RB in the setting of acquired resistance to CDK4/6 inhibitors.

Multiple markers will likely be necessary to assess AKT pathway activation by IHC. Staining for phosphorylated AKT was generally depressed throughout the entire cohort when compared to results with phosphorylated S6. Several features may account for this discrepancy, including the nature of the antibody itself (with inferior performance characteristics and limited binding overall) or the tissue conditions, as archival specimens can experience tissue degradation that leads to false negative staining. Furthermore, the variability in staining observed with stathmin in *AKT1*-mutant samples may be because stathmin is a better measurement of PI3K signaling rather than AKT activity (301). Despite these caveats, the three *AKT1*-mutant samples generally demonstrated relatively high levels of S6 and RB phosphorylation, suggesting that the *AKT1* mutations are activating and that the cells have bypassed the G1-S cell cycle checkpoint.

In our studies, co-treatment with MK-2206 abrogated AKT-mediated resistance and re-sensitized cells to CDK4/6 inhibition. However, only modest responses were observed in a phase I study of ER+ breast cancer patients treated with MK-2206 and endocrine therapy (185). Selection for patients with activating *AKT1* mutations may enrich for sensitivity to MK-2206. AKT inhibitors such as MK-2206 and AZD5363 significantly reduced proliferation of breast cancer explant models with homozygous AKT^{E17K} mutations (305). A partial response to AZD5363 monotherapy was also observed in ER+/HER2- patient harboring an AKT^{E17K} mutation. Therefore, patients who have progressed on a CDK4/6 inhibitor and have an activating *AKT1* mutation may derive clinical benefit from AKT inhibitor therapy.

We have found that AKT-mediated resistance to CDK4/6 inhibition is also mTOR-dependent. The mTOR inhibitor everolimus in combination with the aromatase inhibitor exemestane is currently FDA approved in the second-line metastatic setting for patients who have progressed on nonsteroidal aromatase inhibitors (166). Early data from a phase II clinical trial suggests that triple combination therapy with a everolimus, a CDK4/6 inhibitor (ribociclib) and exemestane is tolerated in patients with metastatic ER+ breast cancer (239). Our follow-up

studies suggest that breast cancers with activated AKT1 and AKT2 may respond to triple combination therapy.

In summary, systematic functional studies coupled with clinical sequencing information greatly enhance our understanding of resistance to targeted therapies, and can aid in guiding patient stratification. This approach identified AKT as a key mediator of resistance to CDK4/6 inhibition and nominated several strategies to re-sensitize cells with activated AKT1 to palbociclib and abemaciclib. Further clinical investigation is necessary to validate PH domain mutations in *AKT1* as a biomarker of resistance to CDK4/6 inhibition.

Materials and Methods

Cell Culture and Reagents

T47D, MCF7 and ZR-75-1 cells were purchased from ATCC between 2012-2016 and cultured in RPMI-1640 (no phenol red, Life Technologies #11835055) + 10% fetal bovine serum (FBS, Gemini Bio-products). Cells were grown for less than 10 passages after thawing. T47D cells were authenticated with STR profiling prior to beginning the screens. Charcoal-stripped serum (CSS) was obtained from Life Technologies. Palbociclib, abemaciclib, everolimus (RAD001) and MK-2206 were purchased from Selleckchem, while rapamycin was purchased from LC Laboratories. Palbociclib was dissolved in water. All other drugs were dissolved in DMSO.

Virus Production and Lentiviral Vectors

To generate virus, we transfected HEK 293T cells with lentiviral constructs, and the packaging plasmids delta 8.9 and pVSVG. Fugene 6 (Roche) was used for transfections. Virus was harvested 72 hours after transfection, aliquoted and frozen at -80^{o}C. Cells were spin-infected with lentivirus in FBS media in 6 well plates with 4μg/ml polybrene. Plates were

centrifuged at 2250rpm for 30min at 30°C. Fresh FBS media was replaced the next day and cells were selected with 1μg/ml puromycin or 35μg/ml blasticidin in FBS media for four days.

Lentiviral vectors encoding candidate resistance open reading frames (ORFs) in the pLX_TRC317 backbone were obtained from the Broad Institute. The pLX_TRC317 vector is a gateway-compatible vector, drives gene expression from EF1a promoter and confers puromycin resistance. The vector also encodes a V5 tag but all constructs in validation studies contain a stop codon prior to V5 tag unless otherwise noted. The following pLX_317 constructs were obtained from the Genetic Perturbation Platform at the Broad Institute: TRCN0000491814 (AKT1), TRCN0000488903 (AKT2), TRCN0000489669 (AKT3), TRCN0000488331 (CDK6), TRCN0000474343 (CCNE2 LMW-V5) and TRCN0000489590 ($EGFR^{L858R}$). CMV-gateway-GFP-V5-puromycin lentiviral vector was also obtained from the Broad Institute and is used as an expression control unless otherwise noted. Myr-AKT is in the pLX304, a CMV-gateway-V5-blasticidin vector, as previously described (178). Corresponding GFP vector in pLX304 was used for myr-AKT experiments.

Pooled Lentiviral ORF Screens

For the primary screen, 3x10^6 T47D cells were seeded into 12-well plates and infected at MOI of 0.3 with pooled virus encoding a 17,255 ORF pooled library (encoding 12,732 human genes) with 4μg/ml polybrene. A total of 2.83x10^8 cells were infected. Plates were centrifuged at 2000rpm at 30°C for 2 hours followed by an immediate media change. 24 hours later, cells were split into T225 flasks and selected with 1.5μg/ml puromycin for 6 days (fresh media with puromycin was replaced at day 4). Then, 2x10^7 cells were collected and frozen at -80°C to determine ORF representation at this early time point. There were 3 replicates (2x10^7 cells treated per replicate) per treatment condition. ORF-infected cells for all CSS-containing arms of the screen were washed 3 times in CSS media to remove residual estrogen. Cells were grown in T225 or T162 flasks with the following media and drug conditions: FBS + 1μM palbociclib,

FBS + 300nM abemaciclib, CSS alone, CSS+100nM palbociclib and CSS+30nM abemaciclib. Control uninfected T47D cells were grown and treated in parallel. Media and drug was changed every 2-6 days for all replicates of a given treatment. When cells became confluent, they were split and at least 20 million cells were replated. For replicates with less than 20 million cells, all cells in the replicate were replated. TrypLE express enzyme (1x) from Gibco was used for trypsinization during the screen as it has no phenol red. Uninfected cells were passaged in parallel to monitor spontaneous resistance; none was observed during the screen. Cells were collected for the "late time point" at day 28 for all FBS conditions or day 31 for all CSS treatment arms and pellets were frozen at -80^{o}C.

In secondary screens conducted by the Genetic Perturbation Platform, there were two replicates for the early time point. Secondary screens were similarly infected as in primary screen but cells were split every 3-4 days for two weeks and cultured in the presence of FBS media, FBS + 1μM palbociclib and CSS+1μM palbociclib. FBS treatment was done in duplicate, while all other screening arms were done in quadruplicate.

Genomic DNA from ORF-infected cells was isolated with the QIAamp blood midi kit. ORFs were PCR-amplified and then sequenced (Illumina). Detailed protocols for lentiviral production, PCR amplification and sequencing of screens may be found at the Broad Institute's Genetic Perturbation platform portal at (www.broadinstitute.org/rnai/public).

Screen Analysis

For each replicate, ORF representation was determined by calculating the log normalized score: $\log_2$(# sequencing reads/total number of reads *10^6+1). Enrichment of each ORF was determined by calculating the log fold change (LFC): the log normalized score for each ORF at the end of the screen (late time point) minus the log normalized score for each ORF at the beginning of the screen (early time point). ORFs with a median LFC of >2 were considered candidate resistance hits in the primary screen. Any ORF with a z score >3 in the

secondary screen was also considered a hit. Deconvolution data did not include mutation status for each ORF. Mutation status for select ORFs (KRAS, EGFR, AKT1/2/3, CDK6, CCNE2 and SRC) were identified manually and are indicated.

Cell Viability Assays

0.5-3x10^3 cells were plated in 96 well plates. The next day, cells were infected at 1:10-1:20 with dilution of lentivirus encoding ORF of interest and 4µg/ml polybrene. Mock transfected cells were only incubated with polybrene. Lentivirus was produced in 293T cells as previously described (266). Plates were spun for 30 minutes at 2250rpm and 30^{o}C and the media was replaced the next day (with 10% FBS or 10% CSS depending on final treatment conditions). 48-72 hours after infection, the media was changed again and cells were treated with compounds. After 6 days of drug treatment, 100µl DMEM (with phenol red) + 10% FBS was added to each well followed by 10µl WST-1 reagent (Abcam and SIGMA/ROCHE) to assess cell viability according to manufacturers' instructions unless otherwise indicated. Viability at a given dose of inhibitor was calculated as a percentage of viability in FBS vehicle-treated cells after background subtraction. Dose response curves were generated with Prism software.

Colony Formation Assays

3x10^3 cells were plated in 12 well plates in native growing condition (FBS+/- CDK4/6 inhibitor). The next day, cells were treated with 1µM palbociclib, 300nM abemaciclib and/or 500nM MK-2206. Cells were cultured for two weeks with media and drug refreshed every 3-5 days. Cells were fixed with 100% methanol and stained with 0.5% crystal violet. Plates were washed with distilled water and subsequently imaged.

Western Blot Analysis

1.5-3x10^5 ORF-infected or cultured to resistance cells were plated in 6 wells. The next day, ORF-infected cells were grown for at least two days in CSS media to remove residual estrogen and subsequently treated for another 48 hours with compounds in CSS media. Cultured to resistance cells were plated in FBS media containing relevant dose of palbociclib or abemaciclib overnight and subsequently treated with compounds for 48 hours in FBS media. Cells were washed with PBS and lysed with RIPA buffer (SIGMA) containing a protease inhibitor cocktail (cOmplete, EDTA-free, SIGMA Aldrich) and phosphatase inhibitors (PhosSTOP, SIGMA). After protein concentrations were determined with the Bio-Rad protein assay and normalized, lysates were resolved with SDS-PAGE protein gels and transferred onto PVDF membranes. All antibodies were from Cell Signaling Technologies except vinculin (EMD Millipore), P-AKT (S473, Cell Signaling and Santa Cruz) and cyclin D1 (Neomarkers).

Cell Cycle Analysis

Cells were treated as described for western blots. Cells were subsequently trypsinized, resuspended in 70% ethanol in PBS and fixed for at least 24 hours. Pellets were washed in PBS and stained with 200µl propidium iodide (PI)/tritonX-100 solution (PBS with 0.1% TritonX-100, 0.2mg/ml RNase A and 20µg/ml PI) for 30 minutes at room temperature in the dark. 300 µl PBS was added after the incubation and flow cytometry was performed with BD LSRFortessa at 605nm wavelength. ModFit software was used to analyze the percentage of cells in S phase from FCS files.

Clinical Sequencing and Annotation

We performed targeted genomic sequencing on a panel of more than 300 cancer-related genes (OncoPanel), whole exome sequencing (WES) and transcriptome sequencing (RNA-seq) on metastatic tumor biopsies from more than 150 patients with metastatic breast cancer who were treated at the Dana-Farber Cancer Institute/Harvard Cancer Center (297,298). Patient

consent and participation was obtained in accordance with the cancer center's Institutional Review Board (IRB) and the Declaration of Helsinki. Tumors were analyzed for point mutations, insertions/deletions, copy number alterations, and gene expression. For all patients enrolled in the research cohort, detailed clinicopathologic data was collected from our institution's electronic medical record. For pathology samples, the patient's biopsy result, tumor yield within the biopsy sample, receptor status (estrogen receptor, progesterone receptor), and HER2 status (including immunohistochemistry and FISH results) were collected. A detailed clinical database was established for this research cohort – all patient charts were reviewed systemically and all treatment regimens were identified and collated. These include therapies deployed in the neoadjuvant, adjuvant, and metastatic settings, along with start/stop date, best overall response, and reason for stopping therapy. If the patient was on a clinical trial, this information was included as well.

The genomic OncoPanel and WES data described above was then retrospectively searched for all variants of interest (e.g. *AKT1*, *AKT2*, *AKT3* mutations). All patients harboring mutational events in the gene of interest (which include point mutations, splice variants, and copy number changes) were then queried as to their exposure to anti-estrogen and CDK4/6 inhibitor therapy. Patients harboring a mutation in AKT1/2/3 with exposure to hormonal therapy and CDK4/6 inhibition were collected for additional review. Representative cases were outlined in a chronological fashion, incorporating the patient's initial diagnosis date, age at the time of diagnosis, receptor/HER2 status, timing of biopsy events, and sequence of clinical therapies. The acquisition of mutational variants of interest, identified via OncoPanel sequencing, were highlighted along this chronology. OncoPanel data for all *AKT1*-mutant patients is provided in **(Table 3.6).** LA indicates low amplification.

These patients were further filtered via timing of tumor biopsy relative to CDK4/6 therapy and assigned as follows: *sensitive* (patient with clinical response or stable disease clearly documented via at least one interval radiographic study and biopsy obtained prior to treatment;

typical duration between imaging studies 8-12 weeks, variable by attending physician and clinical status); *intrinsic resistant* (patient with clinical disease progression prior to first imaging study and/or progression on first radiographic study; biopsy obtained either immediately prior to or subsequent to CDK 4/6 therapy); or *acquired resistant* (patient with initial sensitivity to therapy with subsequent tumor progression; biopsy obtained shortly before or after radiographic progression).

In the cohort analysis, resistant patients include both intrinsic and acquired resistance. The *unknown group* includes patients who have not had exposure to CDK4/6 therapy, patients who clinical data has not be fully annotated, and patients who have recently started CDK4/6 inhibitor therapy but have not yet had their first interval radiographic assessment.

Immunohistochemistry (IHC) Staining

Archival tissue specimens fixed in formalin and paraffin-embedded (FFPE) were collected for additional pathology and immunohistochemical assessment. All IHC staining was performed on the Leica Bond automated staining platform with Citrate antigen retrieval for 30min. The Leica Refine DAB Detection kit was used with the included hematoxylin. The antibody vendors, catalogue numbers and dilutions are as follows: Total Rb- BD Biosciences-554136 clone G3-245 (mouse) 1:75, Phospho Rb- CST-9308 clone s807/811 (rabbit) 1:100, Phospho AKT- CST- 4060 clone ser473 (rabbit) 1:100, Stathmin- CST-13655 clone D1Y5A (rabbit) 1:1200 & Phospho S6–CST 4858 clone ser235/236 (rabbit) 1:100. These samples were scored in a blinded fashion by our collaborator in the Dana Farber Cancer Institute pathology division (Dr. J Geradts). For the various immunostains of interest, each tumor specimen was reviewed and scored for both the proportion of tumor cells positive for the target protein (percent, 0-100) as well as the average staining intensity across all positive tumor cells (1-3+). These two scores were multiplied to create a dynamic “IHC score” (0-300).

.

CHAPTER 4

CONCLUSION AND FUTURE DIRECTIONS

Summary

CDK4/6 inhibition in combination with endocrine therapy is the new standard of care for patients with metastatic ER+ breast cancer. While ER positivity is currently the best clinical predictor of sensitivity to CDK4/6 inhibitors, some ER+ breast cancer patients are intrinsically resistant to CDK4/6 inhibition, while other patients are developing resistance. By leveraging clinical sequencing data and unbiased screening approaches, the two projects described in this work nominate several novel markers of response and resistance to CDK4/6 inhibition.

In chapter 2, we investigated the targetable vulnerabilities of ER-mutant breast cancer cells. We have found that ER ligand binding domain (LBD) mutations upregulate cyclin D1 and E2F1 expression under estrogen-deprived conditions, rendering cells resistant to estrogen-deprivation but sensitive to CDK4/6 inhibition with palbociclib. Furthermore, sensitivity to CDK4/6 inhibition is contingent upon RB1. These results are consistent with Dr. Rinath Jeselsohn's work in Dr. Myles Brown's laboratory and with Wardell *et al.*'s publication (262). Both groups found that the selective ER modulator/selective ER degrader hybrid bazedoxifene acts synergistically with palbociclib to inhibit the growth of ER-mutant breast cancer cells. Thus, breast cancer patients with activating *ESR1* mutations may benefit from combined endocrine therapy and CDK4/6 inhibition.

In chapter 3, our screens enabled comprehensive and unbiased characterization of the landscape of resistance to CDK4/6 inhibition. Since CDK4/6 inhibitors are only FDA-approved in combination with endocrine therapy, the use of estrogen-deprived charcoal-stripped serum media (CSS) better recapitulates clinical treatment of patients compared to normal growth media containing fetal bovine serum (FBS). Our screens identified AKT as a key mediator of resistance to palbociclib and abemaciclib under estrogen-deprived conditions. Validation studies suggest that AKT drives resistance to CDK4/6 inhibition by promoting RB phosphorylation and progression into S phase. Mechanistically, AKT phosphorylates and

inactivates GSK3β despite CDK4/6 inhibition, which stabilizes cyclin D1. Work from Herrera-Abreu *et al.* suggests that cyclin D1 forms noncanonical interactions with CDK2 to promote RB phosphorylation and bypass CDK4/6 inhibition (248). Furthermore, we found that AKT promotes p21 phosphorylation at threonine 145, which could also activate CDK2. These results are consistent with a model in which AKT signaling upregulates CDK2 activity to inactivate RB (**Fig. 4.1**). We also found that triple combination therapy with estrogen deprivation, CDK4/6 inhibition and AKT inhibition mitigates AKT-driven resistance. Furthermore, AKT's mechanism of action is mTOR-dependent; rapamycin treatment sensitives cells to palbociclib and abemaciclib in CSS media.

Collaborations with Dr. Seth Wander, Dr. Nikhil Wagle and the Center for Cancer Precision Medicine at the Dana Farber Cancer Institute have allowed us to assess the clinical relevance of our findings. Preliminary data suggest that oncogenic mutations in *AKT1* but not *PIK3CA* are associated with acquired resistance to CDK4/6 inhibition in patient samples. Importantly, RB is expressed and highly phosphorylated in *AKT1*-mutant tumors, consistent with AKT activation. A recent phase II clinical trial is evaluating triple combination therapy of a mTOR inhibitor (everolimus), an aromatase inhibitor (exemestane) and a CDK4/6 inhibitor (ribociclib) in ER+ metastatic breast cancer patients. Encouragingly, triple combination therapy is tolerable and shows clinical activity (239). Our data suggests that patients with activating *AKT1* mutations may benefit from triple combination therapy.

Limitations of this study

One potential limitation of our work is the use of charcoal-stripped serum. Although charcoal treatment does reduce estrogen levels in growth serum, it also nonspecifically removes growth factors. To specifically test the role of estrogen, one could add β-estradiol to the CSS media. Ping Mao in Nikhil Wagle's group has also conducted similar ORF resistance screens in T47D cells in FBS media with ER degraders, such as fulvestrant. Encouragingly, many of the

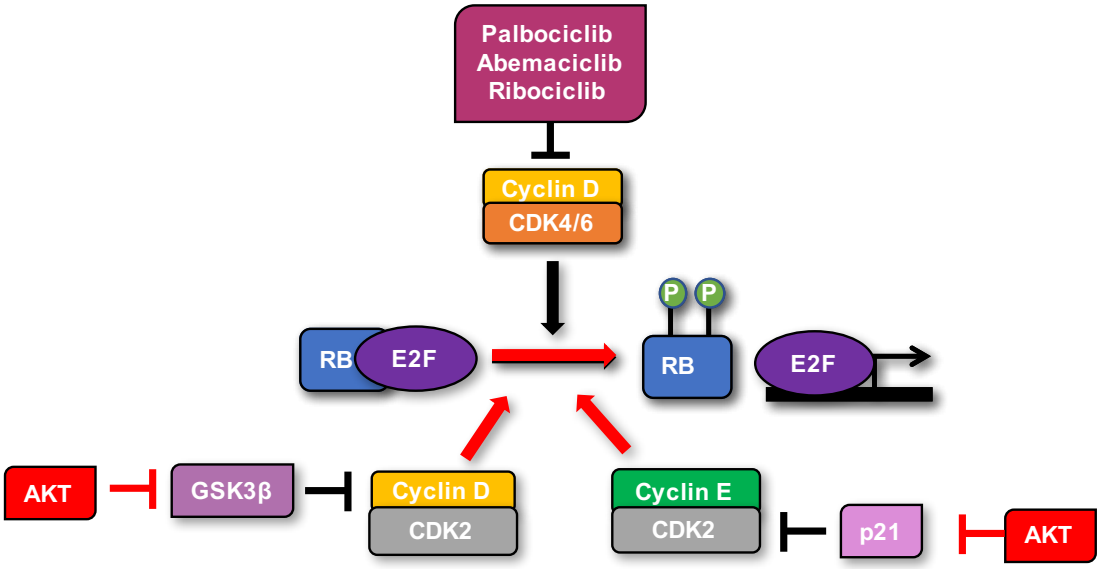

Figure 4.1. Model for AKT-mediated resistance to CDK4/6 inhibition.

top hits in our CSS screen overlap with those in the fulvestrant screen, suggesting that the screen identified on-target resistance mechanisms to anti-estrogen therapy.

Furthermore, the use of lentiviral ORF constructs may result in non-physiological gene expression. We attempted to account for potential artifacts of overexpression by using pharmacological inhibitors to rescue our phenotypes and by using alternative methods to activate AKT (such as with a constitutively active EGFR construct). To drive protein expression from endogenous promoters, one could use CRISPR activation (CRISPRa) technology (306). Experiments with mutant ORFs could also be confounded by the presence of the endogenous wild-type protein. In our studies with mutant ER, we attempted to account for this by conducting experiments under estrogen-deprived conditions, where the wild-type ER is non-functional. One could also use CRISPRs to engineer point mutations into the endogenous *ESR1* locus.

While T47D, MCF7 and ZR-75-1 cells were chosen based on their sensitivity to CDK4/6 inhibition, lentiviral infectability and growth rate, they all harbor genetic alterations in the PI3K pathway. Both T47D and MCF7 cells have an activating mutation in *PIK3CA.* T47D cells have an H1047R kinase domain mutation and MCF7 cells have a E545K helical mutation. ZR-75-1 cells are PTEN null. Our patient data, however, suggest that mutations in the PI3K pathway are likely not a pre-requisite for subsequent activating mutations in *AKT1*. *AKT1* mutations are observed in the absence of *PIK3CA* or *PTEN* mutations. Larger patient populations would be necessary to determine whether *PIK3CA* mutations pre-disposes tumors to additional *AKT* mutations.

Our validation studies also relied heavily on the *in vitro* cell culture models described above. Mouse xenograft experiments are currently underway to assess the efficacy of mTOR inhibition, CDK4/6 inhibition and estrogen deprivation in inhibiting the growth of ER+ breast cancer cells overexpressing AKT1. Since expression of wild-type AKT1 may not fully recapitulate the effects of mutant AKT1, the AKT1 mutations identified in patients will need to be

tested to determine whether they confer resistance to CDK4/6 inhibition. Patient-derived xenografts with activating mutations in AKT1 could also be used to test combination therapies.

Future Directions

Patient stratification is critical for identification of sensitive populations and in determination of alternative treatment strategies to combat resistance to CDK4/6 inhibitors. Our characterization of ER mutations and large scale ORF screens have opened many exciting avenues for future investigation. As outlined below, these studies highlight a need for further characterization of AKT-mediated resistance to CDK4/6 inhibition, sequencing of additional CDK4/6 inhibitor-treated breast cancer patients, and identification of targetable vulnerabilities in cells with inactivated RB.

Elucidating AKT's mechanism of action in CDK4/6 inhibitor resistance

In our study, AKT activation validated across many contexts as a driver of resistance to CDK4/6 inhibition. Since AKT has many downstream effectors, AKT may drive resistance to CDK4/6 inhibition through several mechanisms. Further study of AKT targets will inform clinical treatment and the development of novel therapies.

The role of cyclin D1 in response and resistance to CDK4/6 inhibition is unclear. In chapter 2, we found that cells expressing ER LBD mutants upregulate cyclin D1 expression and are sensitive to CDK4/6 inhibition. Similarly, high cyclin D1 expression and low p16 expression are predictive of sensitivity to palbociclib *in vitro* (4). Clinically, however, genetic amplification of *CCND1*, which encodes cyclin D1, is not associated with response to palbociclib and letrozole (252). In our resistance studies described in chapter 3, AKT's inactivation of GSK3β stabilizes cyclin D1 levels. Noncanonical interactions between cyclin D1 and CDK2 have been detected in ER+ breast cancer cells, which likely drive RB phosphorylation and adaptive resistance to

CDK4/6 inhibition (248). To further complicate matters, CDK4/6 inhibitor treatment increases cyclin D1 levels (Chapter 3, (247,248)).

One possible explanation for the data described above is that there is a difference between amplification of the *CCND1* gene and stabilization of cyclin D1 protein levels. While treatment with either palbociclib or abemaciclib increases cyclin D1 levels in sensitive cells, cyclin D1 levels are significantly higher in cells overexpressing AKT1, AKT2 and $EGFR^{L858R}$ (Chapter 3). Furthermore, we found *CCND1* amplification and *AKT1* mutations co-occur in CDK4/6 inhibitor-resistant tumor biopsies. Thus, the level of cyclin D1 induced by ER expression or *CCND1* gene expression may be sufficient to drive S phase progression, but render cells sensitive to CDK4/6 inhibitor. In contrast, stabilization of cyclin D1 levels by AKT may confer resistance to CDK4/6 inhibition.

To test whether cyclin D1 stabilization is sufficient to bypass CDK4/6 inhibition, one could use a non-degradable cyclin D1 mutant. AKT signaling prevents GSK3β from phosphorylating threonine 286 (T286) on cyclin D1 and inhibits cyclin D1 degradation (134,149). Substitution of T286 for alanine in cyclin D1 prevents GSK3β phosphorylation and inhibits cyclin D1 turnover. If stabilization of cyclin D1 confers resistance to CDK4/6 inhibition, then cells expressing the T286A cyclin D1 mutant (33) should be insensitive to CDK4/6 inhibitor treatment. Immunohistochemistry analysis of patient samples is needed to determine whether there is a correlation between cyclin D1 protein levels and resistance to CDK4/6 inhibition.

In chapter 3, our studies support an emerging hypothesis that CDK2 is a key node of resistance to CDK4/6 inhibition (219,247,248,277). Overexpression of AKT maintains CDK2 activation and mediates resistance to CDK4/6 inhibitors under estrogen-deprived conditions. AKT signaling upregulates cyclin D1 levels, increases p21 phosphorylation at T145 and maintains CDK2 phosphorylation at T160 despite CDK4/6 inhibition. Knockdown studies are needed to confirm the role of CDK2 in AKT-mediated resistance. In addition to AKT, we found that overexpression of a CCNE2 mutant predicted to constitutively activate CDK2 rendered cells

insensitive to CDK4/6 inhibition. Similarly, cyclin E1/2 expression bypassed CDK4/6 inhibition and cyclin E1 is amplified in MCF7 cells with acquired resistance to palbociclib (248,250). These results support the clinical development of CDK2 inhibitors.

Historically, most CDK2 inhibitors have failed in the clinic due to low specificity and lack of patient stratification (204). For example, CDK2 inhibitors, like dinaciclib, often co-target CDK1 (307). Whereas CDK2, CDK4 and CDK6 are dispensable for the proliferation of many cell types (246,308-310), CDK1 appears to be universally essential (311). Identification of synthetic lethal interactions with CDK2 inhibition or predictive biomarkers of sensitivity may lower the concentration of CDK2 inhibitor needed for efficacy and potentially limit toxicity. CDK4/6 inhibitor-resistant patients with CCNE1/2 amplification or lower molecular weight isoforms of CCNE2 may be particularly responsive to CDK2 inhibition. If patient stratification does not improve the therapeutic window for current CDK inhibitors, compounds with increased selectivity for CDK2 may be more useful.

Since AKT-mediated resistance to CDK4/6 inhibition requires mTOR, it will be important to assess whether mTOR mutations bypass the dependency of breast cancer cells on CDK4/6. Activating mutations in mTOR are well-characterized and sensitize cells to rapamycin treatment (312). If mTOR mutants also drive resistance to CDK4/6 inhibition, they should be assessed clinically. ER+ breast cancer patients may derive clinical benefit from combined CDK4/6 and mTOR inhibition.

Genome characterization

Clinical sequencing of additional patient samples will be needed to assess the generalizability of our findings and to build on our work. With a larger cohort of patients, one could determine whether *ESR1*-mutant patients with wild-type RB are significantly more sensitive to CDK4/6 inhibition and aromatase inhibitor therapy compared to patients with wild-type *ESR1*. Unbiased genomic characterization of patients with exquisite sensitivity to CDK4/6

inhibition could also reveal novel biomarkers for patient stratification. This approach has been used to study exceptional responders to everolimus (an mTOR inhibitor). Whole-exome sequencing of a patient who had a complete response to pazopanib (tyrosine kinase inhibitor) and everolimus (an mTOR inhibitor) treatment for two years uncovered activating mTOR mutations (313). Although sensitizing mutations like the ones found in mTOR may be rare on a population level, studies of exceptional responders can help identify their clinical significance. As CDK4/6 inhibitors are often used with ER-directed therapy and increasingly with other targeted agents, further sequencing studies will also identify genetic alterations that sensitize tumors to combination therapies.

Characterization of additional matched pre-treatment and post-relapse samples would reveal whether activating *AKT1* mutations are significantly associated with acquired resistance to CDK4/6 inhibition. Gene expression profiling of treatment-naïve and post-relapse biopsies from patients treated with endocrine therapy and CDK4/6 inhibitors would greatly complement our gain-of-function screens. These studies would reveal whether patients with acquired resistance to hormonal therapy and/or CDK4/6 inhibition show upregulation of our candidate resistance genes. Since our screens identified a diverse array of resistance mechanisms, RNA sequencing analysis of patient biopsies will also help prioritize clinically relevant hits for further validation.

Identifying differences between CDK4/6 inhibitors

While our work focused on convergent mechanisms of resistance to palbociclib and abemaciclib, differences between the inhibitors may also be clinically relevant. For patients with ER+ metastatic breast cancer, the clinical benefit rate of palbociclib monotherapy is only 21% compared to 44.7% for abemaciclib (230,241). Toxicity profiles also differ between the two drugs; palbociclib generally induces neutropenia (230,231), while abemaciclib treatment often triggers diarrhea (241,244). An understanding of the underlying differences between palbociclib

and abemaciclib will enable patient stratification and development of alternative treatment strategies.

Our studies provide several insights into potential mechanistic differences between the inhibitors, which warrant further investigation. Since RB is the main gatekeeper of the G1-S restriction point, RB loss should confer complete resistance to CDK4/6 inhibition. As described in Chapter 2, we used CRISPR technology to generate isogenic T47D cell lines with and without RB (**Fig. 3.2A**). Genetic loss of RB1 increased the GI_{50} of to the CDK4/6 inhibitor palbociclib by approximately 100-fold (**Fig. 3.2B**). Cell cycle analysis indicates that while palbociclib arrests cells with intact RB1 in G1, RB1 null cells progress into S phase despite palbociclib treatment (**Fig. 3.2C**). RB1 loss also renders cells resistant to abemaciclib, but only shifts the GI_{50} approximately 10-fold (**Fig. 3.2D**). Thus, abemaciclib can inhibit cell growth in a RB-independent manner at higher concentrations. Consistent with these findings, abemaciclib inhibits activity of additional kinases like CDK2 and PIM1 at micromolar concentrations (7).

Comparison of resistance profiles in our screens further suggests that abemaciclib has off-target activity. In viability assays conducted in chapter 3, AKT1, AKT2 and activated EGFR conferred resistance to both CDK4/6 inhibitors but higher doses of abemaciclib partially reduced cell viability. Cells expressing these genes were completely resistant to palbociclib up to 10μM at which point palbociclib is toxic. Thus, abemaciclib may have relevant off-target activity at concentrations greater than 1μM. Notably, CDK2 overexpression also conferred resistance to abemaciclib but not palbociclib; these observations are consistent with CDK2 being a target unique to abemaciclib but these observations would need to be validated.

Expression profiling and resistance screens conducted at higher concentrations of abemaciclib may be beneficial in determining the biological relevance of abemaciclib's off-target activity. The doses of abemaciclib and palbociclib used in our screens were chosen for on-target activity. RB null cells were continued to grow at 1μM palbociclib and 0.3μM abemaciclib in FBS media, whereas parental cells were sensitive. Similarly, in CSS media, *ESR1*^{Y537S}-mutant

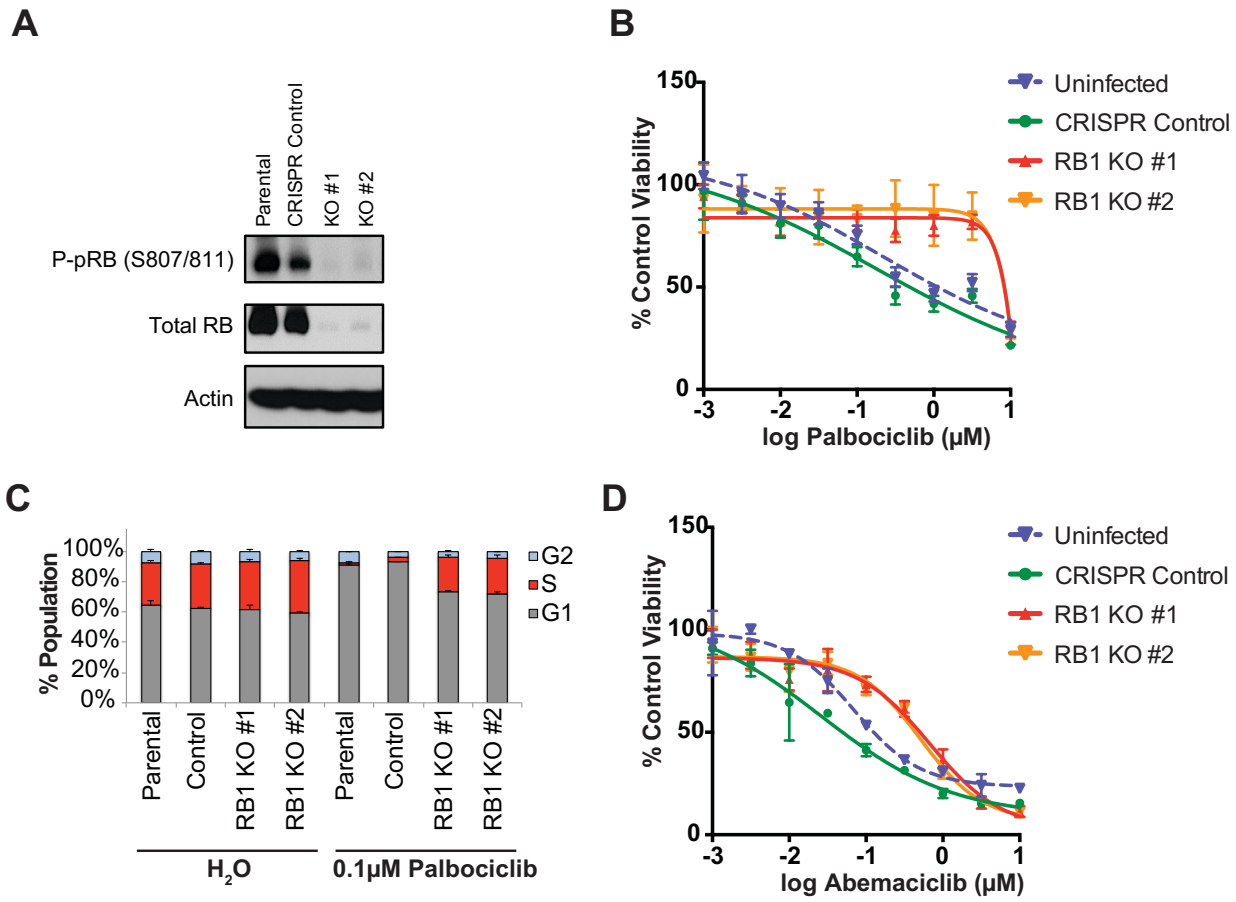

Figure 3.2. Knockout (KO) of RB1 reveals differences between CDK4/6 inhibitors. (A) Western blot analysis of T47D cells expressing control or RB1 CRISPRs. Cells were grown in full serum (FBS containing media). (B) Cells in (A) were plated in 96-well format and subsequently treated with indicated palbociclib concentrations in FBS media. %viability (determined by MTS assay) relative to vehicle control for 6 replicates +/- SD is shown after 6-day treatment. **(C)** Cell cycle analysis of T47D cells +/- RB treated with H2O (vehicle control) or palbociclib for 24 hours. Cells were stained with propidium iodide and indicated cell cycle phases were analyzed by flow cytometry and 2 replicates shown. **(D)** Same as (B) except cells were treated with abemaciclib and average for 3 replicates is shown. See Chapter 2 for additional methods.

cells with RB loss were insensitive to CDK4/6 inhibition. Abemaciclib, however, reduces the viability of RB null cells at higher concentrations (1-2μM) in FBS media. Comparison of the gene expression profiles at 0.3μM and 2μM of abemaciclib treatment may provide insights into the compound's off-target activity. Furthermore, resistance drivers in FBS palbociclib identified in the primary screen can be used to generate a mini pool of ORFs. ER+ breast cancer cells can then be infected with this mini pool and screened at 2μM of abemaciclib. Any hits that no longer score at this higher concentration of abemaciclib may be clinically relevant. It remains to be determined whether patients that progress on palbociclib may benefit from abemaciclib treatment.

Mapping the targetable vulnerabilities of RB null cells

All resistance mechanisms characterized in this work ultimately impinge on RB inactivation. In chapter 2, RB loss or co-expression of CDK6 and cyclin D1 rendered *ESR1*-mutant cells insensitive to palbociclib. In chapter 3, expression of AKT1, AKT2 and activated EGFR maintained RB phosphorylation despite CDK4/6 inhibitor treatment. Similarly, palbociclib and abemaciclib treatment was unable to reduce RB phosphorylation in cells cultured to resistance to CDK4/6 inhibition. For cells with hyperphosphorylated RB, treatment with other targeted therapies like AKT inhibitors may be sufficient to re-sensitize cells to CDK4/6 inhibition. In cells that have lost RB expression, however, treatment with a CDK4/6 inhibitor is no longer a viable option. Thus, the genetic dependencies of RB-null cells must be understood.

Loss of function screens can be utilized to identify synthetic lethal interactions with RB loss in ER+ breast cancer cells. This approach was used to identify a TBK1 co-dependency in *KRAS*-mutant cancer cells (314). Genetic knockout screens can be conducted with the Broad Institute's barcoded CRISPR library (315). Isogenic T47D cells with and without RB can be infected with Cas9 and the CRISPR guide library. Cells can then be cultured to determine which genes are selectively depleted in RB null cells. Knowledge of the dependencies unique

to RB null cells will enable the design of rational therapies with a high therapeutic window to combat resistance to CDK4/6 inhibition.

Concluding Remarks

This dissertation provides a framework for understanding the molecular determinants of response and resistance to CDK4/6 inhibition in ER+ breast cancer. Characterization of endocrine therapy-associated *ESR1* mutations reveals a dependency on CDK4/6 and underscores a need to identify exceptional responders to CDK4/6 inhibition. We conducted the first comprehensive gain-of-function screens to uncover drivers of resistance to CDK4/6 inhibitor monotherapy and in combination with estrogen deprivation in ER+ breast cancer. In addition to identifying AKT as a key bypass mechanism, these screens lay the groundwork for studies of CDK4/6 inhibitors in other genetic contexts and provide a functional map of resistance for clinical reference. Such integrative systematic studies will engender the development of novel therapeutic strategies to combat resistance to targeted therapy.

REFERENCES

1. Global Burden of Disease Cancer C, Fitzmaurice C, Allen C, Barber RM, Barregard L, Bhutta ZA*, et al.* Global, Regional, and National Cancer Incidence, Mortality, Years of Life Lost, Years Lived With Disability, and Disability-Adjusted Life-years for 32 Cancer Groups, 1990 to 2015: A Systematic Analysis for the Global Burden of Disease Study. JAMA Oncol **2016** doi 10.1001/jamaoncol.2016.5688.

2. Torre LA, Bray F, Siegel RL, Ferlay J, Lortet-Tieulent J, Jemal A. Global cancer statistics, 2012. CA Cancer J Clin **2015**;65(2):87-108 doi 10.3322/caac.21262.

3. Althuis MD, Dozier JM, Anderson WF, Devesa SS, Brinton LA. Global trends in breast cancer incidence and mortality 1973-1997. Int J Epidemiol **2005**;34(2):405-12 doi 10.1093/ije/dyh414.

4. Finn RS, Dering J, Conklin D, Kalous O, Cohen DJ, Desai AJ*, et al.* PD 0332991, a selective cyclin D kinase 4/6 inhibitor, preferentially inhibits proliferation of luminal estrogen receptor-positive human breast cancer cell lines in vitro. Breast Cancer Res **2009**;11(5):R77 doi 10.1186/bcr2419.

5. Toogood PL, Harvey PJ, Repine JT, Sheehan DJ, VanderWel SN, Zhou H*, et al.* Discovery of a potent and selective inhibitor of cyclin-dependent kinase 4/6. J Med Chem **2005**;48(7):2388-406 doi 10.1021/jm049354h.

6. Fry DW, Harvey PJ, Keller PR, Elliott WL, Meade M, Trachet E*, et al.* Specific inhibition of cyclin-dependent kinase 4/6 by PD 0332991 and associated antitumor activity in human tumor xenografts. Mol Cancer Ther **2004**;3(11):1427-38.

7. Gelbert LM, Cai S, Lin X, Sanchez-Martinez C, Del Prado M, Lallena MJ*, et al.* Preclinical characterization of the CDK4/6 inhibitor LY2835219: in-vivo cell cycle-dependent/independent anti-tumor activities alone/in combination with gemcitabine. Invest New Drugs **2014**;32(5):825-37 doi 10.1007/s10637-014-0120-7.

8. Kim S, Loo A, Chopra R, Caponigro G, Huang A, Vora S*, et al.* Abstract PR02: LEE011: An orally bioavailable, selective small molecule inhibitor of CDK4/6– Reactivating Rb in cancer. Molecular Cancer Therapeutics **2013**;12(11 Supplement):PR02-PR doi 10.1158/1535-7163.targ-13-pr02.

9. Nevins JR. E2F: a link between the Rb tumor suppressor protein and viral oncoproteins. Science **1992**;258(5081):424-9.

10. Sherr CJ, Beach D, Shapiro GI. Targeting CDK4 and CDK6: From Discovery to Therapy. Cancer Discov **2016**;6(4):353-67 doi 10.1158/2159-8290.CD-15-0894.

11. Flemington EK, Speck SH, Kaelin WG, Jr. E2F-1-mediated transactivation is inhibited by complex formation with the retinoblastoma susceptibility gene product. Proc Natl Acad Sci U S A **1993**;90(15):6914-8.

12. Sarcevic B, Lilischkis R, Sutherland RL. Differential phosphorylation of T-47D human breast cancer cell substrates by D1-, D3-, E-, and A-type cyclin-CDK complexes. J Biol Chem **1997**;272(52):33327-37.

13. Dickson C, Fantl V, Gillett C, Brookes S, Bartek J, Smith R*, et al.* Amplification of chromosome band 11q13 and a role for cyclin D1 in human breast cancer. Cancer Lett **1995**;90(1):43-50.

14. Florenes VA, Faye RS, Maelandsmo GM, Nesland JM, Holm R. Levels of cyclin D1 and D3 in malignant melanoma: deregulated cyclin D3 expression is associated with poor clinical outcome in superficial melanoma. Clin Cancer Res **2000**;6(9):3614-20.

15. Radulovich N, Pham NA, Strumpf D, Leung L, Xie W, Jurisica I*, et al.* Differential roles of cyclin D1 and D3 in pancreatic ductal adenocarcinoma. Mol Cancer **2010**;9:24 doi 10.1186/1476-4598-9-24.

16. Sherr CJ, Roberts JM. CDK inhibitors: positive and negative regulators of G1-phase progression. Genes Dev **1999**;13(12):1501-12.

17. Meyerson M, Harlow E. Identification of G1 kinase activity for cdk6, a novel cyclin D partner. Mol Cell Biol **1994**;14(3):2077-86.

18. Kato J, Matsushime H, Hiebert SW, Ewen ME, Sherr CJ. Direct binding of cyclin D to the retinoblastoma gene product (pRb) and pRb phosphorylation by the cyclin D-dependent kinase CDK4. Genes Dev **1993**;7(3):331-42.

19. Matsushime H, Ewen ME, Strom DK, Kato JY, Hanks SK, Roussel MF*, et al.* Identification and properties of an atypical catalytic subunit (p34PSK-J3/cdk4) for mammalian D type G1 cyclins. Cell **1992**;71(2):323-34.

20. Nevins JR. The Rb/E2F pathway and cancer. Hum Mol Genet **2001**;10(7):699-703.

21. Beijersbergen RL, Carlee L, Kerkhoven RM, Bernards R. Regulation of the retinoblastoma protein-related p107 by G1 cyclin complexes. Genes Dev **1995**;9(11):1340-53.

22. Xiao ZX, Ginsberg D, Ewen M, Livingston DM. Regulation of the retinoblastoma protein-related protein p107 by G1 cyclin-associated kinases. Proc Natl Acad Sci U S A **1996**;93(10):4633-7.

23. Tedesco D, Lukas J, Reed SI. The pRb-related protein p130 is regulated by phosphorylation-dependent proteolysis via the protein-ubiquitin ligase SCF(Skp2). Genes Dev **2002**;16(22):2946-57 doi 10.1101/gad.1011202.

24. Zarkowska T, Mittnacht S. Differential phosphorylation of the retinoblastoma protein by G1/S cyclin-dependent kinases. J Biol Chem **1997**;272(19):12738-46.

25. Lundberg AS, Weinberg RA. Functional inactivation of the retinoblastoma protein requires sequential modification by at least two distinct cyclin-cdk complexes. Mol Cell Biol **1998**;18(2):753-61.

26. Schulze A, Zerfass K, Spitkovsky D, Middendorp S, Berges J, Helin K*, et al.* Cell cycle regulation of the cyclin A gene promoter is mediated by a variant E2F site. Proc Natl Acad Sci U S A **1995**;92(24):11264-8.

27. Botz J, Zerfass-Thome K, Spitkovsky D, Delius H, Vogt B, Eilers M*, et al.* Cell cycle regulation of the murine cyclin E gene depends on an E2F binding site in the promoter. Mol Cell Biol **1996**;16(7):3401-9.

28. Hurford RK, Jr., Cobrinik D, Lee MH, Dyson N. pRB and p107/p130 are required for the regulated expression of different sets of E2F responsive genes. Genes Dev **1997**;11(11):1447-63.

29. Glotzer M, Murray AW, Kirschner MW. Cyclin is degraded by the ubiquitin pathway. Nature **1991**;349(6305):132-8 doi 10.1038/349132a0.

30. Ludlow JW, Shon J, Pipas JM, Livingston DM, DeCaprio JA. The retinoblastoma susceptibility gene product undergoes cell cycle-dependent dephosphorylation and binding to and release from SV40 large T. Cell **1990**;60(3):387-96.

31. Sweeney KJ, Swarbrick A, Sutherland RL, Musgrove EA. Lack of relationship between CDK activity and G1 cyclin expression in breast cancer cells. Oncogene **1998**;16(22):2865-78 doi 10.1038/sj.onc.1201814.

32. Alt JR, Cleveland JL, Hannink M, Diehl JA. Phosphorylation-dependent regulation of cyclin D1 nuclear export and cyclin D1-dependent cellular transformation. Genes Dev **2000**;14(24):3102-14.

33. Diehl JA, Zindy F, Sherr CJ. Inhibition of cyclin D1 phosphorylation on threonine-286 prevents its rapid degradation via the ubiquitin-proteasome pathway. Genes Dev **1997**;11(8):957-72.

34. Chytil A, Waltner-Law M, West R, Friedman D, Aakre M, Barker D*, et al.* Construction of a cyclin D1-Cdk2 fusion protein to model the biological functions of cyclin D1-Cdk2 complexes. J Biol Chem **2004**;279(46):47688-98 doi 10.1074/jbc.M405938200.

35. Serrano M, Hannon GJ, Beach D. A new regulatory motif in cell-cycle control causing specific inhibition of cyclin D/CDK4. Nature **1993**;366(6456):704-7 doi 10.1038/366704a0.

36. Hannon GJ, Beach D. p15INK4B is a potential effector of TGF-beta-induced cell cycle arrest. Nature **1994**;371(6494):257-61 doi 10.1038/371257a0.

37. Guan KL, Jenkins CW, Li Y, Nichols MA, Wu X, O'Keefe CL*, et al.* Growth suppression by p18, a p16INK4/MTS1- and p14INK4B/MTS2-related CDK6 inhibitor, correlates with wild-type pRb function. Genes Dev **1994**;8(24):2939-52.

38. Hirai H, Roussel MF, Kato JY, Ashmun RA, Sherr CJ. Novel INK4 proteins, p19 and p18, are specific inhibitors of the cyclin D-dependent kinases CDK4 and CDK6. Mol Cell Biol **1995**;15(5):2672-81.

39. Chan FK, Zhang J, Cheng L, Shapiro DN, Winoto A. Identification of human and mouse p19, a novel CDK4 and CDK6 inhibitor with homology to p16ink4. Mol Cell Biol **1995**;15(5):2682-8.

40. el-Deiry WS, Tokino T, Velculescu VE, Levy DB, Parsons R, Trent JM*, et al.* WAF1, a potential mediator of p53 tumor suppression. Cell **1993**;75(4):817-25.

41. Xiong Y, Hannon GJ, Zhang H, Casso D, Kobayashi R, Beach D. p21 is a universal inhibitor of cyclin kinases. Nature **1993**;366(6456):701-4 doi 10.1038/366701a0.

42. Harper JW, Adami GR, Wei N, Keyomarsi K, Elledge SJ. The p21 Cdk-interacting protein Cip1 is a potent inhibitor of G1 cyclin-dependent kinases. Cell **1993**;75(4):805-16.

43. Gu Y, Turck CW, Morgan DO. Inhibition of CDK2 activity in vivo by an associated 20K regulatory subunit. Nature **1993**;366(6456):707-10 doi 10.1038/366707a0.

44. Dulic V, Kaufmann WK, Wilson SJ, Tlsty TD, Lees E, Harper JW*, et al.* p53-dependent inhibition of cyclin-dependent kinase activities in human fibroblasts during radiation-induced G1 arrest. Cell **1994**;76(6):1013-23.

45. Noda A, Ning Y, Venable SF, Pereira-Smith OM, Smith JR. Cloning of senescent cell-derived inhibitors of DNA synthesis using an expression screen. Exp Cell Res **1994**;211(1):90-8 doi 10.1006/excr.1994.1063.

46. Polyak K, Kato JY, Solomon MJ, Sherr CJ, Massague J, Roberts JM*, et al.* p27Kip1, a cyclin-Cdk inhibitor, links transforming growth factor-beta and contact inhibition to cell cycle arrest. Genes Dev **1994**;8(1):9-22.

47. Polyak K, Lee MH, Erdjument-Bromage H, Koff A, Roberts JM, Tempst P*, et al.* Cloning of p27Kip1, a cyclin-dependent kinase inhibitor and a potential mediator of extracellular antimitogenic signals. Cell **1994**;78(1):59-66.

48. Toyoshima H, Hunter T. p27, a novel inhibitor of G1 cyclin-Cdk protein kinase activity, is related to p21. Cell **1994**;78(1):67-74.

49. Lee MH, Reynisdottir I, Massague J. Cloning of p57KIP2, a cyclin-dependent kinase inhibitor with unique domain structure and tissue distribution. Genes Dev **1995**;9(6):639-49.

50. Matsuoka S, Edwards MC, Bai C, Parker S, Zhang P, Baldini A*, et al.* p57KIP2, a structurally distinct member of the p21CIP1 Cdk inhibitor family, is a candidate tumor suppressor gene. Genes Dev **1995**;9(6):650-62.

51. Xiong Y, Zhang H, Beach D. Subunit rearrangement of the cyclin-dependent kinases is associated with cellular transformation. Genes Dev **1993**;7(8):1572-83.

52. Perou CM, Sorlie T, Eisen MB, van de Rijn M, Jeffrey SS, Rees CA*, et al.* Molecular portraits of human breast tumours. Nature **2000**;406(6797):747-52 doi 10.1038/35021093.

53. Sorlie T, Perou CM, Tibshirani R, Aas T, Geisler S, Johnsen H*, et al.* Gene expression patterns of breast carcinomas distinguish tumor subclasses with clinical implications. Proc Natl Acad Sci U S A **2001**;98(19):10869-74 doi 10.1073/pnas.191367098.

54. Parker JS, Mullins M, Cheang MC, Leung S, Voduc D, Vickery T*, et al.* Supervised risk predictor of breast cancer based on intrinsic subtypes. J Clin Oncol **2009**;27(8):1160-7 doi 10.1200/JCO.2008.18.1370.

55. Cancer Genome Atlas N. Comprehensive molecular portraits of human breast tumours. Nature **2012**;490(7418):61-70 doi 10.1038/nature11412.

56. Brenton JD, Carey LA, Ahmed AA, Caldas C. Molecular classification and molecular forecasting of breast cancer: ready for clinical application? J Clin Oncol **2005**;23(29):7350-60 doi 10.1200/JCO.2005.03.3845.

57. Palmieri C, Cheng GJ, Saji S, Zelada-Hedman M, Warri A, Weihua Z*, et al.* Estrogen receptor beta in breast cancer. Endocr Relat Cancer **2002**;9(1):1-13.

58. Fuqua SA, Schiff R, Parra I, Moore JT, Mohsin SK, Osborne CK*, et al.* Estrogen receptor beta protein in human breast cancer: correlation with clinical tumor parameters. Cancer Res **2003**;63(10):2434-9.

59. Cheang MC, Chia SK, Voduc D, Gao D, Leung S, Snider J*, et al.* Ki67 index, HER2 status, and prognosis of patients with luminal B breast cancer. J Natl Cancer Inst **2009**;101(10):736-50 doi 10.1093/jnci/djp082.

60. Dai X, Li T, Bai Z, Yang Y, Liu X, Zhan J*, et al.* Breast cancer intrinsic subtype classification, clinical use and future trends. Am J Cancer Res **2015**;5(10):2929-43.

61. Pollack JR, Perou CM, Alizadeh AA, Eisen MB, Pergamenschikov A, Williams CF*, et al.* Genome-wide analysis of DNA copy-number changes using cDNA microarrays. Nat Genet **1999**;23(1):41-6 doi 10.1038/12640.

62. Pauletti G, Godolphin W, Press MF, Slamon DJ. Detection and quantitation of HER-2/neu gene amplification in human breast cancer archival material using fluorescence in situ hybridization. Oncogene **1996**;13(1):63-72.

63. Cadoo KA, Gucalp A, Traina TA. Palbociclib: an evidence-based review of its potential in the treatment of breast cancer. Breast Cancer (Dove Med Press) **2014**;6:123-33 doi 10.2147/BCTT.S46725.

64. Milde-Langosch K, Bamberger AM, Rieck G, Kelp B, Loning T. Overexpression of the p16 cell cycle inhibitor in breast cancer is associated with a more malignant phenotype. Breast Cancer Res Treat **2001**;67(1):61-70.

65. Wang TC, Cardiff RD, Zukerberg L, Lees E, Arnold A, Schmidt EV. Mammary hyperplasia and carcinoma in MMTV-cyclin D1 transgenic mice. Nature **1994**;369(6482):669-71 doi 10.1038/369669a0.

66. Yu Q, Geng Y, Sicinski P. Specific protection against breast cancers by cyclin D1 ablation. Nature **2001**;411(6841):1017-21 doi 10.1038/35082500.

67. Bowe DB, Kenney NJ, Adereth Y, Maroulakou IG. Suppression of Neu-induced mammary tumor growth in cyclin D1 deficient mice is compensated for by cyclin E. Oncogene **2002**;21(2):291-8 doi 10.1038/sj.onc.1205025.

68. Landis MW, Pawlyk BS, Li T, Sicinski P, Hinds PW. Cyclin D1-dependent kinase activity in murine development and mammary tumorigenesis. Cancer Cell **2006**;9(1):13-22 doi 10.1016/j.ccr.2005.12.019.

69. Greene GL, Gilna P, Waterfield M, Baker A, Hort Y, Shine J. Sequence and expression of human estrogen receptor complementary DNA. Science **1986**;231(4742):1150-4.

70. Heldring N, Pike A, Andersson S, Matthews J, Cheng G, Hartman J*, et al.* Estrogen receptors: how do they signal and what are their targets. Physiol Rev **2007**;87(3):905-31 doi 10.1152/physrev.00026.2006.

71. Nilsson S, Makela S, Treuter E, Tujague M, Thomsen J, Andersson G*, et al.* Mechanisms of estrogen action. Physiol Rev **2001**;81(4):1535-65.

72. Mangelsdorf DJ, Thummel C, Beato M, Herrlich P, Schutz G, Umesono K*, et al.* The nuclear receptor superfamily: the second decade. Cell **1995**;83(6):835-9.

73. Lupien M, Meyer CA, Bailey ST, Eeckhoute J, Cook J, Westerling T*, et al.* Growth factor stimulation induces a distinct ER(alpha) cistrome underlying breast cancer endocrine resistance. Genes Dev **2010**;24(19):2219-27 doi 10.1101/gad.1944810.

74. Klinge CM. Estrogen receptor interaction with estrogen response elements. Nucleic Acids Res **2001**;29(14):2905-19.

75. Klinge CM. Estrogen receptor interaction with co-activators and co-repressors. Steroids **2000**;65(5):227-51.

76. Kushner PJ, Agard DA, Greene GL, Scanlan TS, Shiau AK, Uht RM*, et al.* Estrogen receptor pathways to AP-1. J Steroid Biochem Mol Biol **2000**;74(5):311-7.

77. Shao W, Brown M. Advances in estrogen receptor biology: prospects for improvements in targeted breast cancer therapy. Breast Cancer Res **2004**;6(1):39-52 doi 10.1186/bcr742.

78. Gillett C, Fantl V, Smith R, Fisher C, Bartek J, Dickson C*, et al.* Amplification and overexpression of cyclin D1 in breast cancer detected by immunohistochemical staining. Cancer Res **1994**;54(7):1812-7.

79. Herber B, Truss M, Beato M, Muller R. Inducible regulatory elements in the human cyclin D1 promoter. Oncogene **1994**;9(4):1295-304.

80. Sabbah M, Courilleau D, Mester J, Redeuilh G. Estrogen induction of the cyclin D1 promoter: involvement of a cAMP response-like element. Proc Natl Acad Sci U S A **1999**;96(20):11217-22.

81. Castro-Rivera E, Samudio I, Safe S. Estrogen regulation of cyclin D1 gene expression in ZR-75 breast cancer cells involves multiple enhancer elements. J Biol Chem **2001**;276(33):30853-61 doi 10.1074/jbc.M103339200.

82. Cicatiello L, Addeo R, Sasso A, Altucci L, Petrizzi VB, Borgo R*, et al.* Estrogens and progesterone promote persistent CCND1 gene activation during G1 by inducing transcriptional derepression via c-Jun/c-Fos/estrogen receptor (progesterone receptor) complex assembly to a distal regulatory element and recruitment of cyclin D1 to its own gene promoter. Mol Cell Biol **2004**;24(16):7260-74 doi 10.1128/MCB.24.16.7260-7274.2004.

83. Eeckhoute J, Carroll JS, Geistlinger TR, Torres-Arzayus MI, Brown M. A cell-type-specific transcriptional network required for estrogen regulation of cyclin D1 and cell cycle progression in breast cancer. Genes Dev **2006**;20(18):2513-26 doi 10.1101/gad.1446006.

84. Zwijsen RM, Wientjens E, Klompmaker R, van der Sman J, Bernards R, Michalides RJ. CDK-independent activation of estrogen receptor by cyclin D1. Cell **1997**;88(3):405-15.

85. Neuman E, Ladha MH, Lin N, Upton TM, Miller SJ, DiRenzo J*, et al.* Cyclin D1 stimulation of estrogen receptor transcriptional activity independent of cdk4. Mol Cell Biol **1997**;17(9):5338-47.

86. Garraway LA, Sellers WR. Lineage dependency and lineage-survival oncogenes in human cancer. Nat Rev Cancer **2006**;6(8):593-602 doi 10.1038/nrc1947.

87. Osborne CK. Tamoxifen in the treatment of breast cancer. N Engl J Med **1998**;339(22):1609-18 doi 10.1056/NEJM199811263392207.

88. Nayfield SG, Karp JE, Ford LG, Dorr FA, Kramer BS. Potential role of tamoxifen in prevention of breast cancer. J Natl Cancer Inst **1991**;83(20):1450-9.

89. Fisher B, Costantino JP, Redmond CK, Fisher ER, Wickerham DL, Cronin WM. Endometrial cancer in tamoxifen-treated breast cancer patients: findings from the National Surgical Adjuvant Breast and Bowel Project (NSABP) B-14. J Natl Cancer Inst **1994**;86(7):527-37.

90. Kedar RP, Bourne TH, Powles TJ, Collins WP, Ashley SE, Cosgrove DO*, et al.* Effects of tamoxifen on uterus and ovaries of postmenopausal women in a randomised breast cancer prevention trial. Lancet **1994**;343(8909):1318-21.

91. Buzdar AU. Superior efficacy of letrozole versus tamoxifen as first-line therapy. Journal of clinical oncology : official journal of the American Society of Clinical Oncology **2002**;20(3):876-8.

92. Nabholtz JM, Buzdar A, Pollak M, Harwin W, Burton G, Mangalik A*, et al.* Anastrozole is superior to tamoxifen as first-line therapy for advanced breast cancer in postmenopausal women: results of a North American multicenter randomized trial. Arimidex Study Group. Journal of clinical oncology : official journal of the American Society of Clinical Oncology **2000**;18(22):3758-67.

93. Bonneterre J, Thurlimann B, Robertson JF, Krzakowski M, Mauriac L, Koralewski P*, et al.* Anastrozole versus tamoxifen as first-line therapy for advanced breast cancer in 668 postmenopausal women: results of the Tamoxifen or Arimidex Randomized Group Efficacy and Tolerability study. Journal of clinical oncology : official journal of the American Society of Clinical Oncology **2000**;18(22):3748-57.

94. Lonning PE, Geisler J. Indications and limitations of third-generation aromatase inhibitors. Expert Opin Investig Drugs **2008**;17(5):723-39 doi 10.1517/13543784.17.5.723.

95. Geisler J. Differences between the non-steroidal aromatase inhibitors anastrozole and letrozole--of clinical importance? British journal of cancer **2011**;104(7):1059-66 doi 10.1038/bjc.2011.58.

96. Geisler J, Haynes B, Anker G, Dowsett M, Lonning PE. Influence of letrozole and anastrozole on total body aromatization and plasma estrogen levels in postmenopausal breast cancer patients evaluated in a randomized, cross-over study. J Clin Oncol **2002**;20(3):751-7 doi 10.1200/JCO.2002.20.3.751.

97. Dowsett M, Jones A, Johnston SR, Jacobs S, Trunet P, Smith IE. In vivo measurement of aromatase inhibition by letrozole (CGS 20267) in postmenopausal patients with breast cancer. Clin Cancer Res **1995**;1(12):1511-5.

98. Wakeling AE, Dukes M, Bowler J. A potent specific pure antiestrogen with clinical potential. Cancer Res **1991**;51(15):3867-73.

99. Bross PF, Baird A, Chen G, Jee JM, Lostritto RT, Morse DE*, et al.* Fulvestrant in postmenopausal women with advanced breast cancer. Clin Cancer Res **2003**;9(12):4309-17.

100. Dauvois S, Danielian PS, White R, Parker MG. Antiestrogen ICI 164,384 reduces cellular estrogen receptor content by increasing its turnover. Proc Natl Acad Sci U S A **1992**;89(9):4037-41.

101. Gibson MK, Nemmers LA, Beckman WC, Jr., Davis VL, Curtis SW, Korach KS. The mechanism of ICI 164,384 antiestrogenicity involves rapid loss of estrogen receptor in uterine tissue. Endocrinology **1991**;129(4):2000-10 doi 10.1210/endo-129-4-2000.

102. Reese JC, Katzenellenbogen BS. Examination of the DNA-binding ability of estrogen receptor in whole cells: implications for hormone-independent transactivation and the actions of antiestrogens. Mol Cell Biol **1992**;12(10):4531-8.

103. Ma CX, Reinert T, Chmielewska I, Ellis MJ. Mechanisms of aromatase inhibitor resistance. Nat Rev Cancer **2015**;15(5):261-75 doi 10.1038/nrc3920.

104. Osborne CK, Schiff R. Mechanisms of endocrine resistance in breast cancer. Annu Rev Med **2011**;62:233-47 doi 10.1146/annurev-med-070909-182917.

105. Mouridsen H, Gershanovich M, Sun Y, Perez-Carrion R, Boni C, Monnier A*, et al.* Superior efficacy of letrozole versus tamoxifen as first-line therapy for postmenopausal women with advanced breast cancer: results of a phase III study of the International Letrozole Breast Cancer Group. J Clin Oncol **2001**;19(10):2596-606 doi 10.1200/JCO.2001.19.10.2596.

106. Mouridsen H, Gershanovich M, Sun Y, Perez-Carrion R, Boni C, Monnier A*, et al.* Phase III study of letrozole versus tamoxifen as first-line therapy of advanced breast cancer in postmenopausal women: analysis of survival and update of efficacy from the International Letrozole Breast Cancer Group. J Clin Oncol **2003**;21(11):2101-9 doi 10.1200/JCO.2003.04.194.

107. Ingle JN, Suman VJ, Rowland KM, Mirchandani D, Bernath AM, Camoriano JK*, et al.* Fulvestrant in women with advanced breast cancer after progression on prior aromatase inhibitor therapy: North Central Cancer Treatment Group Trial N0032. J Clin Oncol **2006**;24(7):1052-6 doi 10.1200/JCO.2005.04.1053.

108. Zhang QX, Borg A, Wolf DM, Oesterreich S, Fuqua SA. An estrogen receptor mutant with strong hormone-independent activity from a metastatic breast cancer. Cancer Res **1997**;57(7):1244-9.

109. Ellis MJ, Ding L, Shen D, Luo J, Suman VJ, Wallis JW*, et al.* Whole-genome analysis informs breast cancer response to aromatase inhibition. Nature **2012**;486(7403):353-60 doi 10.1038/nature11143.

110. Toy W, Shen Y, Won H, Green B, Sakr RA, Will M*, et al.* ESR1 ligand-binding domain mutations in hormone-resistant breast cancer. Nat Genet **2013**;45(12):1439-45 doi 10.1038/ng.2822.

111. Jeselsohn R, Yelensky R, Buchwalter G, Frampton G, Meric-Bernstam F, Gonzalez-Angulo AM*, et al.* Emergence of constitutively active estrogen receptor-alpha mutations in pretreated advanced estrogen receptor-positive breast cancer. Clin Cancer Res **2014**;20(7):1757-67 doi 10.1158/1078-0432.CCR-13-2332.

112. Robinson DR, Wu YM, Vats P, Su F, Lonigro RJ, Cao X*, et al.* Activating ESR1 mutations in hormone-resistant metastatic breast cancer. Nature genetics **2013**;45(12):1446-51 doi 10.1038/ng.2823.

113. Li S, Shen D, Shao J, Crowder R, Liu W, Prat A*, et al.* Endocrine-therapy-resistant ESR1 variants revealed by genomic characterization of breast-cancer-derived xenografts. Cell Rep **2013**;4(6):1116-30 doi 10.1016/j.celrep.2013.08.022.

114. Segal CV, Dowsett M. Estrogen receptor mutations in breast cancer--new focus on an old target. Clin Cancer Res **2014**;20(7):1724-6 doi 10.1158/1078-0432.CCR-14-0067.

115. Baselga J, Piccart M, Rugo H, Chen D, Burris HA, Campone M*, et al.* Abstract 4564: Assessment of genetic alterations using next-generation sequencing in postmenopausal women with hormone receptor-positive, HER2-negative advanced breast cancer: results from the BOLERO-2 phase III trial. Cancer Research **2013**;73(8 Supplement):4564- doi 10.1158/1538-7445.am2013-4564.

116. Merenbakh-Lamin K, Ben-Baruch N, Yeheskel A, Dvir A, Soussan-Gutman L, Jeselsohn R*, et al.* D538G mutation in estrogen receptor-alpha: A novel mechanism for acquired endocrine resistance in breast cancer. Cancer Res **2013**;73(23):6856-64 doi 10.1158/0008-5472.CAN-13-1197.

117. Toy W, Weir H, Razavi P, Lawson M, Goeppert AU, Mazzola AM*, et al.* Activating ESR1 Mutations Differentially Affect the Efficacy of ER Antagonists. Cancer Discov **2017**;7(3):277-87 doi 10.1158/2159-8290.CD-15-1523.

118. Spoerke JM, Gendreau S, Walter K, Qiu J, Wilson TR, Savage H*, et al.* Heterogeneity and clinical significance of ESR1 mutations in ER-positive metastatic breast cancer patients receiving fulvestrant. Nat Commun **2016**;7:11579 doi 10.1038/ncomms11579.

119. Schiavon G, Hrebien S, Garcia-Murillas I, Cutts RJ, Pearson A, Tarazona N*, et al.* Analysis of ESR1 mutation in circulating tumor DNA demonstrates evolution during therapy for metastatic breast cancer. Sci Transl Med **2015**;7(313):313ra182 doi 10.1126/scitranslmed.aac7551.

120. Harris AL, Nicholson S, Sainsbury JR, Farndon J, Wright C. Epidermal growth factor receptors in breast cancer: association with early relapse and death, poor response to hormones and interactions with neu. J Steroid Biochem **1989**;34(1-6):123-31.

121. Wright C, Nicholson S, Angus B, Sainsbury JR, Farndon J, Cairns J*, et al.* Relationship between c-erbB-2 protein product expression and response to endocrine therapy in advanced breast cancer. British journal of cancer **1992**;65(1):118-21.

122. Borg A, Baldetorp B, Ferno M, Killander D, Olsson H, Ryden S*, et al.* ERBB2 amplification is associated with tamoxifen resistance in steroid-receptor positive breast cancer. Cancer Lett **1994**;81(2):137-44.

123. Carlomagno C, Perrone F, Gallo C, De Laurentiis M, Lauria R, Morabito A*, et al.* c-erb B2 overexpression decreases the benefit of adjuvant tamoxifen in early-stage breast cancer without axillary lymph node metastases. J Clin Oncol **1996**;14(10):2702-8 doi 10.1200/JCO.1996.14.10.2702.

124. Houston SJ, Plunkett TA, Barnes DM, Smith P, Rubens RD, Miles DW. Overexpression of c-erbB2 is an independent marker of resistance to endocrine therapy in advanced breast cancer. British journal of cancer **1999**;79(7-8):1220-6 doi 10.1038/sj.bjc.6690196.

125. Zhang Y, Moerkens M, Ramaiahgari S, de Bont H, Price L, Meerman J*, et al.* Elevated insulin-like growth factor 1 receptor signaling induces antiestrogen resistance through the MAPK/ERK and PI3K/Akt signaling routes. Breast Cancer Res **2011**;13(3):R52 doi 10.1186/bcr2883.

126. Turner N, Pearson A, Sharpe R, Lambros M, Geyer F, Lopez-Garcia MA*, et al.* FGFR1 amplification drives endocrine therapy resistance and is a therapeutic target in breast cancer. Cancer Res **2010**;70(5):2085-94 doi 10.1158/0008-5472.CAN-09-3746.

127. McClelland RA, Barrow D, Madden TA, Dutkowski CM, Pamment J, Knowlden JM*, et al.* Enhanced epidermal growth factor receptor signaling in MCF7 breast cancer cells after long-term culture in the presence of the pure antiestrogen ICI 182,780 (Faslodex). Endocrinology **2001**;142(7):2776-88 doi 10.1210/endo.142.7.8259.

128. Lemmon MA, Schlessinger J. Cell signaling by receptor tyrosine kinases. Cell **2010**;141(7):1117-34 doi 10.1016/j.cell.2010.06.011.

129. Levin ER. Elusive extranuclear estrogen receptors in breast cancer. Clin Cancer Res **2012**;18(1):6-8 doi 10.1158/1078-0432.CCR-11-2547.

130. Kato S, Endoh H, Masuhiro Y, Kitamoto T, Uchiyama S, Sasaki H*, et al.* Activation of the estrogen receptor through phosphorylation by mitogen-activated protein kinase. Science **1995**;270(5241):1491-4.

131. Font de Mora J, Brown M. AIB1 is a conduit for kinase-mediated growth factor signaling to the estrogen receptor. Mol Cell Biol **2000**;20(14):5041-7.

132. Cantley LC. The phosphoinositide 3-kinase pathway. Science **2002**;296(5573):1655-7 doi 10.1126/science.296.5573.1655.

133. Liang J, Zubovitz J, Petrocelli T, Kotchetkov R, Connor MK, Han K*, et al.* PKB/Akt phosphorylates p27, impairs nuclear import of p27 and opposes p27-mediated G1 arrest. Nat Med **2002**;8(10):1153-60 doi 10.1038/nm761.

134. Diehl JA, Cheng M, Roussel MF, Sherr CJ. Glycogen synthase kinase-3beta regulates cyclin D1 proteolysis and subcellular localization. Genes Dev **1998**;12(22):3499-511.

135. Manning BD, Cantley LC. AKT/PKB signaling: navigating downstream. Cell **2007**;129(7):1261-74 doi 10.1016/j.cell.2007.06.009.

136. Laplante M, Sabatini DM. mTOR signaling in growth control and disease. Cell **2012**;149(2):274-93 doi 10.1016/j.cell.2012.03.017.

137. Creighton CJ, Hilger AM, Murthy S, Rae JM, Chinnaiyan AM, El-Ashry D. Activation of mitogen-activated protein kinase in estrogen receptor alpha-positive breast cancer cells in vitro induces an in vivo molecular phenotype of estrogen receptor alpha-negative human breast tumors. Cancer Res **2006**;66(7):3903-11 doi 10.1158/0008-5472.CAN-05-4363.

138. Oh AS, Lorant LA, Holloway JN, Miller DL, Kern FG, El-Ashry D. Hyperactivation of MAPK induces loss of ERalpha expression in breast cancer cells. Mol Endocrinol **2001**;15(8):1344-59 doi 10.1210/mend.15.8.0678.

139. Bayliss J, Hilger A, Vishnu P, Diehl K, El-Ashry D. Reversal of the estrogen receptor negative phenotype in breast cancer and restoration of antiestrogen response. Clin Cancer Res **2007**;13(23):7029-36 doi 10.1158/1078-0432.CCR-07-0587.

140. Wong KK, Engelman JA, Cantley LC. Targeting the PI3K signaling pathway in cancer. Curr Opin Genet Dev **2010**;20(1):87-90 doi 10.1016/j.gde.2009.11.002.

141. Yuan TL, Cantley LC. PI3K pathway alterations in cancer: variations on a theme. Oncogene **2008**;27(41):5497-510 doi 10.1038/onc.2008.245.

142. Saal LH, Holm K, Maurer M, Memeo L, Su T, Wang X*, et al.* PIK3CA mutations correlate with hormone receptors, node metastasis, and ERBB2, and are mutually exclusive with PTEN loss in human breast carcinoma. Cancer Res **2005**;65(7):2554-9 doi 10.1158/0008-5472-CAN-04-3913.

143. Samuels Y, Wang Z, Bardelli A, Silliman N, Ptak J, Szabo S*, et al.* High frequency of mutations of the PIK3CA gene in human cancers. Science **2004**;304(5670):554 doi 10.1126/science.1096502.

144. Thorpe LM, Yuzugullu H, Zhao JJ. PI3K in cancer: divergent roles of isoforms, modes of activation and therapeutic targeting. Nat Rev Cancer **2015**;15(1):7-24 doi 10.1038/nrc3860.

145. Alessi DR, James SR, Downes CP, Holmes AB, Gaffney PR, Reese CB*, et al.* Characterization of a 3-phosphoinositide-dependent protein kinase which phosphorylates and activates protein kinase Balpha. Curr Biol **1997**;7(4):261-9.

146. Sarbassov DD, Guertin DA, Ali SM, Sabatini DM. Phosphorylation and regulation of Akt/PKB by the rictor-mTOR complex. Science **2005**;307(5712):1098-101 doi 10.1126/science.1106148.

147. Stal O, Perez-Tenorio G, Akerberg L, Olsson B, Nordenskjold B, Skoog L*, et al.* Akt kinases in breast cancer and the results of adjuvant therapy. Breast Cancer Res **2003**;5(2):R37-44.

148. Stemke-Hale K, Gonzalez-Angulo AM, Lluch A, Neve RM, Kuo WL, Davies M*, et al.* An integrative genomic and proteomic analysis of PIK3CA, PTEN, and AKT mutations in breast cancer. Cancer Res **2008**;68(15):6084-91 doi 10.1158/0008-5472.CAN-07-6854.

149. Fang X, Yu SX, Lu Y, Bast RC, Jr., Woodgett JR, Mills GB. Phosphorylation and inactivation of glycogen synthase kinase 3 by protein kinase A. Proc Natl Acad Sci U S A **2000**;97(22):11960-5 doi 10.1073/pnas.220413597.

150. Rossig L, Jadidi AS, Urbich C, Badorff C, Zeiher AM, Dimmeler S. Akt-dependent phosphorylation of p21(Cip1) regulates PCNA binding and proliferation of endothelial cells. Mol Cell Biol **2001**;21(16):5644-57 doi 10.1128/MCB.21.16.5644-5657.2001.

151. Guertin DA, Sabatini DM. Defining the role of mTOR in cancer. Cancer Cell **2007**;12(1):9-22 doi 10.1016/j.ccr.2007.05.008.

152. Brown EJ, Albers MW, Shin TB, Ichikawa K, Keith CT, Lane WS*, et al.* A mammalian protein targeted by G1-arresting rapamycin-receptor complex. Nature **1994**;369(6483):756-8 doi 10.1038/369756a0.

153. Averous J, Fonseca BD, Proud CG. Regulation of cyclin D1 expression by mTORC1 signaling requires eukaryotic initiation factor 4E-binding protein 1. Oncogene **2008**;27(8):1106-13 doi 10.1038/sj.onc.1210715.

154. Hashemolhosseini S, Nagamine Y, Morley SJ, Desrivieres S, Mercep L, Ferrari S. Rapamycin inhibition of the G1 to S transition is mediated by effects on cyclin D1 mRNA and protein stability. J Biol Chem **1998**;273(23):14424-9.

155. Law M, Forrester E, Chytil A, Corsino P, Green G, Davis B*, et al.* Rapamycin disrupts cyclin/cyclin-dependent kinase/p21/proliferating cell nuclear antigen complexes and cyclin D1 reverses rapamycin action by stabilizing these complexes. Cancer Res **2006**;66(2):1070-80 doi 10.1158/0008-5472.CAN-05-1672.

156. Miller TW, Hennessy BT, Gonzalez-Angulo AM, Fox EM, Mills GB, Chen H*, et al.* Hyperactivation of phosphatidylinositol-3 kinase promotes escape from hormone dependence in estrogen receptor-positive human breast cancer. J Clin Invest **2010**;120(7):2406-13 doi 10.1172/JCI41680.

157. Serra V, Markman B, Scaltriti M, Eichhorn PJ, Valero V, Guzman M*, et al.* NVP-BEZ235, a dual PI3K/mTOR inhibitor, prevents PI3K signaling and inhibits the growth of cancer cells with activating PI3K mutations. Cancer Res **2008**;68(19):8022-30 doi 10.1158/0008-5472.CAN-08-1385.

158. Sanchez CG, Ma CX, Crowder RJ, Guintoli T, Phommaly C, Gao F*, et al.* Preclinical modeling of combined phosphatidylinositol-3-kinase inhibition with endocrine therapy for estrogen receptor-positive breast cancer. Breast Cancer Res **2011**;13(2):R21 doi 10.1186/bcr2833.

159. Miller TW, Perez-Torres M, Narasanna A, Guix M, Stal O, Perez-Tenorio G*, et al.* Loss of Phosphatase and Tensin homologue deleted on chromosome 10 engages ErbB3 and insulin-like growth factor-I receptor signaling to promote antiestrogen resistance in breast cancer. Cancer Res **2009**;69(10):4192-201 doi 10.1158/0008-5472.CAN-09-0042.

160. Beeram M, Tan QT, Tekmal RR, Russell D, Middleton A, DeGraffenried LA. Akt-induced endocrine therapy resistance is reversed by inhibition of mTOR signaling. Ann Oncol **2007**;18(8):1323-8 doi 10.1093/annonc/mdm170.

161. Kaufman B, Mackey JR, Clemens MR, Bapsy PP, Vaid A, Wardley A*, et al.* Trastuzumab plus anastrozole versus anastrozole alone for the treatment of postmenopausal women with human epidermal growth factor receptor 2-positive, hormone receptor-positive metastatic breast cancer: results from the randomized phase III TAnDEM study. J Clin Oncol **2009**;27(33):5529-37 doi 10.1200/JCO.2008.20.6847.

162. Marcom PK, Isaacs C, Harris L, Wong ZW, Kommarreddy A, Novielli N*, et al.* The combination of letrozole and trastuzumab as first or second-line biological therapy produces durable responses in a subset of HER2 positive and ER positive advanced breast cancers. Breast Cancer Res Treat **2007**;102(1):43-9 doi 10.1007/s10549-006-9307-8.

163. Beaver JA, Park BH. The BOLERO-2 trial: the addition of everolimus to exemestane in the treatment of postmenopausal hormone receptor-positive advanced breast cancer. Future Oncol **2012**;8(6):651-7 doi 10.2217/fon.12.49.

164. Johnston S, Pippen J, Jr., Pivot X, Lichinitser M, Sadeghi S, Dieras V*, et al.* Lapatinib combined with letrozole versus letrozole and placebo as first-line therapy for postmenopausal hormone receptor-positive metastatic breast cancer. J Clin Oncol **2009**;27(33):5538-46 doi 10.1200/JCO.2009.23.3734.

165. Schwartzberg LS, Franco SX, Florance A, O'Rourke L, Maltzman J, Johnston S. Lapatinib plus letrozole as first-line therapy for HER-2+ hormone receptor-positive metastatic breast cancer. Oncologist **2010**;15(2):122-9 doi 10.1634/theoncologist.2009-0240.

166. Baselga J, Campone M, Piccart M, Burris HA, 3rd, Rugo HS, Sahmoud T*, et al.* Everolimus in postmenopausal hormone-receptor-positive advanced breast cancer. N Engl J Med **2012**;366(6):520-9 doi 10.1056/NEJMoa1109653.

167. Bachelot T, Bourgier C, Cropet C, Ray-Coquard I, Ferrero JM, Freyer G*, et al.* Randomized phase II trial of everolimus in combination with tamoxifen in patients with hormone receptor-positive, human epidermal growth factor receptor 2-negative metastatic breast cancer with prior exposure to aromatase inhibitors: a GINECO study. J Clin Oncol **2012**;30(22):2718-24 doi 10.1200/JCO.2011.39.0708.

168. O'Reilly KE, Rojo F, She QB, Solit D, Mills GB, Smith D*, et al.* mTOR inhibition induces upstream receptor tyrosine kinase signaling and activates Akt. Cancer Res **2006**;66(3):1500-8 doi 10.1158/0008-5472.CAN-05-2925.

169. Wan X, Harkavy B, Shen N, Grohar P, Helman LJ. Rapamycin induces feedback activation of Akt signaling through an IGF-1R-dependent mechanism. Oncogene **2007**;26(13):1932-40 doi 10.1038/sj.onc.1209990.

170. Dienstmann R, Rodon J, Serra V, Tabernero J. Picking the point of inhibition: a comparative review of PI3K/AKT/mTOR pathway inhibitors. Mol Cancer Ther **2014**;13(5):1021-31 doi 10.1158/1535-7163.MCT-13-0639.

171. Massarweh S, Osborne CK, Creighton CJ, Qin L, Tsimelzon A, Huang S*, et al.* Tamoxifen resistance in breast tumors is driven by growth factor receptor signaling with repression of classic estrogen receptor genomic function. Cancer Res **2008**;68(3):826-33 doi 10.1158/0008-5472.CAN-07-2707.

172. Osborne CK, Neven P, Dirix LY, Mackey JR, Robert J, Underhill C*, et al.* Gefitinib or placebo in combination with tamoxifen in patients with hormone receptor-positive metastatic breast cancer: a randomized phase II study. Clin Cancer Res **2011**;17(5):1147-59 doi 10.1158/1078-0432.CCR-10-1869.

173. Kaufman P, Ferrero J, Bourgeois H, Kennecke H, De Boer R, Jacot W*, et al.* Abstract S1-4: A Randomized, Double-Blind, Placebo-Controlled, Phase 2 Study of AMG 479 With Exemestane (E) or Fulvestrant (F) in Postmenopausal Women With Hormone-Receptor Positive (HR+) Metastatic (M) or Locally Advanced (LA) Breast Cancer (BC). Cancer Research **2010**;70(24 Supplement):S1-4-S1-4 doi 10.1158/0008-5472.sabcs10-s1-4.

174. Bendell JC, Rodon J, Burris HA, de Jonge M, Verweij J, Birle D*, et al.* Phase I, dose-escalation study of BKM120, an oral pan-Class I PI3K inhibitor, in patients with advanced solid tumors. J Clin Oncol **2012**;30(3):282-90 doi 10.1200/JCO.2011.36.1360.

175. O'Brien C, Wallin JJ, Sampath D, GuhaThakurta D, Savage H, Punnoose EA*, et al.* Predictive biomarkers of sensitivity to the phosphatidylinositol 3' kinase inhibitor GDC-0941 in breast cancer preclinical models. Clin Cancer Res **2010**;16(14):3670-83 doi 10.1158/1078-0432.CCR-09-2828.

176. Juric D, Rodon J, Gonzalez-Angulo AM, Burris HA, Bendell J, Berlin JD*, et al.* Abstract CT-01: BYL719, a next generation PI3K alpha specific inhibitor: Preliminary safety, PK, and efficacy results from the first-in-human study. AACR; 2012.

177. Mayer IA, Abramson VG, Formisano L, Balko JM, Estrada MV, Sanders ME*, et al.* A Phase Ib Study of Alpelisib (BYL719), a PI3Kalpha-Specific Inhibitor, with Letrozole in ER+/HER2- Metastatic Breast Cancer. Clin Cancer Res **2017**;23(1):26-34 doi 10.1158/1078-0432.CCR-16-0134.

178. Le X, Antony R, Razavi P, Treacy DJ, Luo F, Ghandi M*, et al.* Systematic Functional Characterization of Resistance to PI3K Inhibition in Breast Cancer. Cancer Discov **2016**;6(10):1134-47 doi 10.1158/2159-8290.CD-16-0305.

179. Vora SR, Juric D, Kim N, Mino-Kenudson M, Huynh T, Costa C*, et al.* CDK 4/6 inhibitors sensitize PIK3CA mutant breast cancer to PI3K inhibitors. Cancer Cell **2014**;26(1):136-49 doi 10.1016/j.ccr.2014.05.020.

180. Bosch A, Li Z, Bergamaschi A, Ellis H, Toska E, Prat A*, et al.* PI3K inhibition results in enhanced estrogen receptor function and dependence in hormone receptor-positive breast cancer. Sci Transl Med **2015**;7(283):283ra51 doi 10.1126/scitranslmed.aaa4442.

181. Costa C, Ebi H, Martini M, Beausoleil SA, Faber AC, Jakubik CT*, et al.* Measurement of PIP3 levels reveals an unexpected role for p110beta in early adaptive responses to p110alpha-specific inhibitors in luminal breast cancer. Cancer Cell **2015**;27(1):97-108 doi 10.1016/j.ccell.2014.11.007.

182. Juric D, Castel P, Griffith M, Griffith OL, Won HH, Ellis H*, et al.* Convergent loss of PTEN leads to clinical resistance to a PI(3)Kalpha inhibitor. Nature **2015**;518(7538):240-4 doi 10.1038/nature13948.

183. Elkabets M, Vora S, Juric D, Morse N, Mino-Kenudson M, Muranen T*, et al.* mTORC1 inhibition is required for sensitivity to PI3K p110α inhibitors in PIK3CA-mutant breast cancer. Science translational medicine **2013**;5(196):196ra99-ra99.

184. Yap TA, Yan L, Patnaik A, Fearen I, Olmos D, Papadopoulos K*, et al.* First-in-man clinical trial of the oral pan-AKT inhibitor MK-2206 in patients with advanced solid tumors. J Clin Oncol **2011**;29(35):4688-95 doi 10.1200/JCO.2011.35.5263.

185. Ma CX, Sanchez C, Gao F, Crowder R, Naughton M, Pluard T*, et al.* A Phase I Study of the AKT Inhibitor MK-2206 in Combination with Hormonal Therapy in Postmenopausal Women with Estrogen Receptor-Positive Metastatic Breast Cancer. Clin Cancer Res **2016**;22(11):2650-8 doi 10.1158/1078-0432.CCR-15-2160.

186. Jansen VM, Mayer IA, Arteaga CL. Is There a Future for AKT Inhibitors in the Treatment of Cancer? Clinical Cancer Research **2016**;22(11):2599-601 doi 10.1158/1078-0432.ccr-16-0100.

187. Gonzalez-Malerva L, Park J, Zou L, Hu Y, Moradpour Z, Pearlberg J*, et al.* High-throughput ectopic expression screen for tamoxifen resistance identifies an atypical kinase that blocks autophagy. Proc Natl Acad Sci U S A **2011**;108(5):2058-63 doi 10.1073/pnas.1018157108.

188. Fox EM, Miller TW, Balko JM, Kuba MG, Sanchez V, Smith RA*, et al.* A kinome-wide screen identifies the insulin/IGF-I receptor pathway as a mechanism of escape from hormone dependence in breast cancer. Cancer Res **2011**;71(21):6773-84 doi 10.1158/0008-5472.CAN-11-1295.

189. Mendes-Pereira AM, Sims D, Dexter T, Fenwick K, Assiotis I, Kozarewa I*, et al.* Genome-wide functional screen identifies a compendium of genes affecting sensitivity to tamoxifen. Proc Natl Acad Sci U S A **2012**;109(8):2730-5 doi 10.1073/pnas.1018872108.

190. Meijer D, van Agthoven T, Bosma PT, Nooter K, Dorssers LC. Functional screen for genes responsible for tamoxifen resistance in human breast cancer cells. Mol Cancer Res **2006**;4(6):379-86 doi 10.1158/1541-7786.MCR-05-0156.

191. Dorssers LC, Veldscholte J. Identification of a novel breast-cancer-anti-estrogen-resistance (BCAR2) locus by cell-fusion-mediated gene transfer in human breast-cancer cells. Int J Cancer **1997**;72(4):700-5.

192. Dorssers LC, van Agthoven T, Dekker A, van Agthoven TL, Kok EM. Induction of antiestrogen resistance in human breast cancer cells by random insertional mutagenesis using defective retroviruses: identification of bcar-1, a common integration site. Mol Endocrinol **1993**;7(7):870-8 doi 10.1210/mend.7.7.8413311.

193. Musgrove EA, Sutherland RL. Biological determinants of endocrine resistance in breast cancer. Nat Rev Cancer **2009**;9(9):631-43 doi 10.1038/nrc2713.

194. Miller TW, Balko JM, Fox EM, Ghazoui Z, Dunbier A, Anderson H*, et al.* ERalpha-dependent E2F transcription can mediate resistance to estrogen deprivation in human breast cancer. Cancer Discov **2011**;1(4):338-51 doi 10.1158/2159-8290.CD-11-0101.

195. Wang W, Dong L, Saville B, Safe S. Transcriptional activation of E2F1 gene expression by 17beta-estradiol in MCF-7 cells is regulated by NF-Y-Sp1/estrogen receptor interactions. Molecular endocrinology **1999**;13(8):1373-87 doi 10.1210/mend.13.8.0323.

196. Doisneau-Sixou SF, Sergio CM, Carroll JS, Hui R, Musgrove EA, Sutherland RL. Estrogen and antiestrogen regulation of cell cycle progression in breast cancer cells. Endocr Relat Cancer **2003**;10(2):179-86.

197. Watts CK, Brady A, Sarcevic B, deFazio A, Musgrove EA, Sutherland RL. Antiestrogen inhibition of cell cycle progression in breast cancer cells in associated with inhibition of cyclin-dependent kinase activity and decreased retinoblastoma protein phosphorylation. Mol Endocrinol **1995**;9(12):1804-13 doi 10.1210/mend.9.12.8614416.

198. Prall OW, Rogan EM, Musgrove EA, Watts CK, Sutherland RL. c-Myc or cyclin D1 mimics estrogen effects on cyclin E-Cdk2 activation and cell cycle reentry. Mol Cell Biol **1998**;18(8):4499-508.

199. Hui R, Finney GL, Carroll JS, Lee CS, Musgrove EA, Sutherland RL. Constitutive overexpression of cyclin D1 but not cyclin E confers acute resistance to antiestrogens in T-47D breast cancer cells. Cancer Res **2002**;62(23):6916-23.

200. Caldon CE, Sergio CM, Schutte J, Boersma MN, Sutherland RL, Carroll JS*, et al.* Estrogen regulation of cyclin E2 requires cyclin D1 but not c-Myc. Mol Cell Biol **2009**;29(17):4623-39 doi 10.1128/MCB.00269-09.

201. Cariou S, Donovan JC, Flanagan WM, Milic A, Bhattacharya N, Slingerland JM. Down-regulation of p21WAF1/CIP1 or p27Kip1 abrogates antiestrogen-mediated cell cycle arrest in human breast cancer cells. Proc Natl Acad Sci U S A **2000**;97(16):9042-6 doi 10.1073/pnas.160016897.

202. Thangavel C, Dean JL, Ertel A, Knudsen KE, Aldaz CM, Witkiewicz AK*, et al.* Therapeutically activating RB: reestablishing cell cycle control in endocrine therapy-resistant breast cancer. Endocr Relat Cancer **2011**;18(3):333-45 doi 10.1530/ERC-10-0262.

203. Dowsett M, Smith IE, Ebbs SR, Dixon JM, Skene A, A'Hern R*, et al.* Prognostic value of Ki67 expression after short-term presurgical endocrine therapy for primary breast cancer. J Natl Cancer Inst **2007**;99(2):167-70 doi 10.1093/jnci/djk020.

204. Asghar U, Witkiewicz AK, Turner NC, Knudsen ES. The history and future of targeting cyclin-dependent kinases in cancer therapy. Nat Rev Drug Discov **2015**;14(2):130-46 doi 10.1038/nrd4504.

205. Abraham RT, VanArsdale T, Shields DV, Lee NV, Koehler M, Arndt K. Abstract SY34-03: Braking the cycle: Inhibition of the cyclin D-Cdk4/6 pathway in breast cancer. Cancer Research **2014**;74(19 Supplement):SY34-03-SY34-03 doi 10.1158/1538-7445.am2014-sy34-03.

206. Rader J, Russell MR, Hart LS, Nakazawa MS, Belcastro LT, Martinez D*, et al.* Dual CDK4/CDK6 inhibition induces cell-cycle arrest and senescence in neuroblastoma. Clin Cancer Res **2013**;19(22):6173-82 doi 10.1158/1078-0432.CCR-13-1675.

207. Zhang YX, Sicinska E, Czaplinski JT, Remillard SP, Moss S, Wang Y*, et al.* Antiproliferative effects of CDK4/6 inhibition in CDK4-amplified human liposarcoma in vitro and in vivo. Mol Cancer Ther **2014**;13(9):2184-93 doi 10.1158/1535-7163.MCT-14-0387.

208. O'Leary B, Finn RS, Turner NC. Treating cancer with selective CDK4/6 inhibitors. Nat Rev Clin Oncol **2016**;13(7):417-30 doi 10.1038/nrclinonc.2016.26.

209. Chen P, Lee NV, Hu W, Xu M, Ferre RA, Lam H*, et al.* Spectrum and Degree of CDK Drug Interactions Predicts Clinical Performance. Mol Cancer Ther **2016**;15(10):2273-81 doi 10.1158/1535-7163.MCT-16-0300.

210. VanArsdale T, Boshoff C, Arndt KT, Abraham RT. Molecular Pathways: Targeting the Cyclin D-CDK4/6 Axis for Cancer Treatment. Clin Cancer Res **2015**;21(13):2905-10 doi 10.1158/1078-0432.CCR-14-0816.

211. Raub TJ, Wishart GN, Kulanthaivel P, Staton BA, Ajamie RT, Sawada GA*, et al.* Brain Exposure of Two Selective Dual CDK4 and CDK6 Inhibitors and the Antitumor Activity of CDK4 and CDK6 Inhibition in Combination with Temozolomide in an Intracranial Glioblastoma Xenograft. Drug Metab Dispos **2015**;43(9):1360-71 doi 10.1124/dmd.114.062745.

212. Garriga J, Grana X. Cellular control of gene expression by T-type cyclin/CDK9 complexes. Gene **2004**;337:15-23 doi 10.1016/j.gene.2004.05.007.

213. Peterlin BM, Price DH. Controlling the elongation phase of transcription with P-TEFb. Mol Cell **2006**;23(3):297-305 doi 10.1016/j.molcel.2006.06.014.

214. Chen R, Keating MJ, Gandhi V, Plunkett W. Transcription inhibition by flavopiridol: mechanism of chronic lymphocytic leukemia cell death. Blood **2005**;106(7):2513-9 doi 10.1182/blood-2005-04-1678.

215. Christian BA, Grever MR, Byrd JC, Lin TS. Flavopiridol in chronic lymphocytic leukemia: a concise review. Clin Lymphoma Myeloma **2009**;9 Suppl 3:S179-85 doi 10.3816/CLM.2009.s.009.

216. Johnson N, Shapiro GI. Cyclin-dependent kinases (cdks) and the DNA damage response: rationale for cdk inhibitor-chemotherapy combinations as an anticancer strategy for solid tumors. Expert Opin Ther Targets **2010**;14(11):1199-212 doi 10.1517/14728222.2010.525221.

217. Johnson J, Thijssen B, McDermott U, Garnett M, Wessels LF, Bernards R. Targeting the RB-E2F pathway in breast cancer. Oncogene **2016**;35(37):4829-35 doi 10.1038/onc.2016.32.

218. Dean JL, McClendon AK, Hickey TE, Butler LM, Tilley WD, Witkiewicz AK*, et al.* Therapeutic response to CDK4/6 inhibition in breast cancer defined by ex vivo analyses of human tumors. Cell Cycle **2012**;11(14):2756-61 doi 10.4161/cc.21195.

219. Dean JL, Thangavel C, McClendon AK, Reed CA, Knudsen ES. Therapeutic CDK4/6 inhibition in breast cancer: key mechanisms of response and failure. Oncogene **2010**;29(28):4018-32 doi 10.1038/onc.2010.154.

220. Cen L, Carlson BL, Schroeder MA, Ostrem JL, Kitange GJ, Mladek AC*, et al.* p16-Cdk4-Rb axis controls sensitivity to a cyclin-dependent kinase inhibitor PD0332991 in glioblastoma xenograft cells. Neuro Oncol **2012**;14(7):870-81 doi 10.1093/neuonc/nos114.

221. Wiedemeyer WR, Dunn IF, Quayle SN, Zhang J, Chheda MG, Dunn GP*, et al.* Pattern of retinoblastoma pathway inactivation dictates response to CDK4/6 inhibition in GBM. Proc Natl Acad Sci U S A **2010**;107(25):11501-6 doi 10.1073/pnas.1001613107.

222. Logan JE, Mostofizadeh N, Desai AJ, E VONE, Conklin D, Konkankit V*, et al.* PD-0332991, a potent and selective inhibitor of cyclin-dependent kinase 4/6, demonstrates inhibition of proliferation in renal cell carcinoma at nanomolar concentrations and molecular markers predict for sensitivity. Anticancer Res **2013**;33(8):2997-3004.

223. Lee NV, Yuan J, Eisele K, Cao JQ, Painter CL, Chionis J*, et al.* Abstract LB-136: Mechanistic exploration of combined CDK4/6 and ER inhibition in ER-positive breast cancer. Cancer Research **2014**;74(19 Supplement):LB-136-LB- doi 10.1158/1538-7445.am2014-lb-136.

224. Anders L, Ke N, Hydbring P, Choi YJ, Widlund HR, Chick JM*, et al.* A systematic screen for CDK4/6 substrates links FOXM1 phosphorylation to senescence suppression in cancer cells. Cancer Cell **2011**;20(5):620-34 doi 10.1016/j.ccr.2011.10.001.

225. Goel S, Wang Q, Watt AC, Tolaney SM, Dillon DA, Li W*, et al.* Overcoming Therapeutic Resistance in HER2-Positive Breast Cancers with CDK4/6 Inhibitors. Cancer Cell **2016**;29(3):255-69 doi 10.1016/j.ccell.2016.02.006.

226. Kwong LN, Costello JC, Liu H, Jiang S, Helms TL, Langsdorf AE*, et al.* Oncogenic NRAS signaling differentially regulates survival and proliferation in melanoma. Nat Med **2012**;18(10):1503-10 doi 10.1038/nm.2941.

227. Ziemke EK, Dosch JS, Maust JD, Shettigar A, Sen A, Welling TH*, et al.* Sensitivity of KRAS-Mutant Colorectal Cancers to Combination Therapy That Cotargets MEK and CDK4/6. Clin Cancer Res **2016**;22(2):405-14 doi 10.1158/1078-0432.CCR-15-0829.

228. Baughn LB, Di Liberto M, Wu K, Toogood PL, Louie T, Gottschalk R*, et al.* A novel orally active small molecule potently induces G1 arrest in primary myeloma cells and prevents tumor growth by specific inhibition of cyclin-dependent kinase 4/6. Cancer Res **2006**;66(15):7661-7 doi 10.1158/0008-5472.CAN-06-1098.

229. Menu E, Garcia J, Huang X, Di Liberto M, Toogood PL, Chen I*, et al.* A novel therapeutic combination using PD 0332991 and bortezomib: study in the 5T33MM myeloma model. Cancer Res **2008**;68(14):5519-23 doi 10.1158/0008-5472.CAN-07-6404.

230. DeMichele A, Clark AS, Tan KS, Heitjan DF, Gramlich K, Gallagher M*, et al.* CDK 4/6 inhibitor palbociclib (PD0332991) in Rb+ advanced breast cancer: phase II activity, safety, and predictive biomarker assessment. Clin Cancer Res **2015**;21(5):995-1001 doi 10.1158/1078-0432.CCR-14-2258.

231. Finn RS, Crown JP, Lang I, Boer K, Bondarenko IM, Sergey OK*, et al.* Final results of a randomized Phase II study of PD 0332991, a cyclin-dependent kinase (CDK)-4/6 inhibitor, in combination with letrozole vs letrozole alone for first-line treatment of ER+/HER2- advanced breast cancer (PALOMA-1; TRIO-18). AACR Annual Meeting 2014. San Diego, CA2014.

232. Beaver JA, Amiri-Kordestani L, Charlab R, Chen W, Palmby T, Tilley A*, et al.* FDA Approval: Palbociclib for the Treatment of Postmenopausal Patients with Estrogen Receptor-Positive, HER2-Negative Metastatic Breast Cancer. Clin Cancer Res **2015**;21(21):4760-6 doi 10.1158/1078-0432.CCR-15-1185.

233. Turner NC, Huang Bartlett C, Cristofanilli M. Palbociclib in Hormone-Receptor-Positive Advanced Breast Cancer. N Engl J Med **2015**;373(17):1672-3 doi 10.1056/NEJMc1510345.

234. Cristofanilli M, Turner NC, Bondarenko I, Ro J, Im SA, Masuda N*, et al.* Fulvestrant plus palbociclib versus fulvestrant plus placebo for treatment of hormone-receptor-positive, HER2-negative metastatic breast cancer that progressed on previous endocrine therapy (PALOMA-3): final analysis of the multicentre, double-blind, phase 3 randomised controlled trial. Lancet Oncol **2016**;17(4):425-39 doi 10.1016/S1470-2045(15)00613-0.

235. Walker AJ, Wedam S, Amiri-Kordestani L, Bloomquist E, Tang S, Sridhara R*, et al.* FDA Approval of Palbociclib in Combination with Fulvestrant for the Treatment of Hormone Receptor-Positive, HER2-Negative Metastatic Breast Cancer. Clin Cancer Res **2016**;22(20):4968-72 doi 10.1158/1078-0432.CCR-16-0493.

236. Infante JR, Cassier PA, Gerecitano JF, Witteveen PO, Chugh R, Ribrag V*, et al.* A Phase I Study of the Cyclin-Dependent Kinase 4/6 Inhibitor Ribociclib (LEE011) in Patients with Advanced Solid Tumors and Lymphomas. Clin Cancer Res **2016**;22(23):5696-705 doi 10.1158/1078-0432.CCR-16-1248.

237. Hortobagyi GN, Stemmer SM, Burris HA, Yap YS, Sonke GS, Paluch-Shimon S*, et al.* Ribociclib as First-Line Therapy for HR-Positive, Advanced Breast Cancer. N Engl J Med **2016**;375(18):1738-48 doi 10.1056/NEJMoa1609709.

238. O'Brien NA, Tomaso ED, Ayala R, Tong L, Issakhanian S, Linnartz R*, et al.* Abstract 4756: In vivo efficacy of combined targeting of CDK4/6, ER and PI3K signaling in ER+ breast cancer. Cancer Research **2014**;74(19 Supplement):4756- doi 10.1158/1538-7445.am2014-4756.

239. Bardia A, Modi S, Oliveira M, Campone M, Ma B, Dirix L*, et al.* Abstract P6-13-01: Triplet therapy with ribociclib, everolimus, and exemestane in women with HR+/HER2– advanced breast cancer. Cancer Research **2016**;76(4 Supplement):P6-13-01-P6-13-01 doi 10.1158/1538-7445.sabcs15-p6-13-01.

240. Shapiro G, Rosen LS, Tolcher AW, Goldman JW, Gandhi L, Papadopoulos KP*, et al.* A first-in-human phase I study of the CDK4/6 inhibitor, LY2835219, for patients with advanced cancer. Journal of Clinical Oncology **2013**;31(15_suppl):2500- doi 10.1200/jco.2013.31.15_suppl.2500.

241. Dickler M, Tolaney S, Rugo H, Cortes J, Dieras V, Patt D*, et al.* MONARCH1: results from a phase II study of abemaciclib, a CDK4 and CDK6 inhibitor, as monotherapy, in patients with HR+/HER2-breast cancer, after chemotherapy for advanced disease. J Clin Oncol **2016**;34(suppl; abstr 510).

242. Patnaik A, Rosen LS, Tolaney SM, Tolcher AW, Goldman JW, Gandhi L*, et al.* Abstract CT232: Clinical activity of LY2835219, a novel cell cycle inhibitor selective for CDK4 and CDK6, in patients with metastatic breast cancer. Cancer Research **2014**;74(19 Supplement):CT232-CT doi 10.1158/1538-7445.am2014-ct232.

243. Tolaney SM, Rosen LS, Beeram M, Goldman JW, Gandhi L, Tolcher AW*, et al.* Abstract P5-19-13: Clinical activity of abemaciclib, an oral cell cycle inhibitor, in metastatic breast cancer. Cancer Research **2015**;75(9 Supplement):P5-19-3-P5--3 doi 10.1158/1538-7445.sabcs14-p5-19-13.

244. Patnaik A, Rosen LS, Tolaney SM, Tolcher AW, Goldman JW, Gandhi L*, et al.* Efficacy and Safety of Abemaciclib, an Inhibitor of CDK4 and CDK6, for Patients with Breast Cancer, Non-Small Cell Lung Cancer, and Other Solid Tumors. Cancer Discov **2016**;6(7):740-53 doi 10.1158/2159-8290.CD-16-0095.

245. Hu MG, Deshpande A, Enos M, Mao D, Hinds EA, Hu GF*, et al.* A requirement for cyclin-dependent kinase 6 in thymocyte development and tumorigenesis. Cancer Res **2009**;69(3):810-8 doi 10.1158/0008-5472.CAN-08-2473.

246. Malumbres M, Sotillo R, Santamaria D, Galan J, Cerezo A, Ortega S*, et al.* Mammalian cells cycle without the D-type cyclin-dependent kinases Cdk4 and Cdk6. Cell **2004**;118(4):493-504 doi 10.1016/j.cell.2004.08.002.

247. Jansen VM, Bhola NE, Bauer JA, Formisano L, Lee KM, Hutchinson KE*, et al.* Kinome-wide RNA interference screen reveals a role for PDK1 in acquired resistance to CDK4/6 inhibition in ER-positive breast cancer. Cancer Res **2017** doi 10.1158/0008-5472.CAN-16-2653.

248. Herrera-Abreu MT, Palafox M, Asghar U, Rivas MA, Cutts RJ, Garcia-Murillas I*, et al.* Early Adaptation and Acquired Resistance to CDK4/6 Inhibition in Estrogen Receptor-Positive Breast Cancer. Cancer Res **2016**;76(8):2301-13 doi 10.1158/0008-5472.CAN-15-0728.

249. Yang C, Li Z, Bhatt T, Dickler M, Giri D, Scaltriti M*, et al.* Acquired CDK6 amplification promotes breast cancer resistance to CDK4/6 inhibitors and loss of ER signaling and dependence. Oncogene **2016** doi 10.1038/onc.2016.379.

250. Caldon CE, Sergio CM, Kang J, Muthukaruppan A, Boersma MN, Stone A*, et al.* Cyclin E2 overexpression is associated with endocrine resistance but not insensitivity to CDK2 inhibition in human breast cancer cells. Mol Cancer Ther **2012**;11(7):1488-99 doi 10.1158/1535-7163.MCT-11-0963.

251. Akiyama T, Ohuchi T, Sumida S, Matsumoto K, Toyoshima K. Phosphorylation of the retinoblastoma protein by cdk2. Proc Natl Acad Sci U S A **1992**;89(17):7900-4.

252. Finn RS, Crown JP, Lang I, Boer K, Bondarenko IM, Kulyk SO*, et al.* The cyclin-dependent kinase 4/6 inhibitor palbociclib in combination with letrozole versus letrozole alone as first-line treatment of oestrogen receptor-positive, HER2-negative, advanced breast cancer (PALOMA-1/TRIO-18): a randomised phase 2 study. Lancet Oncol **2015**;16(1):25-35 doi 10.1016/S1470-2045(14)71159-3.

253. Finn RS, Martin M, Rugo HS, Jones S, Im SA, Gelmon K*, et al.* Palbociclib and Letrozole in Advanced Breast Cancer. N Engl J Med **2016**;375(20):1925-36 doi 10.1056/NEJMoa1607303.

254. Lonning PE, Bajetta E, Murray R, Tubiana-Hulin M, Eisenberg PD, Mickiewicz E*, et al.* Activity of exemestane in metastatic breast cancer after failure of nonsteroidal

aromatase inhibitors: a phase II trial. Journal of clinical oncology : official journal of the American Society of Clinical Oncology **2000**;18(11):2234-44.

255. Ingle JN. Sequencing of endocrine therapy in postmenopausal women with advanced breast cancer. Clinical cancer research : an official journal of the American Association for Cancer Research **2004**;10(1 Pt 2):362S-7S.

256. Turner NC, Ro J, Andre F, Loi S, Verma S, Iwata H*, et al.* Palbociclib in Hormone-Receptor-Positive Advanced Breast Cancer. N Engl J Med **2015**;373(3):209-19 doi 10.1056/NEJMoa1505270.

257. Foster JS, Wimalasena J. Estrogen regulates activity of cyclin-dependent kinases and retinoblastoma protein phosphorylation in breast cancer cells. Mol Endocrinol **1996**;10(5):488-98 doi 10.1210/mend.10.5.8732680.

258. Prall OW, Sarcevic B, Musgrove EA, Watts CK, Sutherland RL. Estrogen-induced activation of Cdk4 and Cdk2 during G1-S phase progression is accompanied by increased cyclin D1 expression and decreased cyclin-dependent kinase inhibitor association with cyclin E-Cdk2. J Biol Chem **1997**;272(16):10882-94.

259. Planas-Silva MD, Weinberg RA. Estrogen-dependent cyclin E-cdk2 activation through p21 redistribution. Mol Cell Biol **1997**;17(7):4059-69.

260. Shi H, Moriceau G, Kong X, Lee MK, Lee H, Koya RC*, et al.* Melanoma whole-exome sequencing identifies (V600E)B-RAF amplification-mediated acquired B-RAF inhibitor resistance. Nat Commun **2012**;3:724 doi 10.1038/ncomms1727.

261. Gazdar AF. Activating and resistance mutations of EGFR in non-small-cell lung cancer: role in clinical response to EGFR tyrosine kinase inhibitors. Oncogene **2009**;28 Suppl 1:S24-31 doi 10.1038/onc.2009.198.

262. Wardell SE, Ellis MJ, Alley HM, Eisele K, VanArsdale T, Dann SG*, et al.* Efficacy of SERD/SERM Hybrid-CDK4/6 Inhibitor Combinations in Models of Endocrine Therapy-Resistant Breast Cancer. Clin Cancer Res **2015**;21(22):5121-30 doi 10.1158/1078-0432.CCR-15-0360.

263. Fribbens C, O'Leary B, Kilburn L, Hrebien S, Garcia-Murillas I, Beaney M*, et al.* Plasma ESR1 Mutations and the Treatment of Estrogen Receptor-Positive Advanced Breast Cancer. J Clin Oncol **2016**;34(25):2961-8 doi 10.1200/JCO.2016.67.3061.

264. Bosco EE, Wang Y, Xu H, Zilfou JT, Knudsen KE, Aronow BJ*, et al.* The retinoblastoma tumor suppressor modifies the therapeutic response of breast cancer. J Clin Invest **2007**;117(1):218-28 doi 10.1172/JCI28803.

265. Cohen O, Kim D, Oh C, Waks A, Oliver N, Helvie K*, et al.* Abstract S1-01. Whole exome and transcriptome sequencing of resistant ER+ metastatic breast cancer. SABCS **2016**.

266. Whittaker SR, Theurillat JP, Van Allen E, Wagle N, Hsiao J, Cowley GS*, et al.* A genome-scale RNA interference screen implicates NF1 loss in resistance to RAF inhibition. Cancer Discov **2013**;3(3):350-62 doi 10.1158/2159-8290.CD-12-0470.

267. Juric D, Hamilton E, Estévez LG, De Boer RH, Mayer I, Campone M*, et al.* Abstract P5-19-24: Phase Ib/II study of LEE011 and BYL719 and letrozole in ER+, HER2–breast cancer: Safety, preliminary efficacy and molecular analysis. Cancer Research **2015**;75:P5-19-24.

268. Shapiro G, Rosen LS, Tolcher AW, Goldman JW, Gandhi L, Papadopoulos KP*, et al.* A first-in-human phase I study of the CDK4/6 inhibitor, LY2835219, for patients with advanced cancer. Journal of Clinical Oncology **2013**;31(15):suppl; abstr 2500.

269. Chang F, Lee JT, Navolanic PM, Steelman LS, Shelton JG, Blalock WL*, et al.* Involvement of PI3K/Akt pathway in cell cycle progression, apoptosis, and neoplastic transformation: a target for cancer chemotherapy. Leukemia **2003**;17(3):590-603 doi 10.1038/sj.leu.2402824.

270. Arpino G, De Angelis C, Giuliano M, Giordano A, Falato C, De Laurentiis M*, et al.* Molecular mechanism and clinical implications of endocrine therapy resistance in breast cancer. Oncology **2009**;77 Suppl 1:23-37 doi 10.1159/000258493.

271. Arpino G, Green SJ, Allred DC, Lew D, Martino S, Osborne CK*, et al.* HER-2 amplification, HER-1 expression, and tamoxifen response in estrogen receptor-positive metastatic breast cancer: a southwest oncology group study. Clinical cancer research : an official journal of the American Association for Cancer Research **2004**;10(17):5670-6 doi 10.1158/1078-0432.CCR-04-0110.

272. Harwell RM, Porter DC, Danes C, Keyomarsi K. Processing of cyclin E differs between normal and tumor breast cells. Cancer Res **2000**;60(2):481-9.

273. Wang XD, Rosales JL, Magliocco A, Gnanakumar R, Lee KY. Cyclin E in breast tumors is cleaved into its low molecular weight forms by calpain. Oncogene **2003**;22(5):769-74 doi 10.1038/sj.onc.1206166.

274. Nielsen NH, Arnerlov C, Emdin SO, Landberg G. Cyclin E overexpression, a negative prognostic factor in breast cancer with strong correlation to oestrogen receptor status. British journal of cancer **1996**;74(6):874-80.

275. Keyomarsi K, Conte D, Jr., Toyofuku W, Fox MP. Deregulation of cyclin E in breast cancer. Oncogene **1995**;11(5):941-50.

276. Akli S, Zheng PJ, Multani AS, Wingate HF, Pathak S, Zhang N*, et al.* Tumor-specific low molecular weight forms of cyclin E induce genomic instability and resistance to p21, p27, and antiestrogens in breast cancer. Cancer Res **2004**;64(9):3198-208.

277. Wang L, Wang J, Blaser BW, Duchemin AM, Kusewitt DF, Liu T*, et al.* Pharmacologic inhibition of CDK4/6: mechanistic evidence for selective activity or acquired resistance in acute myeloid leukemia. Blood **2007**;110(6):2075-83 doi 10.1182/blood-2007-02-071266.

278. Vivanco I, Sawyers CL. The phosphatidylinositol 3-Kinase AKT pathway in human cancer. Nat Rev Cancer **2002**;2(7):489-501 doi 10.1038/nrc839.

279. Godin-Heymann N, Bryant I, Rivera MN, Ulkus L, Bell DW, Riese DJ, 2nd*, et al.* Oncogenic activity of epidermal growth factor receptor kinase mutant alleles is enhanced by the T790M drug resistance mutation. Cancer Res **2007**;67(15):7319-26 doi 10.1158/0008-5472.CAN-06-4625.

280. Di Nicolantonio F, Arena S, Tabernero J, Grosso S, Molinari F, Macarulla T*, et al.* Deregulation of the PI3K and KRAS signaling pathways in human cancer cells determines their response to everolimus. J Clin Invest **2010**;120(8):2858-66 doi 10.1172/JCI37539.

281. Bleeker FE, Felicioni L, Buttitta F, Lamba S, Cardone L, Rodolfo M*, et al.* AKT1(E17K) in human solid tumours. Oncogene **2008**;27(42):5648-50 doi 10.1038/onc.2008.170.

282. Kohn AD, Takeuchi F, Roth RA. Akt, a pleckstrin homology domain containing kinase, is activated primarily by phosphorylation. J Biol Chem **1996**;271(36):21920-6.

283. Johannessen CM, Boehm JS, Kim SY, Thomas SR, Wardwell L, Johnson LA*, et al.* COT drives resistance to RAF inhibition through MAP kinase pathway reactivation. Nature **2010**;468(7326):968-72 doi 10.1038/nature09627.

284. Emery CM, Vijayendran KG, Zipser MC, Sawyer AM, Niu L, Kim JJ*, et al.* MEK1 mutations confer resistance to MEK and B-RAF inhibition. Proceedings of the National Academy of Sciences of the United States of America **2009**;106(48):20411-6 doi 10.1073/pnas.0905833106.

285. Tate SC, Cai S, Ajamie RT, Burke T, Beckmann RP, Chan EM*, et al.* Semi-mechanistic pharmacokinetic/pharmacodynamic modeling of the antitumor activity of LY2835219, a new cyclin-dependent kinase 4/6 inhibitor, in mice bearing human tumor xenografts. Clin Cancer Res **2014**;20(14):3763-74 doi 10.1158/1078-0432.CCR-13-2846.

286. Cross DA, Alessi DR, Cohen P, Andjelkovich M, Hemmings BA. Inhibition of glycogen synthase kinase-3 by insulin mediated by protein kinase B. Nature **1995**;378(6559):785-9 doi 10.1038/378785a0.

287. Dudek H, Datta SR, Franke TF, Birnbaum MJ, Yao R, Cooper GM*, et al.* Regulation of neuronal survival by the serine-threonine protein kinase Akt. Science **1997**;275(5300):661-5.

288. Hirai H, Sootome H, Nakatsuru Y, Miyama K, Taguchi S, Tsujioka K*, et al.* MK-2206, an allosteric Akt inhibitor, enhances antitumor efficacy by standard chemotherapeutic agents or molecular targeted drugs in vitro and in vivo. Mol Cancer Ther **2010**;9(7):1956-67 doi 10.1158/1535-7163.MCT-09-1012.

289. Zhou BP, Liao Y, Xia W, Spohn B, Lee MH, Hung MC. Cytoplasmic localization of p21Cip1/WAF1 by Akt-induced phosphorylation in HER-2/neu-overexpressing cells. Nat Cell Biol **2001**;3(3):245-52 doi 10.1038/35060032.

290. Xia W, Chen JS, Zhou X, Sun PR, Lee DF, Liao Y*, et al.* Phosphorylation/cytoplasmic localization of p21Cip1/WAF1 is associated with HER2/neu overexpression and provides a novel combination predictor for poor prognosis in breast cancer patients. Clin Cancer Res **2004**;10(11):3815-24 doi 10.1158/1078-0432.CCR-03-0527.

291. Gu Y, Rosenblatt J, Morgan DO. Cell cycle regulation of CDK2 activity by phosphorylation of Thr160 and Tyr15. EMBO J **1992**;11(11):3995-4005.

292. Inoki K, Li Y, Zhu T, Wu J, Guan KL. TSC2 is phosphorylated and inhibited by Akt and suppresses mTOR signalling. Nat Cell Biol **2002**;4(9):648-57 doi 10.1038/ncb839.

293. Manning BD, Tee AR, Logsdon MN, Blenis J, Cantley LC. Identification of the tuberous sclerosis complex-2 tumor suppressor gene product tuberin as a target of the phosphoinositide 3-kinase/akt pathway. Mol Cell **2002**;10(1):151-62.

294. Vander Haar E, Lee SI, Bandhakavi S, Griffin TJ, Kim DH. Insulin signalling to mTOR mediated by the Akt/PKB substrate PRAS40. Nat Cell Biol **2007**;9(3):316-23 doi 10.1038/ncb1547.

295. Ballou LM, Lin RZ. Rapamycin and mTOR kinase inhibitors. J Chem Biol **2008**;1(1-4):27-36 doi 10.1007/s12154-008-0003-5.

296. Zhang J, Xu K, Liu P, Geng Y, Wang B, Gan W*, et al.* Inhibition of Rb Phosphorylation Leads to mTORC2-Mediated Activation of Akt. Mol Cell **2016**;62(6):929-42 doi 10.1016/j.molcel.2016.04.023.

297. Wagle N, Berger MF, Davis MJ, Blumenstiel B, Defelice M, Pochanard P*, et al.* High-throughput detection of actionable genomic alterations in clinical tumor samples by targeted, massively parallel sequencing. Cancer Discov **2012**;2(1):82-93 doi 10.1158/2159-8290.CD-11-0184.

298. Van Allen EM, Wagle N, Stojanov P, Perrin DL, Cibulskis K, Marlow S*, et al.* Whole-exome sequencing and clinical interpretation of formalin-fixed, paraffin-embedded tumor samples to guide precision cancer medicine. Nat Med **2014**;20(6):682-8 doi 10.1038/nm.3559.

299. Parikh C, Janakiraman V, Wu WI, Foo CK, Kljavin NM, Chaudhuri S*, et al.* Disruption of PH-kinase domain interactions leads to oncogenic activation of AKT in human cancers. Proc Natl Acad Sci U S A **2012**;109(47):19368-73 doi 10.1073/pnas.1204384109.

300. Burke JE, Perisic O, Masson GR, Vadas O, Williams RL. Oncogenic mutations mimic and enhance dynamic events in the natural activation of phosphoinositide 3-kinase p110alpha (PIK3CA). Proc Natl Acad Sci U S A **2012**;109(38):15259-64 doi 10.1073/pnas.1205508109.

301. Trovik J, Wik E, Stefansson I, Carter SL, Beroukhim R, Oyan AM*, et al.* Stathmin is superior to AKT and phospho-AKT staining for the detection of phosphoinositide 3-kinase activation and aggressive endometrial cancer. Histopathology **2010**;57(4):641-6 doi 10.1111/j.1365-2559.2010.03661.x.

302. Johannessen CM, Johnson LA, Piccioni F, Townes A, Frederick DT, Donahue MK*, et al.* A melanocyte lineage program confers resistance to MAP kinase pathway inhibition. Nature **2013**;504(7478):138-42 doi 10.1038/nature12688.

303. Vasudevan KM, Barbie DA, Davies MA, Rabinovsky R, McNear CJ, Kim JJ*, et al.* AKT-independent signaling downstream of oncogenic PIK3CA mutations in human cancer. Cancer Cell **2009**;16(1):21-32 doi 10.1016/j.ccr.2009.04.012.

304. Alao JP. The regulation of cyclin D1 degradation: roles in cancer development and the potential for therapeutic invention. Mol Cancer **2007**;6:24 doi 10.1186/1476-4598-6-24.

305. Davies BR, Guan N, Logie A, Crafter C, Hanson L, Jacobs V*, et al.* Tumors with AKT1E17K Mutations Are Rational Targets for Single Agent or Combination Therapy with AKT Inhibitors. Mol Cancer Ther **2015**;14(11):2441-51 doi 10.1158/1535-7163.MCT-15-0230.

306. Konermann S, Brigham MD, Trevino AE, Joung J, Abudayyeh OO, Barcena C*, et al.* Genome-scale transcriptional activation by an engineered CRISPR-Cas9 complex. Nature **2015**;517(7536):583-8 doi 10.1038/nature14136.

307. Parry D, Guzi T, Shanahan F, Davis N, Prabhavalkar D, Wiswell D*, et al.* Dinaciclib (SCH 727965), a novel and potent cyclin-dependent kinase inhibitor. Mol Cancer Ther **2010**;9(8):2344-53 doi 10.1158/1535-7163.MCT-10-0324.

308. Rane SG, Dubus P, Mettus RV, Galbreath EJ, Boden G, Reddy EP*, et al.* Loss of Cdk4 expression causes insulin-deficient diabetes and Cdk4 activation results in beta-islet cell hyperplasia. Nat Genet **1999**;22(1):44-52 doi 10.1038/8751.

309. Tsutsui T, Hesabi B, Moons DS, Pandolfi PP, Hansel KS, Koff A*, et al.* Targeted disruption of CDK4 delays cell cycle entry with enhanced p27(Kip1) activity. Mol Cell Biol **1999**;19(10):7011-9.

310. Berthet C, Aleem E, Coppola V, Tessarollo L, Kaldis P. Cdk2 knockout mice are viable. Curr Biol **2003**;13(20):1775-85.

311. Santamaria D, Barriere C, Cerqueira A, Hunt S, Tardy C, Newton K*, et al.* Cdk1 is sufficient to drive the mammalian cell cycle. Nature **2007**;448(7155):811-5 doi 10.1038/nature06046.

312. Grabiner BC, Nardi V, Birsoy K, Possemato R, Shen K, Sinha S*, et al.* A diverse array of cancer-associated MTOR mutations are hyperactivating and can predict rapamycin sensitivity. Cancer Discov **2014**;4(5):554-63 doi 10.1158/2159-8290.CD-13-0929.

313. Wagle N, Grabiner BC, Van Allen EM, Hodis E, Jacobus S, Supko JG*, et al.* Activating mTOR mutations in a patient with an extraordinary response on a phase I trial of everolimus and pazopanib. Cancer Discov **2014**;4(5):546-53 doi 10.1158/2159-8290.CD-13-0353.

314. Barbie DA, Tamayo P, Boehm JS, Kim SY, Moody SE, Dunn IF*, et al.* Systematic RNA interference reveals that oncogenic KRAS-driven cancers require TBK1. Nature **2009**;462(7269):108-12 doi 10.1038/nature08460.

315. Shalem O, Sanjana NE, Hartenian E, Shi X, Scott DA, Mikkelsen TS*, et al.* Genome-scale CRISPR-Cas9 knockout screening in human cells. Science **2014**;343(6166):84-7 doi 10.1126/science.1247005.